NuSTEC Class Notes

Vijay R. Pandharipande

Department of Physics, University of Illinois at Urbana-Champaign, Urbana, IL 61801

Steven C. Pieper

Physics Division, Argonne National Laboratory, Argonne, IL 60439

Rocco Schiavilla

Thomas Jefferson National Accelerator Facility, Newport News, VA 23606
and
Department of Physics, Old Dominion University, Norfolk, VA 23529

This set of class notes for the NUSTEC (Neutrino Scattering Theory Experiment Collaboration) training is based on the draft textbook *Nuclear Forces and Light Nuclei* by the same authors.

Contents

Chapter 1

The Basic Model

The atomic nucleus was discovered by Rutherford in 1911, who also classified nuclear physics as the *unclear physics*. This characterization continues to apply to several areas of nuclear physics even today. The fundamental degrees of freedom in nuclei are believed to be quarks and gluons; however, due to color confinement, they are never visible. At low energies, quantum chromodynamics (QCD), which governs the behavior of interacting quarks and gluons, does not have simple solutions. The observed degrees of freedom of nuclear physics are hadrons, protons and neutrons in particular, and a large effort is focused on numerical simulations of hadrons using lattice QCD.

In the past century many interesting models were developed to explain the systematic trends in the low-energy properties of stable and near stable atomic nuclei. They include, for example, the liquid-drop model, the compound-nucleus model, the shell model, the optical model, the collective model, and the interacting boson model. These models have provided deep insights into nuclear structure and reactions, and have been quite successful in correlating many of the nuclear properties. Most of them can be related to the shell model which describes the general theory of quantum liquid drops. They are discussed in various texts of nuclear physics.

The nuclear models primarily address stable or near stable nuclei with mass numbers $A > 10$. (Letters A and Z are used for the total number of nucleons and protons in the nucleus, respectively.) They do not aim at describing all systems and phenomena containing interacting nucleons at low energies. Two extreme examples are the Bethe and Critchfield calculation of the rate for the $p + p \to d + e^+ + \nu_e$ weak capture reaction, which powers the sun, and the structure of neutron stars. We use p, n, and d to denote the proton, neutron and the deuteron. The letter N denotes nucleons, *i.e.* either proton or neutron. Bethe and Critchfield used p-p scattering data and models of the deuteron wave function in their prediction of the $p + p$ weak capture rate, and many calculations of neutron star structure also rely on models of nuclear forces.

All the nuclear models tacitly assume that nuclei are made up of interacting nucleons.

Within this approximation a general theory can be developed for all low-energy phenomena displayed by interacting nucleons, ranging from the deuteron to neutron stars. The present text is aimed at the simplest version of this theory describing low-energy nuclear systems as those composed of nucleons interacting via many-body potentials and many-body electroweak currents. We call it the "basic model." It is likely that the shell model and other models of nuclei can be considered as suitable approximations of this theory for various energy and mass regions of nuclear systems.

The basic model assumes that a Hamiltonian,

$$H = \sum_i \left(m_i + \frac{\mathbf{p}_i^2}{2\, m_i} \right) + \sum_{i<j} v_{ij} + \sum_{i<j<k} V_{ijk} + \ \ldots \ , \tag{1.1}$$

provides a good approximation to the energy of interacting nucleons. The subscripts $i, j, k, ...$ label the nucleons in the system, and we use natural units ($\hbar = 1$ and $c = 1$). Lengths are in fm, momenta are in fm^{-1}, masses and energies are in MeV, and $\hbar\, c \approx 197.327$ MeV fm. The mass m_i is that of a proton or neutron according to the nature of nucleon i.

If electromagnetic interactions and mass differences between charged and neutral nucleons, pions, and other hadrons are neglected, then the proton and neutron can be considered as members of a doublet in a hypothetical "isospin space" with isospin $t = 1/2$, and isospin projections $t_z = +1/2$ and $-1/2$, respectively. Similarly, the positively charged, neutral, and negatively charged pions can be considered as members of a triplet with isospin $t = 1$, having isospin projections $t_z = +1, 0, -1$; and so on. In this approximation the mass m_i in the basic Hamiltonian is replaced by the average value, $m_N = (m_p + m_n)/2$ of the proton and neutron masses, and the small isospin symmetry breaking terms in the potentials v_{ij}, V_{ijk}, ... are ignored. The Hamiltonian then becomes a relatively simpler scalar in isospin space.

The first term of the Hamiltonian is the nonrelativistic part of the relativistic kinetic energy $(m_i^2 + \mathbf{p}_i^2)^{1/2}$ of a free nucleon. Naively including terms of higher order in the nucleon momentum $\mathbf{p}_i$, such as just the next term, $-\mathbf{p}_i^4/(8m_i^3)$, can lead to a Hamiltonian that is unbound from below which is not acceptable. However, the exact expression for the kinetic energy, its nonrelativistic limit and some higher-order approximations can be used safely.

In addition to isospin t=1/2, nucleons have spin s=1/2. It is convenient to introduce the Pauli spin and isospin matrices $\boldsymbol{\sigma}$ and $\boldsymbol{\tau}$, which are related to the spin and isospin operators $\mathbf{s}$ and $\mathbf{t}$ via $\mathbf{s} = \boldsymbol{\sigma}/2$ and $\mathbf{t} = \boldsymbol{\tau}/2$. The state of a nucleon can then be specified by giving its position $\mathbf{r}$, spin projection $\sigma_z = \pm 1$, and isospin projection $\tau_z = \pm 1$. These quantum numbers are collectively denoted by

$$\mathbf{x} \equiv \mathbf{r},\ \sigma_z,\ \tau_z\ . \tag{1.2}$$

The state of A nucleons can be specified by a generalized vector

$$\mathbf{X} = \mathbf{x}_1,\ \mathbf{x}_2, \ldots, \mathbf{x}_A\ , \tag{1.3}$$

in a multidimensional position, spin, and isospin space. The nuclear wave function, $\Psi(\mathbf{X},t)$, is a function of $\mathbf{X}$ and time t. The basic model assumes that at low energies, below the pion production threshold, this wave function obeys the many-body Schrödinger equation:

$$i\frac{\partial}{\partial t}\Psi(\mathbf{X},t) = H\Psi(\mathbf{X},t)\ . \tag{1.4}$$

The potentials v_{ij}, V_{ijk}, ..., are operators on the spins and isospins of the nucleons in the pairs ij, triplets ijk, ..., and depend on interparticle distances, $\mathbf{r}_{ij}$, and so on. They can also contain momentum dependence $\mathbf{p}_i$, $\mathbf{p}_j$, and so on. The ...in the Hamiltonian, Eq. (1.1), denotes four- and higher-body potentials. The series of potentials is assumed to be convergent, and potentials beyond three body are often neglected in present versions of this model.

In order to study and predict rates of electroweak decays and reactions, the model must contain electroweak current operators describing the interaction of nuclei with electroweak fields. They are expanded as a sum of one- and many-body (two-body, three-body, ...) terms. For example, the operators for the electromagnetic charge and current densities of a nucleus, denoted as $\rho_c(\mathbf{r})$ and $\mathbf{j}(\mathbf{r})$, have the form

$$\rho_c(\mathbf{r}) = \sum_i \rho_{c,i}(\mathbf{r}) + \sum_{i<j} \rho_{c,ij}(\mathbf{r}) + \sum_{i<j<k} \rho_{c,ijk}(\mathbf{r}) + \dots\ , \tag{1.5}$$

$$\mathbf{j}(\mathbf{r}) = \sum_i \mathbf{j}_i(\mathbf{r}) + \sum_{i<j} \mathbf{j}_{ij}(\mathbf{r}) + \sum_{i<j<k} \mathbf{j}_{ijk}(\mathbf{r}) + \dots\ , \tag{1.6}$$

where the one-body operators $\rho_{c,i}$ and $\mathbf{j}_i$ describe the current of a free nucleon i, and the two- and three-body operators ρ_{ij}, $\mathbf{j}_{ij}$, and $\rho_{c,ijk}$, $\mathbf{j}_{ijk}$ represent the effects of the interactions v_{ij} and V_{ijk} on the charges and currents of nucleon pairs ij and triplets ijk. There are analogous expansions for the weak vector and axial vector charge and current operators.

The concept of this model is fairly old. For example, the review of nuclear physics by Bethe and Bacher in 1937 already assumes its existence. The validity of the model is based on the convergence of the series describing the interactions and currents. However, these series cannot yet be derived from QCD. The relation between nuclear forces and currents and the underlying degrees of freedom of QCD is probably the most unclear part of nuclear physics, although in the last two decades the emergence of chiral effective field theories has considerably improved our understanding of this connection.

The interactions v_{ij} and V_{ijk}, and the electroweak current operators have to be obtained from experimental data. However, in quantum mechanics these operators are not unique. Let us assume that we have a set of potentials v_{ij}, V_{ijk}, ... that explain all the relevant data using the eigenstates of the Hamiltonian of this set. We can make a unitary transformation U, and define a new set of potentials v'_{ij}, V'_{ijk}, ... and H' such that:

$$H' = UHU^\dagger = \sum_i \frac{\mathbf{p}_i^2}{2\,m_i} + \sum_i \frac{1}{2\,m_i}[U\ ,\ \mathbf{p}_i^2]\,U^\dagger + \sum_{i<j} U\,v_{ij}\,U^\dagger + \sum_{i<j<k} U\,V_{ijk}\,U^\dagger + \dots$$

$$\equiv \sum_i \frac{\mathbf{p}_i^2}{2\,m_i} + \sum_{i<j} v'_{ij} + \sum_{i<j<k} V'_{ijk} + \dots \ . \tag{1.7}$$

The current and other operators O' of the new set are given by $O' \equiv U\,O\,U^\dagger$, and $\Psi'_n \equiv U\,\Psi_n$ are the eigenstates of H' if Ψ_n are those of H.

The potentials v'_{ij}, V'_{ijk}, ... , operators O', and eigenstates Ψ'_n of the new set are as good as those of the first set, and predict the same observables. Many different sets of operators are possible; for brevity we consider only two. There is no experimental method which can be used to choose one set over the other. This choice has to be made by the theory used to describe nuclei, as for example, the choice of gauge in quantum electrodynamics. Ideally one may wish to have a theory manifestly invariant under the unitary transformations of interest, however such a theory is generally less transparent than that in which a suitable choice is made.

Using the two-body Hamiltonians

$$H_2 \equiv \frac{\mathbf{p}_{ij}^2}{2\,m_{ij}} + v_{ij}\ , \qquad H'_2 \equiv \frac{\mathbf{p}_{ij}^2}{2\,m_{ij}} + v'_{ij}\ , \tag{1.8}$$

it is possible to fit all the two-nucleon scattering data with apparently different two-body potentials. Here m_{ij} is the pp, np or nn reduced mass as needed, and $\mathbf{p}_{ij}$ is the relative momentum. The corresponding truncated Hamiltonians H_2 and H'_2, containing only the two-body potentials v_{ij} and v'_{ij}, will generally give different predictions for systems with $A \geq 3$, because the V_{ijk} and V'_{ijk} are different. In principle, the Hamiltonians H_3 and H'_3, including also the three-body potentials V_{ijk} and V'_{ijk} are equivalent in systems with $A \leq 3$. The basic model assumes that the series of two-, three-, and many-body potentials and other operators are rapidly convergent for particular choices of the set. However, this assumption has to be experimentally verified for the chosen set.

In practice, physically correct constraints can be imposed on models of nuclear (and not only nuclear) forces used to fit the data and limit their freedom via unitary transformations. Two sets of constraints have been historically used. The first set limits the ranges of components in nuclear forces using very general arguments. The second set requires the forces to have the maximum locality allowed by the data. From this perspective, for example, while the "unitary freedom" discussed above would allow one, in the case of the hydrogen atom Hamiltonian, to design a unitary transformation that makes the Coulomb potential highly nonlocal at large distances, such freedom is not considered seriously, since a strongly nonlocal Coulomb interaction between slow charges has presumably no physical reality.

Chapter 2

The Yukawa Potential

The dominant terms in nuclear forces are due to exchange of pions. These terms have a complex dependence on the spins and isospins of the interacting nucleons coming from the 0^- spin-parity and unit isospin of the pions. In this chapter we consider the simpler, spin-isospin independent, Yukawa potential due to the coupling of the interacting particles to a massive scalar field. The spins and isospins of the interacting particles are ignored for pedagogical clarity, and the main focus is on the representation of meson exchange interactions by inter-nucleon potentials.

The Yukawa potentials are defined so that the total potential energy in any static configuration of the particles equals the energy of the field in its ground state for that configuration, apart from constants independent of particle positions. The motion of the particles is neglected as, for example, in electrostatic problems. Classical and quantum treatments lead to the same potential, and we discuss the classical description first.

2.1 The Yukawa potential in classical mechanics

The classical Lagrangian density $\mathcal{L}_0(\phi, \dot{\phi}, \boldsymbol{\nabla}\phi)$ of the free scalar field $\phi(\mathbf{r}, t)$ is given by

$$\mathcal{L}_0(\phi, \dot{\phi}, \boldsymbol{\nabla}\phi) = \frac{1}{2}\left[\dot{\phi}^2(\mathbf{r}, t) - |\,\boldsymbol{\nabla}\phi(\mathbf{r}, t)\,|^2 - \mu^2\phi^2(\mathbf{r}, t)\right] \ , \tag{2.1}$$

where $\dot{\phi}(\mathbf{r}, t)$ denotes the partial derivative with respect to time of $\phi(\mathbf{r}, t)$ and μ is a parameter, to be interpreted, after quantization, as the mass of the field excitation quanta. We assume that the scalar field couples to particles numbered 1, 2, ..., A at positions $\mathbf{r}_1$, $\mathbf{r}_2$, ..., $\mathbf{r}_A$ by an additional interaction term in the Lagrangian density

$$\mathcal{L}(\phi, \dot{\phi}, \boldsymbol{\nabla}\phi) = \mathcal{L}_0(\phi, \dot{\phi}, \boldsymbol{\nabla}\phi) + \mathcal{L}_{\rm int}(\phi) \ , \tag{2.2}$$

where

$$\mathcal{L}_{\rm int}(\phi) = -g\,\phi(\mathbf{r},t)\sum_{i=1}^{A}\delta(\mathbf{r}-\mathbf{r}_i)\ , \tag{2.3}$$

and the parameter g is called the coupling constant. The Euler-Lagrange equation,

$$\frac{\partial}{\partial t}\frac{\partial\mathcal{L}}{\partial\dot{\phi}} + \boldsymbol{\nabla}\cdot\frac{\partial\mathcal{L}}{\partial(\boldsymbol{\nabla}\phi)} - \frac{\partial\mathcal{L}}{\partial\phi} = 0\ , \tag{2.4}$$

then leads to

$$\ddot{\phi}(\mathbf{r},t) - \nabla^2\phi(\mathbf{r},t) + \mu^2\phi(\mathbf{r},t) = -g\sum_{i=1}^{A}\delta(\mathbf{r}-\mathbf{r}_i)\ , \tag{2.5}$$

and the classical lowest-energy state of the field is easily calculated from the solution in the static limit, *i.e.* $\phi(\mathbf{r},t)\to\overline{\phi}(\mathbf{r})$:

$$\nabla^2\overline{\phi}(\mathbf{r}) - \mu^2\overline{\phi}(\mathbf{r}) = g\sum_{i=1}^{A}\delta(\mathbf{r}-\mathbf{r}_i)\ . \tag{2.6}$$

The solution of the above equation is a superposition of the fields of all the particles,

$$\overline{\phi}(\mathbf{r}) = \sum_{i=1}^{A}\overline{\phi}_i(\mathbf{r})\ , \tag{2.7}$$

where $\overline{\phi}_i(\mathbf{r})$ is the field of particle i at $\mathbf{r}_i$. It satisfies the equation

$$\nabla^2\overline{\phi}_i(\mathbf{r}) - \mu^2\overline{\phi}_i(\mathbf{r}) = g\,\delta(\mathbf{r}-\mathbf{r}_i)\ , \tag{2.8}$$

whose solution with the boundary condition $\overline{\phi}_i(r\to\infty)\to 0$ is

$$\overline{\phi}_i(\mathbf{r}) = -\frac{g}{4\pi}\frac{e^{-\mu|\mathbf{r}-\mathbf{r}_i|}}{|\mathbf{r}-\mathbf{r}_i|}\ . \tag{2.9}$$

We can now calculate the energy $E_{\overline{\phi}}$ of the static field, given by

$$E_{\overline{\phi}} = -\int d^3r\,\overline{\mathcal{L}}(\overline{\phi},\boldsymbol{\nabla}\overline{\phi}) = \int d^3r\left[\frac{1}{2}\left[|\,\boldsymbol{\nabla}\overline{\phi}(\mathbf{r})\,|^2 + \mu^2\overline{\phi}^2(\mathbf{r})\right] + g\,\overline{\phi}(\mathbf{r})\sum_{i=1}^{A}\delta(\mathbf{r}-\mathbf{r}_i)\right]\ . \tag{2.10}$$

After integrating by parts the $|\,\boldsymbol{\nabla}\overline{\phi}(\mathbf{r})\,|^2$ term, we obtain:

$$E_{\overline{\phi}} = \int d^3r\left[\frac{1}{2}\overline{\phi}(\mathbf{r})\left[-\nabla^2\overline{\phi}(\mathbf{r}) + \mu^2\overline{\phi}(\mathbf{r})\right] + g\,\overline{\phi}(\mathbf{r})\sum_{i=1}^{A}\delta(\mathbf{r}-\mathbf{r}_i)\right]\ , \tag{2.11}$$

which can be further reduced to the form below by using the Euler-Lagrange equation, Eq. (2.6),

$$E_{\overline{\phi}} = \frac{1}{2}\sum_{i=1}^{A} g\,\overline{\phi}(\mathbf{r}_i) \ . \tag{2.12}$$

Substituting the expressions in Eqs. (2.7) and (2.9) in the above $E_{\overline{\phi}}$ yields

$$\begin{aligned} E_{\overline{\phi}} &= -\frac{g^2}{8\pi}\sum_{i,j=1}^{A}\frac{e^{-\mu|\mathbf{r}_i-\mathbf{r}_j|}}{|\mathbf{r}_i-\mathbf{r}_j|} \\ &= -\frac{g^2}{8\pi}\sum_{i=1}^{A}\lim_{r\to 0}\frac{1}{r} - \frac{g^2}{4\pi}\sum_{i<j=1}^{A}\frac{e^{-\mu|\mathbf{r}_i-\mathbf{r}_j|}}{|\mathbf{r}_i-\mathbf{r}_j|} \ . \end{aligned} \tag{2.13}$$

The first term of the above field energy is divergent. It represents the sum of the "self-energies" of the particles due to interaction with their own scalar field. These "self-energies" are independent of the positions of the particles, and are inseparable from the energies, or equivalently the masses, of the isolated particles. The second term of $E_{\overline{\phi}}$ is a sum of pairwise Yukawa potentials defined as

$$v_Y(r_{ij}) = -\frac{g^2}{4\pi}\frac{e^{-\mu r_{ij}}}{r_{ij}} \ , \tag{2.14}$$

where we have used r_{ij} to denote $|\mathbf{r}_i - \mathbf{r}_j|$. In all low energy phenomena, in which the scalar field can be assumed to remain in its lowest energy state, we can replace its energy $E_{\overline{\phi}}$ by the sum of pairwise Yukawa potentials

$$E_{\overline{\phi}} = \sum_{i<j=1}^{A} v_Y(r_{ij}) \ , \tag{2.15}$$

by absorbing the sum of the divergent terms in the sum of the masses of the sources.

The above derivation of the Yukawa potential is very similar to the classical derivation of the Coulomb potential energy of charged particles. In rationalized Heavyside-Lorentz units the Coulomb potential between two unit charges is

$$v_C(r_{ij}) = \frac{e^2}{4\pi}\frac{1}{r_{ij}} \ . \tag{2.16}$$

The electromagnetic field is massless, *i.e.* the photons have zero rest mass, therefore the Coulomb potential does not contain the exponential factor $e^{-\mu r_{ij}}$ in the Yukawa potential. The difference in the signs of the Yukawa and Coulomb potentials is because the former is mediated by a scalar field, while the latter is mediated by a vector field.

2.2 The Yukawa potential in quantum mechanics

The quantization of the free scalar field is discussed in many textbooks. Its excitation quanta appear as particles, called scalar mesons, with spin-parity 0^+ and rest mass μ. Mesons with momentum $\mathbf{k}$ have positive energy denoted by ω_k,

$$\omega_k = \sqrt{\mu^2 + k^2} \ . \tag{2.17}$$

The quantum field operator $\hat{\phi}(\mathbf{r})$ in the Schrödinger picture is time independent, and can be represented in the following two equivalent ways:

$$\begin{aligned} \hat{\phi}(\mathbf{r}) &= \sum_{\mathbf{k}} \frac{1}{\sqrt{2\omega_k}} \left(a_{\mathbf{k}} e^{i\mathbf{k}\cdot\mathbf{r}} + a^\dagger_{\mathbf{k}} e^{-i\mathbf{k}\cdot\mathbf{r}} \right) , \\ &= \int \frac{d^3k}{(2\pi)^3} \frac{1}{\sqrt{2\omega_k}} \left(a_{\mathbf{k}} e^{i\mathbf{k}\cdot\mathbf{r}} + a^\dagger_{\mathbf{k}} e^{-i\mathbf{k}\cdot\mathbf{r}} \right) \ . \end{aligned} \tag{2.18}$$

The operators $a_{\mathbf{k}}$ and $a^\dagger_{\mathbf{k}}$ respectively annihilate and create mesons with momentum $\mathbf{k}$. Normalized plane waves $e^{i\mathbf{k}\cdot\mathbf{r}}/L^{3/2}$, satisfying periodic boundary conditions in a cubic box of volume L^3, are used in the above field operator with an implicit $L \to \infty$ limit. In this limit the sum over $\mathbf{k}$ can be replaced by the integral as in Eq. (2.18). Since physical observables do not depend upon the normalization volume, we have set $L = 1$ for brevity here and in the rest of these notes.

The mesons do not interact with each other, and the Hamiltonian of the free meson field, H_0, is a simple sum of the energies of the individual mesons. It is defined so that the vacuum, denoted by $|0\rangle$, has zero energy, and is given by

$$H_0 = \sum_{\mathbf{k}} \omega_k a^\dagger_{\mathbf{k}} a_{\mathbf{k}} \ . \tag{2.19}$$

Even though the concept of potentials has grown out of classical mechanics, they are equally useful in quantum problems in which the field stays in its ground state, and the particles are either static or slowly moving. This is because in the case of static particles quantum theory gives the same field energy as given by classical mechanics, Eq. (2.13), for the scalar field. In order to prove this important result, we note that the interaction Hamiltonian describing the coupling of the field to the particles is given by

$$H_{\rm int} = -\int d^3r \, \hat{\mathcal{L}}_{\rm int}(\hat{\phi}) = g \int d^3r \, \hat{\phi}(\mathbf{r}) \sum_{i=1}^{A} \delta(\mathbf{r} - \mathbf{r}_i) \ . \tag{2.20}$$

Using the expansion of the quantum field operator in Eq. (2.18) yields

$$H_{\rm int} = g \sum_{i=1}^{A} \sum_{\mathbf{k}} \frac{1}{\sqrt{2\omega_k}} \left(e^{i\mathbf{k}\cdot\mathbf{r}_i} a_{\mathbf{k}} + e^{-i\mathbf{k}\cdot\mathbf{r}_i} a^\dagger_{\mathbf{k}} \right) \ . \tag{2.21}$$

The full Hamiltonian $H = H_0 + H_{\rm int}$ can then be expressed as

$$\begin{aligned} H &= \sum_{\mathbf{k}} \left[\omega_k \left(a^\dagger_{\mathbf{k}} + \frac{\gamma^*_{\mathbf{k}}}{\sqrt{\omega_k}} \right) \left(a_{\mathbf{k}} + \frac{\gamma_{\mathbf{k}}}{\sqrt{\omega_k}} \right) - |\gamma_{\mathbf{k}}|^2 \right] \ , \\ &= \sum_{\mathbf{k}} \left(\omega_k \, A^\dagger_{\mathbf{k}} A_{\mathbf{k}} - |\gamma_{\mathbf{k}}|^2 \right) \ , \end{aligned} \tag{2.22}$$

where the complex function $\gamma_{\mathbf{k}}$ is defined as

$$\gamma_{\mathbf{k}} \equiv \frac{g}{\sqrt{2}\,\omega_k} \sum_{i=1}^{A} \mathrm{e}^{-i\mathbf{k}\cdot\mathbf{r}_i} \ , \tag{2.23}$$

and

$$A_{\mathbf{k}} \equiv a_{\mathbf{k}} + \frac{\gamma_{\mathbf{k}}}{\sqrt{\omega_k}} \ , \tag{2.24}$$

and similarly for $A^\dagger_{\mathbf{k}}$. The transformation $a_{\mathbf{k}}, a^\dagger_{\mathbf{k}} \to A_{\mathbf{k}}, A^\dagger_{\mathbf{k}}$ is canonical, since it preserves the commutation relations, for example $\left[A_{\mathbf{k}} \, , \, A^\dagger_{\mathbf{k}'} \right] = \left[a_{\mathbf{k}} \, , \, a^\dagger_{\mathbf{k}'} \right] = \delta_{\mathbf{k},\mathbf{k}'}$. Therefore, the spectrum of eigenvalues of H is the same as that of the unperturbed Hamiltonian H_0, but for an overall shift in the energy. In particular, for the ground-state energy of H we find

$$\begin{aligned} E_{\overline{\phi}} = -\sum_{\mathbf{k}} |\gamma_{\mathbf{k}}|^2 &= -\frac{g^2}{2} \sum_{i,j=1}^{A} \sum_{\mathbf{k}} \frac{e^{i\mathbf{k}\cdot(\mathbf{r}_i - \mathbf{r}_j)}}{\omega_k^2} \\ &= -\frac{g^2}{8\pi} \sum_{i,j=1}^{A} \frac{e^{-\mu r_{ij}}}{r_{ij}} \ , \end{aligned} \tag{2.25}$$

where use has been made of the following result

$$\sum_{\mathbf{k}} \frac{e^{i\mathbf{k}\cdot\mathbf{r}}}{\omega_k^2} = \int \frac{d^3k}{(2\pi)^3} \frac{e^{i\mathbf{k}\cdot\mathbf{r}}}{k^2 + \mu^2} = \frac{1}{4\pi} \frac{e^{-\mu r}}{r} \ . \tag{2.26}$$

Hence, in both classical and quantum theories the scalar field energy in the presence of static particles can be replaced by a sum of Yukawa potentials between the particles.

2.3 Scattering in the Born approximation

We now consider the interaction between two slowly moving particles coupled to the scalar field. In the first treatment, expecting that the field maintains its ground state during the slow motion of the particles, we replace its energy by the Yukawa potential between the two particles. The Hamiltonian of the particles is then given by

$$H = -\frac{1}{2m}(\nabla_1^2 + \nabla_2^2) + v_Y(r) \ , \tag{2.27}$$

where m is the mass of the particles, including self energies, and the first term is just the sum of their nonrelativistic kinetic energies. For simplicity, we have assumed that the particles have the same mass, however, this is not necessary. The interparticle distance is denoted by $\mathbf{r}=\mathbf{r}_1-\mathbf{r}_2$. The two-body scattering problem for this Hamiltonian can be easily solved with the phase-shift method. However, here we want to study the way in which the Yukawa potential describes meson exchange interactions. Therefore we will use perturbation theory in powers of g^2. Note that the Yukawa potential is of order g^2.

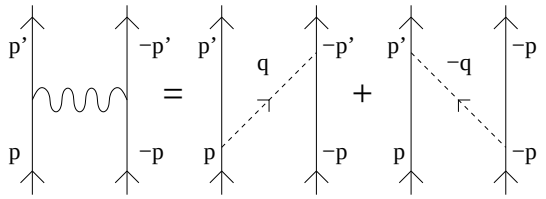

Figure 2.1: The vertical thin lines in these diagrams denote particles with indicated momenta, while the wavy and dashed lines respectively denote the Yukawa potential and the exchanged mesons. The diagrams depict terms in the perturbation theory described in the text. They can also be considered as time ordered diagrams in which time increases from bottom to up, and the potential is instantaneous. The diagram on the left represents the first order Born amplitude for the scattering by the Yukawa potential. It equals the sum of the one meson exchange amplitudes shown on the right side.

The scattering of two particles can be easily calculated from the Hamiltonian (2.27) in the Born approximation, assuming that g^2 is small. In the center-of-mass (CM) frame the particles scatter from initial momenta $\mathbf{p}_1=\mathbf{p}$, $\mathbf{p}_2=-\mathbf{p}$ to final momenta $\mathbf{p}'_1=\mathbf{p}'$, $\mathbf{p}'_2=-\mathbf{p}'$ as illustrated in Fig. 2.1. In this frame the Hamiltonian (2.27) becomes

$$H=-\frac{1}{m}\nabla^2+v_Y(r)\ , \tag{2.28}$$

and energy conservation implies

$$p^2=p'^2=m\,E\ , \tag{2.29}$$

where E is the total kinetic energy. The initial and final states before and after scattering are given, respectively, by

$$|i\rangle=e^{i\mathbf{p}\cdot\mathbf{r}}\ \text{ and }\ |f\rangle=e^{i\mathbf{p}'\cdot\mathbf{r}}\ , \tag{2.30}$$

and are eigenstates of the kinetic energy operator. The Yukawa potential $v_Y(r)$ is the perturbation. We can choose the z-axis to be in the direction of the initial relative momentum $\mathbf{p}$, and the final relative momentum $\mathbf{p}'$ to be within a solid angle $d\Omega$ around the scattering angle θ. Using Fermi's golden rule, the transition rate W_{fi} (probability of transition per unit time) from initial to final state is obtained as

$$W_{fi}=2\pi|\langle f|v_Y|i\rangle|^2\rho(E)\ , \tag{2.31}$$

where $\rho(E)$ is the density of final states

$$\rho(E) = \frac{1}{(2\pi)^3}\frac{m}{2}p' d\Omega \ , \tag{2.32}$$

and the matrix element reads

$$\begin{aligned} \langle f|v_Y|i\rangle &= \int d^3r\, e^{-i\mathbf{p}'\cdot\mathbf{r}} v_Y(r) e^{i\mathbf{p}\cdot\mathbf{r}} \\ &= \int d^3r\, v_Y(r) e^{i\mathbf{q}\cdot\mathbf{r}} \equiv \widetilde{v}_Y(q) \ , \end{aligned} \tag{2.33}$$

i.e. it equals the Fourier transform $\widetilde{v}_Y(q)$ of $v_Y(r)$ in the momentum $\mathbf{q}$,

$$\mathbf{q} = \mathbf{p} - \mathbf{p}' \ , \tag{2.34}$$

transferred by particle 1 to 2 in the collision. The scattering cross section then follows from

$$d\sigma = W_{fi}/(\text{incident flux}) \ , \tag{2.35}$$

where in the assumed unit-normalization volume the incident flux equals the relative velocity $2\,p/m$. Using Eqs. (2.31)–(2.35) and $p{=}p'$ from energy conservation, we obtain

$$\left(\frac{d\sigma}{d\Omega}\right)_{\text{Born}} = \left(\frac{m}{4\pi}\right)^2 \widetilde{v}_Y^2(q) \ . \tag{2.36}$$

For the Yukawa potential

$$\widetilde{v}_Y(q) = -\frac{g^2}{\mu^2 + q^2} \ , \tag{2.37}$$

and the scattering cross-section is:

$$\left(\frac{d\sigma}{d\Omega}\right)_{\text{Born}} = \frac{g^4}{(4\pi)^2}\frac{m^2}{\left(\mu^2 + 4p^2\sin^2\theta/2\right)^2}, \tag{2.38}$$

where, for a given scattering angle θ, the magnitude of the momentum transfer has been expressed as

$$q = 2\,p\sin\theta/2 \ . \tag{2.39}$$

The form of the cross section, Eq. (2.38), for scattering by the Yukawa potential is similar to the well known Rutherford cross-section for scattering by the Coulomb potential. In momentum space the Coulomb potential is given by

$$\widetilde{v}_C(q) = \frac{e^2}{q^2} \ , \tag{2.40}$$

and therefore

$$\left(\frac{d\sigma}{d\Omega}\right)_C = \frac{e^4}{(4\pi)^2}\frac{m^2}{16\,p^4\sin^4\theta/2} \tag{2.41}$$

is the Rutherford cross section. Since the photon has zero mass, the Rutherford cross section has $\mu = 0$. Note that when $q^2 \gg \mu^2$ the Yukawa cross section becomes similar to the Rutherford. On the other hand, when $p^2 \ll \mu^2$, it is spherically symmetric, *i.e.*, independent of θ. The Coulomb potential in Gauss units, e^2/r, differs from that in Heavyside-Lorentz units, Eq. (2.16), by a factor of 4π. The Rutherford cross section in Gauss units does not have the factor $1/(4\pi)^2$ in Eq. (2.41). Also it is well known that the Born approximation is exact for the scattering cross section by a Coulomb potential: higher order corrections only contribute an overall phase factor in the amplitude. However, the Born approximation is not exact in the general case of a Yukawa potential with $\mu \neq 0$.

2.4 One meson exchange scattering

We will now calculate the scattering cross section up to order g^4 directly from meson exchange processes without using the Yukawa potential. The initial and final states are eigenstates of the unperturbed Hamiltonian

$$H_0 = -\frac{1}{2m}\left(\nabla_1^2 + \nabla_2^2\right) + \sum_{\mathbf{k}} \omega_k\, a_{\mathbf{k}}^\dagger a_{\mathbf{k}}\ , \tag{2.42}$$

that describes free particles and mesons. The full $H{=}H_0 + H_{\rm int}$, where $H_{\rm int}$, given by Eq. (2.21), provides the coupling between particles and mesons. The first order amplitude $\langle f|H_{\rm int}|i\rangle$ vanishes, because the initial and final states have no mesons. In second order, the transition probability reads

$$W_{fi} = 2\pi\left|\sum_I \langle f|H_{\rm int}|I\rangle\frac{1}{E-E_I}\langle I|H_{\rm int}|i\rangle\right|^2 \rho(E)\ , \tag{2.43}$$

where $|I\rangle$ are intermediate states with one virtual meson, and $H_0|I\rangle{=}E_I|I\rangle$ as usual. Due to momentum conservation, the meson can only have momentum $\mathbf{q}$ or $-\mathbf{q}$ and, therefore, only two intermediate states $|I\rangle$ contribute to W_{fi}. As illustrated in Fig. 2.1, in the first, denoted by $|\mathbf{p}', -\mathbf{p}, \mathbf{q}\rangle$, particles 1, 2 and the meson have momenta $\mathbf{p}'$, $-\mathbf{p}$ and $\mathbf{q}$ respectively, while in the second $|\mathbf{p}, -\mathbf{p}', -\mathbf{q}\rangle$ they have momenta $\mathbf{p}$, $-\mathbf{p}'$ and $-\mathbf{q}$. In the CM frame $p^2{=}p'^2$, and therefore both states have

$$E_I = \frac{p^2}{m} + \omega_q\ , \tag{2.44}$$

and the energy denominator $E - E_I$ is simply $-\omega_q$. Note that this relation is exact only in the CM frame, corrections to it in other frames are part of relativistic effects. Only the

$e^{-i\mathbf{q}\cdot\mathbf{r}_1}\, a^\dagger_{\mathbf{q}}$ term in $H_{\rm int}$, Eq. (2.21), contributes to the matrix element $\langle \mathbf{p}', -\mathbf{p}, \mathbf{q}|H_{\rm int}|i\rangle$, given by

$$\langle \mathbf{p}', -\mathbf{p}, \mathbf{q}|H_{\rm int}|i\rangle = \frac{g}{\sqrt{2\omega_q}} \int d^3r_1\, d^3r_2\, e^{-i\mathbf{p}'\cdot\mathbf{r}_1} e^{-i\mathbf{q}\cdot\mathbf{r}_1} e^{i\mathbf{p}\cdot\mathbf{r}_1} e^{i\mathbf{p}\cdot\mathbf{r}_2} e^{-i\mathbf{p}\cdot\mathbf{r}_2} = \frac{g}{\sqrt{2\omega_q}}\ , \tag{2.45}$$

due our unit normalization volume. The remaining three matrix elements give the same contribution:

$$\langle \mathbf{p}, -\mathbf{p}', -\mathbf{q}|H_{\rm int}|i\rangle = \langle f|H_{\rm int}|\mathbf{p}, -\mathbf{p}', -\mathbf{q}\rangle = \langle f|H_{\rm int}|\mathbf{p}', -\mathbf{p}, \mathbf{q}\rangle = \frac{g}{\sqrt{2\,\omega_q}}\ , \tag{2.46}$$

and thus the transition rate reads

$$W_{fi} = 2\pi \left| \frac{-g^2}{\omega_q^2} \right|^2 \rho(E)\ , \tag{2.47}$$

which is the same as that obtained from the Yukawa potential since it has $\widetilde{v}_Y(q) = -g^2/\omega_q^2$.

One can consider the equality of the transition amplitudes

$$\langle f|v_Y|i\rangle \equiv \sum_I \langle f|H_{\rm int}|I\rangle \frac{1}{E - E_I} \langle I|H_{\rm int}|i\rangle\ , \tag{2.48}$$

as an alternate definition of the Yukawa potential. The diagrams of Fig. 2.1 suggest a physical interpretation of the scattering in the Born approximation. It occurs due to the absorption by particle 2 of a meson of momentum $\mathbf{q}$ emitted by 1 or by particle 1 absorbing a meson of momentum $-\mathbf{q}$ emitted by 2. The range, of order $1/\mu$, of the Yukawa potential comes from the uncertainty principle. The intermediate state $|I\rangle$ violates energy conservation by $\Delta E \sim \omega_q \sim \mu$. Hence this state can exist only for a time $\Delta t \sim 1/\mu$ during which the virtual meson can propagate through a distance of order $1/\mu$. Therefore the interaction can occur only when the inter-particle distance is of order $1/\mu$ or less. As the meson mass $\mu \to 0$ one obtains the familiar $1/r$ dependence of the Coulomb and gravitational potentials.

2.5 Two meson exchange scattering amplitude

So far we have seen that the Yukawa potential represents the interaction energy for static sources to all orders in the coupling constant g, and the one meson exchange interaction between moving particles. However, when the coupling constant g is large, the particles can exchange many mesons during the scattering. In this case the lowest order one-meson exchange contribution may not provide a good approximation to the total scattering amplitude. In this section we consider the two-meson exchange contribution to the scattering amplitude to further examine the limitations of representing meson exchange interactions by potentials.

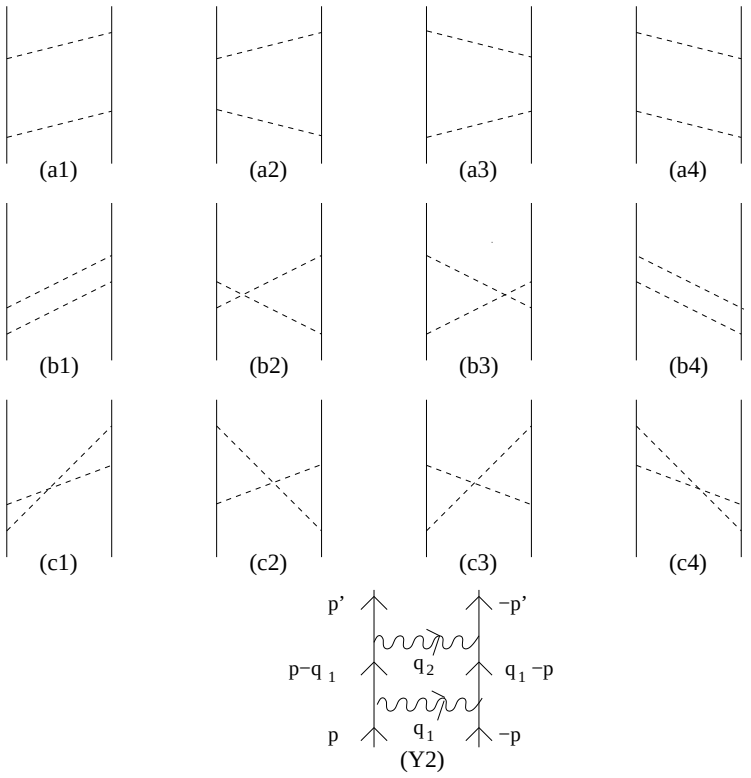

Figure 2.2: Diagrams a1-a4, b1-b4 and c1-c4 show all the two-meson exchange processes that contribute to the scattering of two particles. The second order Yukawa potential amplitude shown by diagram Y2 provides an approximation to the sum of the twelve two-meson exchange amplitudes. This approximation becomes exact for slowly moving particles.

The second order Yukawa potential contribution to scattering is illustrated in diagram $Y2$ of Fig. 2.2. It contains two consecutive momentum transfers, $\mathbf{q}_1$ and $\mathbf{q}_2$, from particle 1 to 2, with a two-particle intermediate state $|I\rangle$. Its contribution to the scattering amplitude is denoted as $A_Y^{(2)}(\mathbf{q}_1, \mathbf{q}_2)$, and reads

$$A_Y^{(2)}(\mathbf{q}_1, \mathbf{q}_2) = \langle f|v_Y|I\rangle \frac{1}{E - E_I} \langle I|v_Y|i\rangle = \frac{-g^4}{\omega_{q_1}^2 \omega_{q_2}^2} \frac{1}{2\,\delta_1} \ , \tag{2.49}$$

where we have defined the energy denominator

$$2\,\delta_1 = E_I - E = \frac{1}{m}\left(q_1^2 - 2\,\mathbf{p}\cdot\mathbf{q}_1\right) \ . \tag{2.50}$$

In terms of meson exchanges this amplitude is given by the sum of all processes in which the first meson with momentum $\mathbf{q}_1$ ($-\mathbf{q}_1$) emitted by particle 1 (2) is absorbed by 2 (1), and

a second meson with momentum $\mathbf{q}_2$ ($-\mathbf{q}_2$) emitted next by 1 (2) is absorbed by 2 (1). The twelve possible processes are shown by diagrams a_1 to c_4 in Fig. 2.2. In processes a_1 to a_4, the second meson is emitted after the first is absorbed, while in b_1 to c_4 it is emitted before. In b_1 to b_4 (c_1 to c_4), the second is absorbed after (before) the first.

The contributions of two-meson exchange diagrams to the scattering amplitude follow from

$$\langle f|H_{\rm int}|I_3\rangle\frac{1}{E-E_{I_3}}\langle I_3|H_{\rm int}|I_2\rangle\frac{1}{E-E_{I_2}}\langle I_2|H_{\rm int}|I_1\rangle\frac{1}{E-E_{I_1}}\langle I_1|H_{\rm int}|i\rangle\ , \tag{2.51}$$

where the intermediate states $|I_1\rangle$, $|I_2\rangle$ and $|I_3\rangle$ can be read off the diagrams a_1 to c_4. The calculation of the sum of two-meson exchange contributions is rather simple. We define δ_2 similarly to δ_1 but with $\mathbf{q}_2$ replacing $\mathbf{q}_1$, and note that in all the diagrams a_1 to c_4 the product of the matrix elements of $H_{\rm int}$ is given by $g^4/(4\,\omega_{q_1}\omega_{q_2})$. We obtain

$$\begin{aligned} A_M^{(2)}(\mathbf{q}_1,\mathbf{q}_2) \;=\; & -\frac{g^4}{4\,\omega_{q_1}\omega_{q_2}}\Bigg\{\frac{4}{2\,\delta_1\,(\delta_1+\omega_{q_2})(\delta_1+\omega_{q_1})}+\frac{2}{(\delta_1+\omega_{q_2})(\omega_{q_1}+\omega_{q_2})(\delta_1+\omega_{q_1})} \\ & +\left[\frac{1}{(\delta_2+\omega_{q_2})(\omega_{q_1}+\omega_{q_2}+\delta_1+\delta_2)(\delta_2+\omega_{q_1})}+(\mathbf{q}_1\rightleftharpoons\mathbf{q}_2)\right] \\ & +\left[\frac{1}{(\delta_1+\omega_{q_1})(\omega_{q_1}+\omega_{q_2})(\delta_2+\omega_{q_1})}+(\mathbf{q}_1\rightleftharpoons\mathbf{q}_2)\right] \\ & +\left[\frac{1}{(\delta_1+\omega_{q_2})(\omega_{q_1}+\omega_{q_2}+\delta_1+\delta_2)(\delta_2+\omega_{q_2})}+(\mathbf{q}_1\rightleftharpoons\mathbf{q}_2)\right]\Bigg\}\ , \end{aligned} \tag{2.52}$$

where diagrams a_1 to a_4, and b_1 and b_4, give the contributions on the first line, diagrams b_2 and b_3, c_1 and c_4, and c_2 and c_3, give the contributions on the second, third, and fourth line of Eq. (2.52), respectively. In the static limit (m large), $\delta_i \ll \omega_{q_1}$ or ω_{q_2} and we may expand the two-meson exchange scattering amplitude in powers of δ_i/ω_q, which gives

$$A_M^{(2)}(\mathbf{q}_1,\mathbf{q}_2) \simeq A_Y^{(2)}(\mathbf{q}_1,\mathbf{q}_2) \text{ up to terms quadratic in } \delta_i\ . \tag{2.53}$$

The processes a_1–a_4 are called meson exchange ladders. In these processes we have intermediate states without mesons as in the second order Yukawa potential scattering diagram $Y2$ of Fig. 2.2. The scattering amplitude in the meson exchange ladder approximation is denoted by $A_{MEL}^{(2)}(\mathbf{q}_1,\mathbf{q}_2)$. Summing the contributions of processes a_1–a_4 leads, in the static limit, to

$$A_{MEL}^{(2)}(\mathbf{q}_1,\mathbf{q}_2) = A_M^{(2)}(\mathbf{q}_1,\mathbf{q}_2)\left[1-\frac{\delta_1(\omega_{q_1}+\omega_{q_2})}{\omega_{q_1}\omega_{q_2}}+...\right]\ , \tag{2.54}$$

where the ellipsis represent terms quadratic in δ_1. In this respect, the Yukawa potential provides a better approximation to the full two-meson exchange scattering amplitude than the meson exchange ladder approximation.

2.6 Corrections to the Yukawa potential

All two meson exchange processes in which $\mathbf{q}_1+\mathbf{q}_2=\mathbf{q}$ contribute to the scattering amplitude with momentum transfer $\mathbf{q}$. Thus the error in the Yukawa potential approximation of the two-meson scattering amplitude is given by

$$D^{(2)}(\mathbf{p},\mathbf{q}) = \int \frac{d^3q_1}{(2\pi)^3}\left[A_M^{(2)}(\mathbf{q}_1,\mathbf{q}_2=\mathbf{q}-\mathbf{q}_1) - A_Y^{(2)}(\mathbf{q}_1,\mathbf{q}_2=\mathbf{q}-\mathbf{q}_1)\right] . \tag{2.55}$$

This error depends on both $\mathbf{p}$ and $\mathbf{q}$ through δ_i and ω_{q_2}. We can define a two-meson exchange potential $v^{(2)}$ such that

$$\langle f|v^{(2)}|i\rangle = D^{(2)}(\mathbf{p},\mathbf{q}) , \tag{2.56}$$

and the two-body potential

$$v = v_Y + v^{(2)} \tag{2.57}$$

then offers a better approximation than the Yukawa; it correctly reproduces the one- and two-meson exchange contributions to the scattering amplitude. Unlike the v_Y potential, $v^{(2)}$ depends upon both $\mathbf{p}$ and $\mathbf{q}$. We can either consider it as a momentum dependent interaction, or as a nonlocal interaction $v^{(2)}(\mathbf{r}',\mathbf{r})$, defined as

$$v^{(2)}(\mathbf{r}',\mathbf{r}) = \int \frac{d^3p}{(2\pi)^3}\frac{d^3q}{(2\pi)^3} e^{i\mathbf{p}\cdot(\mathbf{r}'-\mathbf{r})} e^{-i\mathbf{q}\cdot\mathbf{r}'} D^{(2)}(\mathbf{p},\mathbf{q}) . \tag{2.58}$$

We should note that relativistic effects also generate momentum dependent and nonlocal interactions.

By carrying out this process further we can define $l \geq 2$ meson exchange potentials $v^{(l)}$ such that the scattering amplitude obtained by using the two-body potential

$$v = v_Y + \sum_{l=2}^{n} v^{(l)} , \tag{2.59}$$

correctly reproduces the sum of all amplitudes having up to n exchanged mesons and provides a good approximation for those having more than n exchanged mesons. This procedure is obviously useful when the potentials $v^{(l)}$ become smaller as l increases. The $v^{(l)}$ is proportional to g^{2l}, and thus the series converges trivially when the coupling constant g is small. It also converges when the mass of the interacting particles is large because of the $1/m$ factors contained in the $v^{(l)}$. The ranges of the $v^{(l)}$ are proportional to $1/(l\mu)$. Thus the $v^{(l)}$ form a series of interactions with decreasing ranges.

The above discussion of the two-meson exchange potential is not directly applicable to nuclear forces. It is applicable when the particles and fields are elementary. However, both nucleons and mesons are composite objects with internal degrees of freedom and excitations,

therefore many additional processes (some of which are discussed in the next chapter), contribute to the $D^{(2)}$ amplitude. Models of the interaction potential v_{ij} between nucleons i and j are obtained by reproducing the observed two-nucleon scattering data, which naturally contain all possible many-meson exchange amplitudes. In contrast, the corrections to the Coulomb interaction between electrons due to two-photon exchange processes can be calculated using the techniques presented above, since the electrons and photons are elementary particles without internal degrees of freedom.

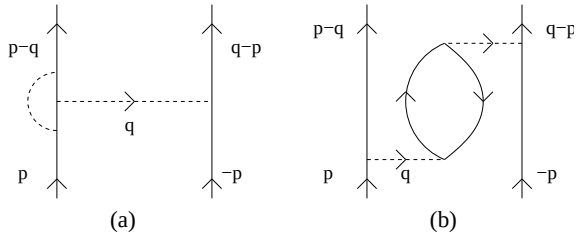

Figure 2.3: Diagrams (a) and (b) respectively show the vertex and vacuum polarization corrections to the one meson exchange interaction between elementary particles.

2.7 Vertex corrections and vacuum polarization

Additional corrections to the Yukawa potential, of order g^4, are obtained from vertex corrections and vacuum polarization diagrams shown in Fig. 2.3. These corrections change the shape of the Yukawa potential at small r, and are important in both quantum electro- and chromo-dynamics. Their role in shaping nuclear forces is not obvious. Nucleons and mesons have a finite size. The short distance behavior of meson exchange interactions between nucleons is modified by their size and internal structure. It is likely that only the long-range parts of nuclear forces can be conveniently described as due to exchange of mesons. In practice, the short range interaction between nucleons is obtained from experimental data along with the two-pion exchange interaction.

Chapter 3

Pion-Exchange Interactions

Pions are the lightest of all the mesons, and thus responsible for the longest range part of the strong forces among nucleons. Their existence as the carriers of nuclear forces was predicted by Yukawa in 1935, and they were first observed in 1947. There is strong evidence for the existence of the one-pion-exchange potential in the nucleon-nucleon experimental scattering data, and pion-exchange interactions can account for much of the potential energy of light nuclei, and possibly all nuclei.

3.1 Pion-nucleon coupling

Pions are pseudoscalar mesons with spin-parity assignment 0^-, and their three charge states, π^+, π^0, π^-, are regarded as members of an isospin t=1 triplet with t_z=+1, 0, –1, respectively. The masses of the charged pions, m_{π^+}=m_{π^-}=139.57 MeV, are a bit larger than the neutral pion mass m_{π^0}=134.98 MeV. This small mass difference is presumably due to electromagnetic forces which violate the isospin symmetry of the strong interaction. To begin with, we ignore this difference along with that between the neutron and proton mass (939.57 MeV and 938.27 MeV, respectively), and use m_π and m_N to denote the average pion and nucleon mass, and assume isospin symmetry; its breaking is considered later in Sec. 3.16.

It is convenient to express the pion field operator $\hat{\boldsymbol{\phi}}(\mathbf{r})$ as a vector in isospin space with three "Cartesian" components a=x, y, z:

$$\hat{\phi}_a(\mathbf{r}) = \sum_{\mathbf{k}} \frac{1}{\sqrt{2\omega_k}} \left(a_{\mathbf{k}\,a} e^{i\mathbf{k}\cdot\mathbf{r}} + a^\dagger_{\mathbf{k}\,a} e^{-i\mathbf{k}\cdot\mathbf{r}} \right) \ . \tag{3.1}$$

The annihilation operators of the charged and neutral pions are related to the Cartesian $a_{\mathbf{k}\,a}$'s in the above field operator by

$$a_{\mathbf{k}\pm} = \frac{1}{\sqrt{2}} \left(a_{\mathbf{k}\,x} \mp i\, a_{\mathbf{k}\,y} \right) \ , \qquad a_{\mathbf{k}\,0} = a_{\mathbf{k}\,z} \ , \tag{3.2}$$

and the charged and neutral pion field operators are defined as

$$\hat{\phi}_{\pm}(\mathbf{r}) = \frac{1}{\sqrt{2}}\left[\hat{\phi}_x(\mathbf{r}) \pm i\,\hat{\phi}_y(\mathbf{r})\right] = \sum_{\mathbf{k}} \frac{1}{\sqrt{2\omega_k}}\left(a_{\mathbf{k}\mp} e^{i\mathbf{k}\cdot\mathbf{r}} + a^{\dagger}_{\mathbf{k}\pm} e^{-i\mathbf{k}\cdot\mathbf{r}}\right) , \tag{3.3}$$

$$\hat{\phi}_0(\mathbf{r}) = \hat{\phi}_z(\mathbf{r}) , \tag{3.4}$$

so that $\hat{\phi}_{+,0,-}$ create $\pi^{+,0,-}$ or annihilate $\pi^{-,0,+}$, respectively.

The spin 1/2 and isospin 1/2 operators of the nucleon are denoted as $\mathbf{s}$ and $\mathbf{t}$ with $\mathbf{s} = \boldsymbol{\sigma}/2$ and $\mathbf{t} = \boldsymbol{\tau}/2$, where $\boldsymbol{\sigma}$ and $\boldsymbol{\tau}$ are Pauli matrices operating in configuration and isospin space, respectively. The isospin matrices are taken as

$$\tau_x = \begin{pmatrix} 0 & 1 \\ 1 & 0 \end{pmatrix} , \qquad \tau_y = \begin{pmatrix} 0 & -i \\ i & 0 \end{pmatrix} , \qquad \tau_z = \begin{pmatrix} 1 & 0 \\ 0 & -1 \end{pmatrix} , \tag{3.5}$$

and proton and neutron states, defined as

$$|p\rangle = \begin{pmatrix} 1 \\ 0 \end{pmatrix} , \qquad |n\rangle = \begin{pmatrix} 0 \\ 1 \end{pmatrix} , \tag{3.6}$$

are eigenstates of τ_z (or, equivalently, t_z) corresponding to eigenvalues ± 1 ($\pm 1/2$), respectively.

The matrices above also represent the Pauli spin matrices σ_x, σ_y, and σ_z in the basis that makes σ_z diagonal. Its eigenstates, correspoding to eigenvalues ± 1 (or $\pm 1/2$ of s_z), are denoted as $|\uparrow\rangle$ and $|\downarrow\rangle$, and are defined in analogy to Eq. (3.6); they are called Pauli spinors. Thus the four possible spin-isospin states of a nucleon are $|\uparrow p\rangle$, $|\downarrow p\rangle$, $|\uparrow n\rangle$, and $|\downarrow n\rangle$.

The operator $\boldsymbol{\tau}\cdot\hat{\boldsymbol{\phi}}$, defined as (the $\mathbf{r}$-dependence is suppressed here for brevity)

$$\begin{aligned} \hat{\boldsymbol{\phi}}\cdot\boldsymbol{\tau} &= \hat{\phi}_x\tau_x + \hat{\phi}_y\tau_y + \hat{\phi}_z\tau_z \\ &= \hat{\phi}_+\tau_- + \hat{\phi}_-\tau_+ + \hat{\phi}_0\tau_0 , \end{aligned} \tag{3.7}$$

with

$$\tau_{\pm} = \frac{1}{\sqrt{2}}\left(\tau_x \pm i\,\tau_y\right) , \qquad \tau_0 = \tau_z , \tag{3.8}$$

being a scalar in isospin space, conserves the total isospin of the pion-nucleon system, and therefore its total charge. Note that the operators τ_+ and τ_- change neutrons into protons and viceversa, *i.e.*

$$\tau_+|p\rangle = 0 , \qquad \tau_+|n\rangle = \sqrt{2}|p\rangle , \qquad \tau_-|n\rangle = 0 , \qquad \tau_-|p\rangle = \sqrt{2}|n\rangle , \tag{3.9}$$

and hence the combination $\hat{\phi}_+\tau_-$ ($\hat{\phi}_-\tau_+$) in Eq. (3.7) either creates a π^+ (π^-) or annihilates a π^- (π^+) while converting a proton (neutron) into a neutron (proton). The combination $\hat{\phi}_0\tau_z$, instead, creates or annihilates a π^0 without changing the nucleon charge.

The interaction of the pion field with a nonrelativistic nucleon at position $\mathbf{r}$ is described by the interaction Hamiltonian

$$H_{\pi NN} = -\frac{f_{\pi NN}}{m_\pi}\boldsymbol{\sigma}\cdot\left[\boldsymbol{\nabla}\hat{\boldsymbol{\phi}}(\mathbf{r})\cdot\boldsymbol{\tau}\right] \ , \tag{3.10}$$

where $f_{\pi NN}$ is the dimensionless pion-nucleon coupling constant. Note that the field $\hat{\phi}$ has dimensions of energy and $\boldsymbol{\nabla}/m_\pi$ is dimensionless. The $H_{\pi NN}$ is a scalar in configuration space, since it contains a dot-product of two pseudo-vectors, $\boldsymbol{\sigma}$ and $\boldsymbol{\nabla}\hat{\boldsymbol{\phi}}(\mathbf{r})\cdot\boldsymbol{\tau}$. It is also a scalar in isospin space, and thus the $H_{\pi NN}$ interaction conserves momentum, angular momentum, parity, and isospin.

Let the nucleon be at the origin so that $H_{\pi NN}$ contains the term $\boldsymbol{\nabla}\hat{\phi}_a(\mathbf{r})$ evaluated at $\mathbf{r}$=0. The plane waves in the pion field operator, Eq. (3.1), can be expanded in eigenfunctions of angular momentum:

$$e^{i\mathbf{k}\cdot\mathbf{r}} = 4\pi\sum_{l=0}^{\infty}\sum_{m=-l}^{l} i^l\, Y^*_{lm}(\theta_k,\phi_k)\, j_l(kr)\, Y_{lm}(\theta,\phi) \ , \tag{3.11}$$

where θ_k, ϕ_k and θ, ϕ are the polar angles of $\mathbf{k}$ and $\mathbf{r}$, respectively. Only the $l = 1$ pion waves, called P-waves in spectroscopic notation, have a finite gradient at the origin, and thus $H_{\pi NN}$ describes the absorption and emission of pions having a unit orbital angular momentum about the nucleon. These pions have even overall parity, since the intrinsic negative parity of pions combines with the negative parity of P-waves.

Since angular momentum and parity are conserved by the strong interaction, only the l=1 π-N state can couple to the nucleon. Conservation of parity requires l be odd, and for $l > 1$ the total angular momentum cannot be 1/2. Therefore, in the limit $k \to 0$ all allowed strong pion-nucleon coupling Hamiltonians reduce to the form given in Eq. (3.10). The most general nonrelativistic $H_{\pi NN}$ is obtained by allowing $f_{\pi NN}$ to depend on the pion momentum k. In relativistic theories the π-N coupling is not unique.

3.2 The one pion-exchange potential

The one-pion-exchange potential (OPEP) between two nucleons, denoted by v^π, can be easily calculated from the one-pion-exchange scattering amplitude as discussed in Sec. 2.4. The two diagrams contributing to this amplitude are as shown in Fig. 2.1. Thus, Eq. (2.48) for the scalar-meson-exchange Yukawa potential reads

$$\langle f|v^\pi|i\rangle \equiv \sum_I \langle f|H_{\pi NN}|I\rangle \frac{1}{E-E_I}\langle I|H_{\pi NN}|i\rangle, \tag{3.12}$$

in the case of OPEP. The main difference is that $H_{\pi NN}$ contains spin, isospin, and gradient operators absent in the simple $H_{\rm int}$ considered in Chapter 2.

We denote the initial and final two-nucleon states by

$$|i\rangle = |\mathbf{p}, \chi_1; -\mathbf{p}, \chi_2\rangle \ , \qquad |f\rangle = |\mathbf{p}', \chi_1'; -\mathbf{p}', \chi_2'\rangle \ , \tag{3.13}$$

where χ_1,χ_2 and χ_1',χ_2' represent the spin-isospin states of nucleons 1 and 2, before and after scattering. In the first process shown in Fig. 2.1, a pion of momentum $\mathbf{q} = \mathbf{p} - \mathbf{p}'$ and charge α=+, 0 or – is emitted by nucleon 1. In this case, the intermediate state $|I\rangle$ is given by

$$|I\rangle = |\mathbf{p}', \chi_1'; -\mathbf{p}, \chi_2; \mathbf{q}, \alpha\rangle \ , \tag{3.14}$$

and the matrix element

$$\langle I|H_{\pi NN}|i\rangle = i\frac{f_{\pi NN}}{m_\pi}\frac{1}{\sqrt{2\omega_q}}\langle\chi_1'|\boldsymbol{\sigma}_1\cdot\mathbf{q}\,\tau_{1,-\alpha}|\chi_1\rangle \tag{3.15}$$

is obtained by noting that here the gradient in $H_{\pi NN}$ operates on the coefficient $e^{-i\mathbf{q}\cdot\mathbf{r}_1}$ of the pion creation operator in $\hat{\phi}_\alpha(\mathbf{r}_1)$, and that the isospin operator $\tau_{1,-\alpha}$ accompanies the creation of a pion of charge α by nucleon 1. The spatial integrals over $\mathbf{r}_1$ and $\mathbf{r}_2$ give unit factors due to our unit normalization volume. The second matrix element is given by

$$\langle f|H_{\pi NN}|I\rangle = -i\frac{f_{\pi NN}}{m_\pi}\frac{1}{\sqrt{2\omega_q}}\langle\chi_2'|\boldsymbol{\sigma}_2\cdot\mathbf{q}\,\tau_{2,\alpha}|\chi_2\rangle \ , \tag{3.16}$$

since here the gradient in $H_{\pi NN}$ operates on the coefficient $e^{i\mathbf{q}\cdot\mathbf{r}_2}$ of the annihilation operator, and the isospin operator $\tau_{2,\alpha}$ goes along with the absorption of a pion of charge α by nucleon 2. The energy denominator in Eq. (3.12) is just $-\omega_q$, and thus the contribution of the first process to the scattering amplitude is

$$-\frac{f_{\pi NN}^2}{m_\pi^2}\frac{1}{2\,\omega_q^2}\langle\chi_1', \chi_2'|\boldsymbol{\sigma}_2\cdot\mathbf{q}\,\boldsymbol{\sigma}_1\cdot\mathbf{q}\,\left(\tau_{2,+}\tau_{1,-} + \tau_{2,0}\tau_{1,0} + \tau_{2,-}\tau_{1,+}\right)|\chi_1, \chi_2\rangle \ , \tag{3.17}$$

where the three isospin terms are associated with π^+-, π^0-, and π^--exchange, respectively. Note that

$$\boldsymbol{\tau}_1\cdot\boldsymbol{\tau}_2 = \tau_{2,+}\tau_{1,-} + \tau_{2,0}\tau_{1,0} + \tau_{2,-}\tau_{1,+} \ , \tag{3.18}$$

and that the second process, in which the exchanged pion has momentum $-\mathbf{q}$, leads to an identical contribution to the scattering amplitude. Thus, from the total scattering amplitude, we define the momentum-space OPEP as

$$\widetilde{v}_{12}^{\pi}(\mathbf{q}) = -\frac{f_{\pi NN}^2}{m_\pi^2}\frac{\boldsymbol{\sigma}_1\cdot\mathbf{q}\,\boldsymbol{\sigma}_2\cdot\mathbf{q}}{q^2+m_\pi^2}\boldsymbol{\tau}_1\cdot\boldsymbol{\tau}_2 \ , \tag{3.19}$$

i.e. as an operator acting in the spin-isospin space of the two nucleons.

The configuration space $v_{12}^{\pi}(\mathbf{r})$ is obtained from the Fourier transform

$$\begin{aligned} v_{12}^{\pi}(\mathbf{r}) = \int \frac{d^3q}{(2\pi)^3} e^{-i\mathbf{q}\cdot\mathbf{r}}\, \widetilde{v}_{12}^{\pi}(\mathbf{q}) &= \frac{f_{\pi NN}^2}{m_\pi^2} \boldsymbol{\tau}_1\cdot\boldsymbol{\tau}_2\, \boldsymbol{\sigma}_1\cdot\boldsymbol{\nabla}\, \boldsymbol{\sigma}_2\cdot\boldsymbol{\nabla} \int \frac{d^3q}{(2\pi)^3} \frac{e^{-i\mathbf{q}\cdot\mathbf{r}}}{q^2+m_\pi^2} \\ &= \frac{f_{\pi NN}^2}{m_\pi^2} \boldsymbol{\tau}_1\cdot\boldsymbol{\tau}_2\, \boldsymbol{\sigma}_1\cdot\boldsymbol{\nabla}\, \boldsymbol{\sigma}_2\cdot\boldsymbol{\nabla} y_\pi(r)\ . \end{aligned} \tag{3.20}$$

The Laplacian, $\nabla^2 y_\pi(r)$, of the Yukawa function,

$$y_\pi(r) = \int \frac{d^3q}{(2\pi)^3} \frac{e^{-i\mathbf{q}\cdot\mathbf{r}}}{q^2+m_\pi^2} = \frac{e^{-m_\pi r}}{4\pi\, r}\ , \tag{3.21}$$

has a δ-function singularity at the origin, since

$$\left(-\nabla^2 + m_\pi^2\right) y_\pi(r) = \delta(\mathbf{r})\ . \tag{3.22}$$

Gradients in Eq. (3.20) have to be evaluated retaining this singularity. To this end, it is first convenient to express the derivatives in the form

$$\boldsymbol{\sigma}_1\cdot\boldsymbol{\nabla}\ \boldsymbol{\sigma}_2\cdot\boldsymbol{\nabla} = \sigma_{1,a}\sigma_{2,b}\left[\left(\nabla_a\nabla_b - \frac{\delta_{a,b}}{3}\nabla^2\right) + \frac{\delta_{a,b}}{3}\nabla^2\right]\ , \tag{3.23}$$

where the sum over the repeated indices $a, b{=}x, y, z$ is understood, and then note that

$$\left(\nabla_a\nabla_b - \frac{\delta_{a,b}}{3}\nabla^2\right) y_\pi(r) = -\int \frac{d^3q}{(2\pi)^3} \left(q_a q_b - \frac{\delta_{a,b}}{3} q^2\right) \frac{e^{-i\mathbf{q}\cdot\mathbf{r}}}{q^2+m_\pi^2}\ . \tag{3.24}$$

The expression in parenthesis on the r.h.s. of the equation above is a symmetric and traceless second-rank tensor, whose integral over the polar angles θ_q, ϕ_q is zero. After expanding the plane wave in eigenfunctions of angular momentum using Eq. (3.11)—or rather its complex conjugate—the contribution proportional to $j_0(qr)$, which is responsible for the δ-function singularity in $\nabla^2 y_\pi(r)$, is found to vanish. Thus, we obtain:

$$\begin{aligned} \boldsymbol{\sigma}_1\cdot\boldsymbol{\nabla}\, \boldsymbol{\sigma}_2\cdot\boldsymbol{\nabla} y_\pi(r) &= \left(\boldsymbol{\sigma}_1\cdot\hat{\mathbf{r}}\ \boldsymbol{\sigma}_2\cdot\hat{\mathbf{r}} - \frac{1}{3}\boldsymbol{\sigma}_1\cdot\boldsymbol{\sigma}_2\right)\left(m_\pi^2 + \frac{3m_\pi}{r} + \frac{3}{r^2}\right) y_\pi(r) \\ &+ \frac{1}{3}\boldsymbol{\sigma}_1\cdot\boldsymbol{\sigma}_2\left[m_\pi^2\, y_\pi(r) - \delta(\mathbf{r})\right]\ , \end{aligned} \tag{3.25}$$

where $\hat{\mathbf{r}}$ denotes the unit vector $\mathbf{r}/r$ and in the second line use has been made of Eq. (3.22).

The OPEP can now be cast in its standard form,

$$v_{12}^{\pi}(\mathbf{r}) = \frac{f_{\pi NN}^2}{4\pi}\frac{m_\pi}{3}\boldsymbol{\tau}_1\cdot\boldsymbol{\tau}_2 \left\{T_\pi(r) S_{12} + \left[Y_\pi(r) - \frac{4\pi}{m_\pi^3}\delta(\mathbf{r})\right]\boldsymbol{\sigma}_1\cdot\boldsymbol{\sigma}_2\right\}\ , \tag{3.26}$$

by defining the tensor operator S_{12},

$$S_{12} = 3\,\boldsymbol{\sigma}_1 \cdot \hat{\mathbf{r}}\,\boldsymbol{\sigma}_2 \cdot \hat{\mathbf{r}} - \boldsymbol{\sigma}_1 \cdot \boldsymbol{\sigma}_2 \ , \tag{3.27}$$

and the dimensionless functions $Y_\pi(r)$ and $T_\pi(r)$,

$$Y_\pi(r) = \frac{e^{-m_\pi r}}{m_\pi r} \ , \tag{3.28}$$

$$T_\pi(r) = \left(1 + \frac{3}{m_\pi r} + \frac{3}{{m_\pi}^2 r^2}\right) Y_\pi(r) \ . \tag{3.29}$$

The OPEP has a range of $1/m_\pi \sim 1.4$ fm. Within this range $(m_\pi r) < 1$, and the function $T_\pi(r)$ is larger than $Y_\pi(r)$ by a factor > 7. The tensor part of OPEP, proportional to the operator S_{12}, is therefore much larger than its Yukawa part with the $Y_\pi(r)$ radial dependence. The volume integral of the Yukawa function,

$$\int d^3r\, Y_\pi(r) = \frac{4\pi}{{m_\pi}^3} \ , \tag{3.30}$$

equals the strength of the contact interaction containing the $\delta(\mathbf{r})$ function. Therefore the volume integral of the $\boldsymbol{\sigma}_1 \cdot \boldsymbol{\sigma}_2$ term, *i.e.* the spin-spin interaction, vanishes.

3.3 Properties of the tensor operator

The Pauli identity, valid for any two vectors or vector operators $\mathbf{A}$ and $\mathbf{B}$,

$$\boldsymbol{\sigma} \cdot \mathbf{A}\,\boldsymbol{\sigma} \cdot \mathbf{B} = \mathbf{A} \cdot \mathbf{B} \ + i\boldsymbol{\sigma} \cdot \mathbf{A} \times \mathbf{B} \tag{3.31}$$

where a 2×2 unit matrix multiplying the scalar product on the r.h.s. is not explicitly indicated, can be used to derive the following two useful properties of the tensor operator S_{12}:

$$\boldsymbol{\sigma}_1 \cdot \boldsymbol{\sigma}_2\, S_{12} = S_{12}\, \boldsymbol{\sigma}_1 \cdot \boldsymbol{\sigma}_2 = S_{12} \ , \tag{3.32}$$

$$S_{12}^2 = 6 + 2\,\boldsymbol{\sigma}_1 \cdot \boldsymbol{\sigma}_2 \ - 2\,S_{12} \ . \tag{3.33}$$

From the first of these it also follows that

$$[S_{12}\,,\, \boldsymbol{\sigma}_1 \cdot \boldsymbol{\sigma}_2] = 0 \ . \tag{3.34}$$

Let S (not to be confused with the tensor operator S_{12}) denote the total spin of the two interacting nucleons. It can have values 0 and 1, and the projection operators for these two-nucleon spin states are given by:

$$P_{S=0} = \frac{1}{4}\,(1 - \boldsymbol{\sigma}_1 \cdot \boldsymbol{\sigma}_2) \ , \tag{3.35}$$

$$P_{S=1} = \frac{1}{4}\,(3 + \boldsymbol{\sigma}_1 \cdot \boldsymbol{\sigma}_2) \ . \tag{3.36}$$

They obey the standard projection operator relations,

$$P_{S=0} + P_{S=1} = 1 \ , \tag{3.37}$$

$$P_S \, P_{S'} = P_S \, \delta_{S,S'} \ , \tag{3.38}$$

and Eqs. (3.32) and (3.34) then imply

$$[P_S \, , \, S_{12}] = 0 \ , \qquad S_{12} \, P_0 = 0 \ , \qquad S_{12} \, P_1 = S_{12} \ . \tag{3.39}$$

The tensor force thus acts only in the S=1 (spin-triplet) states; it is zero in the S=0 (singlet) state.

3.4 One pion-exchange potential in pair spin-isospin channels

The one pion-exchange potential (OPEP) is not spherically symmetric. The expectation value of the tensor operator for two parallel-spin nucleons at distance $\mathbf{r}$ is given by

$$\langle \uparrow, \uparrow | S_{12} | \uparrow, \uparrow \rangle = 3 \cos^2\theta - 1 = 2 \, P_2(\cos\theta) \ , \tag{3.40}$$

where θ is the polar angle between $\mathbf{r}$, the z-axis used to quantize the spin projections, and $P_2(x)$ is the Legendre polynomial of order 2. The expectation values are independent of the azimuthal angle φ of $\mathbf{r}$. Using this result, we obtain:

$$\langle S, M = 1, \pm 1; \mathbf{r} | v^\pi | S, M = 1, \pm 1; \mathbf{r} \rangle = \frac{f^2_{\pi NN}}{4\pi} \frac{m_\pi}{3} \boldsymbol{\tau}_1 \cdot \boldsymbol{\tau}_2 \left[2 \, T_\pi(r) \, P_2(\cos\theta) + Y_\pi(r) - \frac{4\pi}{m_\pi^3} \delta(\mathbf{r}) \right] \ . \tag{3.41}$$

In the $|S, M = 0\rangle$ state the OPEP expectation value is given by

$$\langle S, M = 1, 0; \mathbf{r} | v^\pi | S, M = 1, 0; \mathbf{r} \rangle = \frac{f^2_{\pi NN}}{4\pi} \frac{m_\pi}{3} \boldsymbol{\tau}_1 \cdot \boldsymbol{\tau}_2 \left[-4 \, T_\pi(r) \, P_2(\cos\theta) + Y_\pi(r) - \frac{4\pi}{{m_\pi}^3} \delta(\mathbf{r}) \right] . \tag{3.42}$$

At finite values of r, the sign of the expectation value is dominated by that of the tensor potential, since $T_\pi(r) > Y_\pi(r)$.

The potential is symmetric under $\mathbf{r} \to -\mathbf{r}$ ($\theta \to \pi - \theta$ and $\varphi \to \varphi + \pi$), and as a function of θ it has maxima or minima at $\theta = 0$ and $\pi/2$. The $v^\pi_{T,S=1,M}(r, \theta)$ has opposite signs at $\theta = 0$ and $\pi/2$, and it can be verified that

$$v^\pi_{T,S=1,M=\pm1}(r, \theta = 0) = v^\pi_{T,S=1,M=0}(r, \theta = \pi/2) \ . \tag{3.43}$$

The OPEP in $T = 0$ and 1, $S = 1$ states is shown in Figs. 3.1 and 3.2.

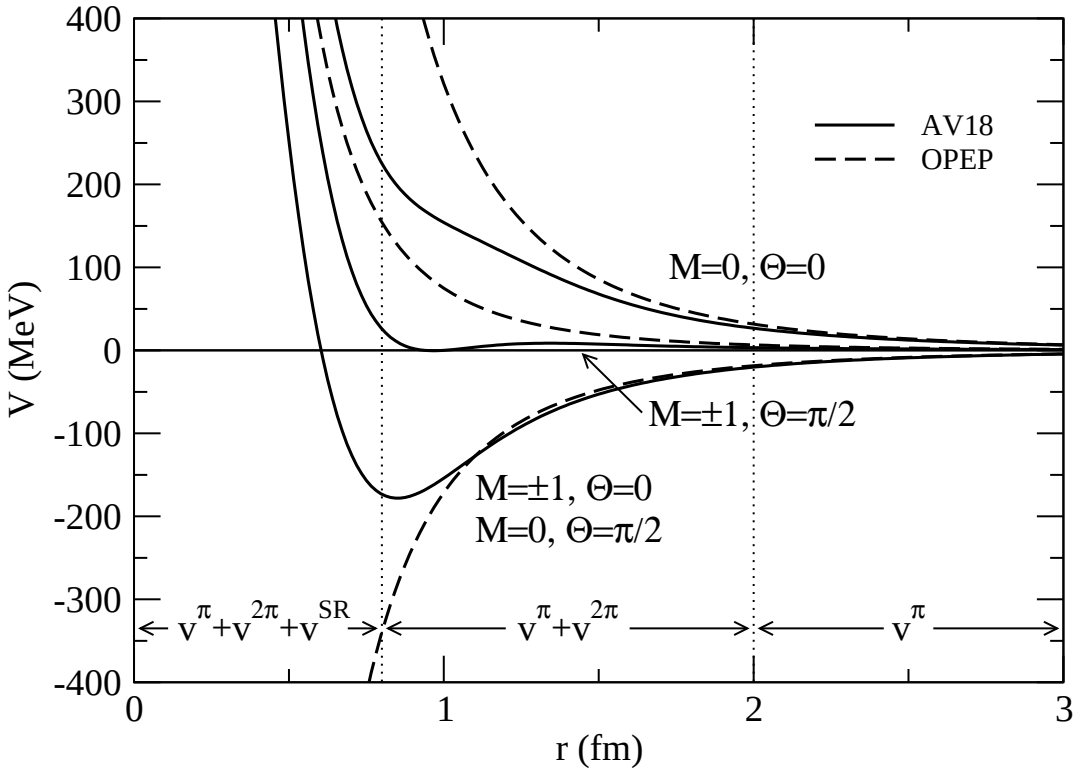

Figure 3.1: The potential in the $T = 0$, $S = 1$, $M = \pm 1$ and 0 states as a function of polar coordinates r and θ. It is independent of the azimuthal angle φ, and is given for $\theta = 0$ and $\pi/2$. The dashed lines show the OPEP, and the solid lines give the static part of the Argonne v_{18} (AV18) potential in the $^3S_1$-$^3D_1$ partial waves coupled by the tensor force.

The v^π in $T = 0$ states has similarities with the interaction between magnetic dipoles discussed in the next section, and its large angular anisotropy has observable effects on the structure of nuclei. We obtain:

$$v^\pi_{T=0,S=1,M}(r,\theta) = -3\ v^\pi_{T=1,S=1,M}(r,\theta)\ , \tag{3.44}$$

from the values of -3 and 1 of $\boldsymbol{\tau}_i \cdot \boldsymbol{\tau}_j$ in $T = 0$ and 1 states. The sum of the expectation values of the tensor potential in the $S = 1; M = 1, 0, -1$ states vanishes.

The tensor operator is identically zero in the $S = 0$ states. Thus the OPEP has the simpler form

$$\langle S, M = 0, 0; \mathbf{r}|v^\pi|S, M = 0, 0; \mathbf{r}\rangle = -\frac{f^2_{\pi NN}}{4\pi}\, m_\pi\, \boldsymbol{\tau}_1 \cdot \boldsymbol{\tau}_2 \left[Y_\pi(r) - \frac{4\pi}{{m_\pi}^3}\delta(\mathbf{r})\right]\ , \tag{3.45}$$

in $S = 0$ states. It is shown in Figs. 3.3 and 3.4. It has the smallest magnitude in $T, S = 1, 0$ states and the largest in 0,1.

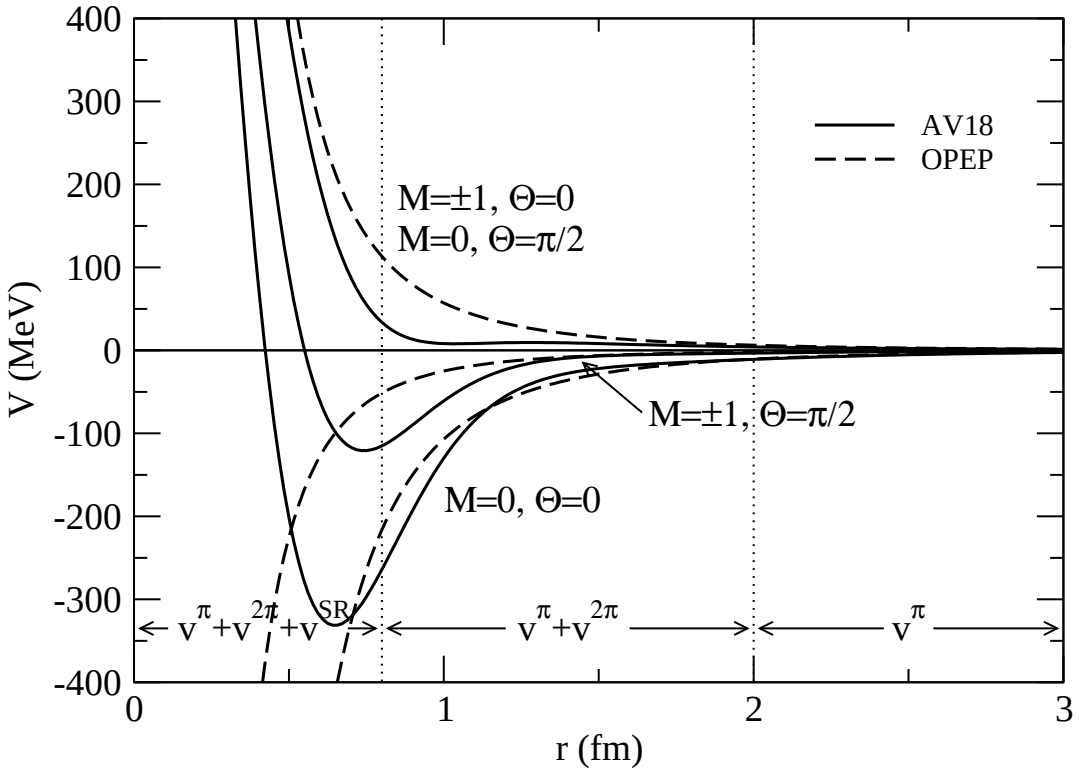

Figure 3.2: The potential in the $T = 1$, $S = 1$, $M = \pm 1$ and 0 states as a function of polar coordinates. The solid lines give the static part of the AV18 potential in the ${}^3P_J$ partial waves with $J = 0, 1$ and 2. See caption of Fig. 3.1 for notation.

The observed NN scattering data supports the assumption that the long-range part of the strong interaction between nucleons is given by OPEP. In 1991 the Nijmegen group fitted that data assuming that the long-range part of v_{ij} is given by the exchange of a pseudoscalar-isovector meson, *i.e.* having the quantum numbers of the pion, but with an unknown mass. They found that the best fit required the unknown mass to be the pion mass with an uncertainty of few MeV.

The description of the long-range parts of the two-nucleon interaction (and current operators, described in later chapter) is therefore relatively simple. It depends on only one parameter, the pion-nucleon coupling constant. The value of this coupling constant, obtained in 1993, is

$$\frac{f^2_{\pi NN}}{4\pi} = 0.075 \ . \tag{3.46}$$

The same value is obtained from analysis of NN or πN scattering data.

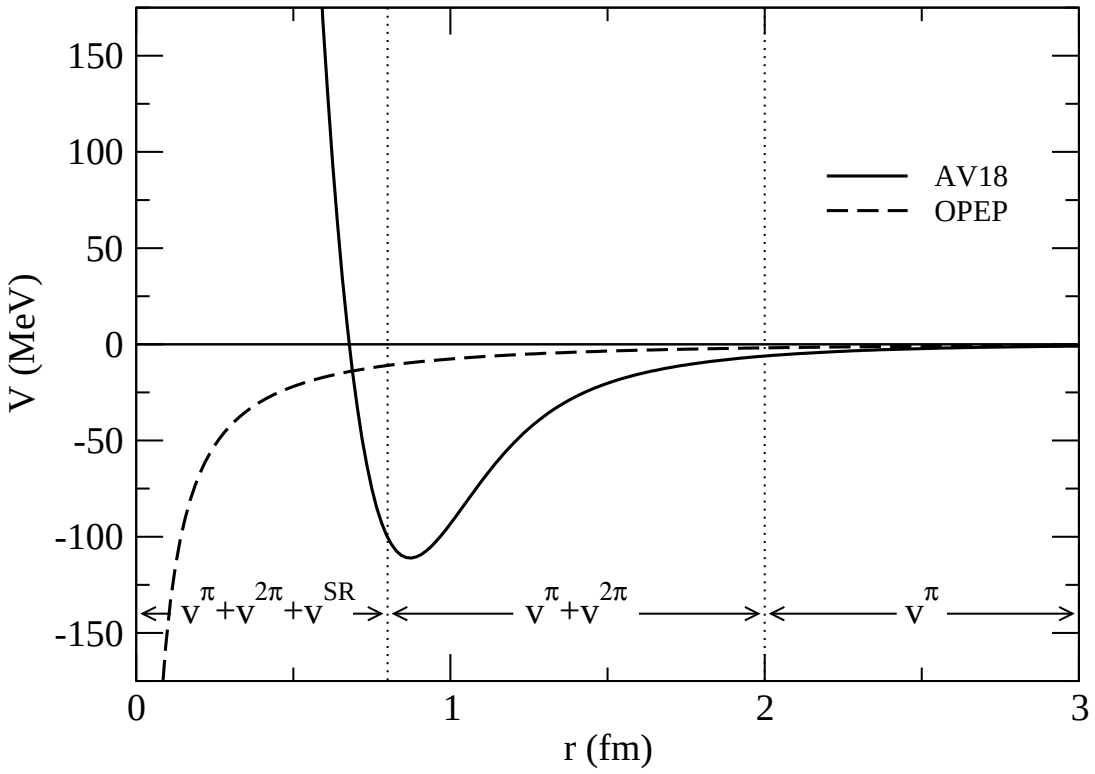

Figure 3.3: The OPEP in $T, S = 1, 0$ states (dashed line) and the AV18 in the $^1S_0$ partial wave.

The rms radius of the Yukawa part of v_{ij}^{π} is given by

$$R_{\rm rms}({\rm OPEP_Y}) = \left[\frac{\int d^3r\, r^2\, Y_\pi(r)}{\int d^3r\, Y_\pi(r)}\right]^{1/2} = \frac{\sqrt{6}}{m_\pi} \sim 3.5 \text{ fm}. \tag{3.47}$$

It is quite large due to the long exponential tail of $Y_\pi(r)$. Figures3.1 to 3.4 show $v(r)$ without the r^2 phase space factor. They therefore suppress the importance of the long-range parts of $v(r)$.

The OPEP is dominated by its tensor part which has a $1/r^3$ divergence at small r; this must be cut off to give a usable potential. Its rms radius is sensitive to the short-range cutoff used for v^π, nevertheless it is smaller than that of the Yukawa part. The experimental value of the effective range of nuclear potentials, obtained from low-energy scattering data, depends on the spin-isospin state of the two nucleons. In states with total orbital angular momentum $L = 0$, which sample the whole of the two-body interaction, the values of the total spin and isospin are restricted to be 0,1 and 1,0 by the antisymmetry of the two-nucleon wave function. The experimental values of the effective-range parameters in these

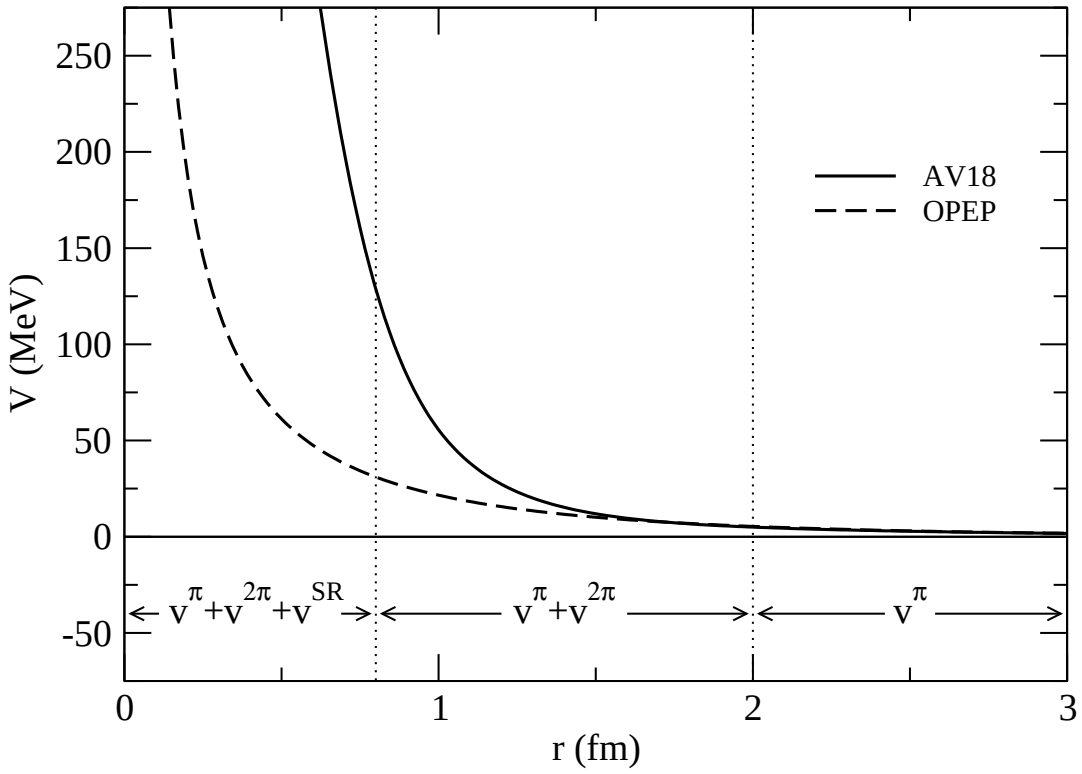

Figure 3.4: The OPEP in the $T, S = 0, 0$ state (dashed line) and the AV18 in the ${}^1P_1$ partial wave.

two states are respectively 2.81(5) fm and 1.760(5) fm. However, the effective range can be very different from the rms radius of the corresponding potential.

Second and higher order terms of v_{ij}^{π} are taken into account when the Schrödinger equation $H\Psi = E\Psi$ is solved with a Hamiltonian including OPEP. They contain two-body terms having $(v_{ij}^{\pi})^{n\geq 2}$, as well as three- and higher-body terms having $v_{ij}^{\pi}\, v_{jk}^{\pi}, \ldots$.

Nuclei are bound states of nucleons, in which, as emphasized by Bethe and Salpeter, the nuclear potentials contribute in all orders. For example, it is not possible to quantify the contributions of the Coulomb potential to the binding energy of the hydrogen atom in first, second, third, ...orders of perturbation theory. However, one can estimate the total Coulomb energy of the hydrogen atom as the expectation value of the Coulomb potential in its ground state. One can similarly calculate the total contribution of OPEP to the potential energy of the nucleus. It is denoted by $\langle v^{\pi} \rangle$, and depends somewhat on the cutoffs used to regulate the divergence of $T_{\pi}(r)$ at small r. However, it provides over half of the potential energy in light nuclei and nuclear matter at equilibrium density, using plausible short-range behaviors.

3.5 The interaction between magnetic dipoles

The interaction between two magnetic dipoles is probably the most familiar example of the tensor force. It can be derived just as OPEP, from the contribution of the one-photon-exchange interaction to the scattering amplitude of two dipoles. The interaction of a dipole at position $\mathbf{r}$ with a magnetic field is given by

$$H_D = -\mu\,\boldsymbol{\sigma}\cdot\hat{\mathbf{B}}(\mathbf{r})\ , \tag{3.48}$$

where μ is the magnetic moment of the particle, which we assume to have spin 1/2, and $\hat{\mathbf{B}}(\mathbf{r})$ is the quantized magnetic field,

$$\hat{\mathbf{B}}(\mathbf{r}) = \sum_{\mathbf{k}}\sum_{\alpha=1}^{2}\frac{i}{\sqrt{2\omega_k}}\mathbf{k}\times\hat{\mathbf{e}}_\alpha\left(a_{\mathbf{k}\,\alpha}\,e^{i\mathbf{k}\cdot\mathbf{r}} - a^\dagger_{\mathbf{k}\,\alpha}\,e^{-i\mathbf{k}\cdot\mathbf{r}}\right)\ . \tag{3.49}$$

The unit polarization vectors $\hat{\mathbf{e}}_1$ and $\hat{\mathbf{e}}_2$ form along with $\hat{\mathbf{k}}$ a right-handed orthonormal system of axes, $\hat{\mathbf{e}}_1\times\hat{\mathbf{e}}_2{=}\hat{\mathbf{k}}$. Thus the interaction Hamiltonian H_D can be written as

$$H_D = -i\,\mu\sum_{\mathbf{k}}\sum_{\alpha=1}^{2}\frac{\hat{\mathbf{e}}_\alpha\cdot(\boldsymbol{\sigma}\times\mathbf{k})}{\sqrt{2\omega_k}}\left(a_{\mathbf{k}\,\alpha}\,e^{i\mathbf{k}\cdot\mathbf{r}} - a^\dagger_{\mathbf{k}\,\alpha}\,e^{-i\mathbf{k}\cdot\mathbf{r}}\right)\ . \tag{3.50}$$

Using this interaction in place of $H_{\pi NN}$ in Eq. (3.12), and intermediate states $|I\rangle$ containing a photon of momentum $\pm\mathbf{q}$, we obtain the scattering amplitude, or equivalently the dipole-dipole interaction $\widetilde{v}^{DD}_{12}(\mathbf{q})$ in momentum space, as

$$\begin{aligned}
\widetilde{v}^{DD}_{12}(\mathbf{q}) &= -\frac{\mu^2}{q^2}\sum_{\alpha=1,2}(\boldsymbol{\sigma}_1\times\mathbf{q})\cdot\hat{\mathbf{e}}_\alpha\ (\boldsymbol{\sigma}_2\times\mathbf{q})\cdot\hat{\mathbf{e}}_\alpha \\
&= -\frac{\mu^2}{q^2}\ (\boldsymbol{\sigma}_1\times\mathbf{q})\cdot(\boldsymbol{\sigma}_2\times\mathbf{q}) \\
&= \frac{\mu^2}{q^2}\left(\boldsymbol{\sigma}_1\cdot\mathbf{q}\,\boldsymbol{\sigma}_2\cdot\mathbf{q}\ -\ q^2\,\boldsymbol{\sigma}_1\cdot\boldsymbol{\sigma}_2\right)\ .
\end{aligned} \tag{3.51}$$

It has a $\boldsymbol{\sigma}_1\cdot\boldsymbol{\sigma}_2$ term absent in the OPEP $\widetilde{v}^{\pi}_{12}(\mathbf{q})$, Eq. (3.19). The configuration-space version of the dipole-dipole potential is obtained by Fourier transform as in Sec. 3.2:

$$\begin{aligned}
v^{DD}_{12}(\mathbf{r}) &= -\mu^2\left(\boldsymbol{\sigma}_1\cdot\boldsymbol{\nabla}\,\boldsymbol{\sigma}_2\cdot\boldsymbol{\nabla}\ -\ \boldsymbol{\sigma}_1\cdot\boldsymbol{\sigma}_2\,\nabla^2\right)\frac{1}{4\pi\,r} \\
&= -\frac{\mu^2}{4\pi}\left[\frac{1}{r^3}S_{12}\ +\ \frac{8\pi}{3}\delta(\mathbf{r})\,\boldsymbol{\sigma}_1\cdot\boldsymbol{\sigma}_2\right]\ .
\end{aligned} \tag{3.52}$$

The total angular momentum of the hydrogen atom having its electron in the $1s_{1/2}$ state is given by the sum of the spins of the electron and the proton, and can have values of 0

and 1. The degeneracy between these two states of the hydrogen atom is removed by the interaction between the magnetic dipole moments of the electron and the proton. In first order perturbation theory, valid for this hyperfine splitting, the tensor part of v_{12}^{DD} does not contribute because of spherical symmetry of the electron wave function, and the $\boldsymbol{\sigma}_1 \cdot \boldsymbol{\sigma}_2$ part lowers the $S = 0$ state below the $S = 1$. The well known 21 cm microwave radiation used by radio astronomers to survey the hydrogen clouds in our galaxy is emitted in the transition from the $S = 1$ state to the ground state. The energy of this transition is accurately predicted by electron-proton dipole-dipole interaction obtained from Eq. (3.52) after replacing μ^2 by $\mu_p \mu_e$ the product of the magnetic moments of the proton and electron. This observation confirms the existence and the strength of the δ-function term in the v_{12}^{DD}.

It is unlikely that the effects of this term in OPEP, Eq. (3.26), can ever be observed experimentally. The electron penetrates the proton without perturbing it excessively, and interacts with the proton's magnetic moment electromagnetically. When two nucleons interpenetrate each other, however, many strong forces besides OPEP can contribute, and the nucleons' quark substructure may become strongly perturbed. Therefore the δ-function term in OPEP is often removed from the v_{12}^{π} and considered together with other short range terms in nuclear forces.

3.6 Pion field of classical sources

In Sec. 2.1 the nonrelativistic scalar meson exchange Yukawa potential is derived using classical mechanics. Here we outline a similar derivation of OPEP. The pion fields $\phi_a(\mathbf{r}, t)$, a=x, y, z, are treated classically without field quantization, and the quantum operators $\boldsymbol{\sigma}$ and $\boldsymbol{\tau}$ in the pion-nucleon interaction Hamiltonian, Eq. (3.10), are replaced by classical spin and isospin vectors, denoted by $\overline{\boldsymbol{\sigma}}$ and $\overline{\boldsymbol{\tau}}$. The classical Lagrangian density $\overline{\mathcal{L}}(\overline{\phi}_a, \boldsymbol{\nabla}\overline{\phi}_a)$ describing the static pion field $\overline{\phi}_a(\mathbf{r})$ (hence, the overline over $\mathcal{L}$ and ϕ_a) coupled to sources $\overline{\boldsymbol{\sigma}}_i$, $\overline{\boldsymbol{\tau}}_i$ at $\mathbf{r}_i$ with i=$1, \ldots, A$ is then given by

$$\overline{\mathcal{L}}(\overline{\phi}_a, \boldsymbol{\nabla}\overline{\phi}_a) = -\frac{1}{2}\sum_a \left[\mid \boldsymbol{\nabla}\overline{\phi}_a(\mathbf{r}) \mid^2 + m_\pi^2 \overline{\phi}_a^2(\mathbf{r}) \right] + \frac{f_{\pi NN}}{m_\pi} \sum_{i=1}^{A} \delta(\mathbf{r} - \mathbf{r}_i) \overline{\tau}_{i,a}\, \overline{\boldsymbol{\sigma}}_i \cdot \boldsymbol{\nabla}\overline{\phi}_a(\mathbf{r}) \ , \quad (3.53)$$

and the sum over repeated indices a is understood. The Euler-Lagrange equations for the pion fields (in the static limit) read

$$\nabla^2 \overline{\phi}_a(\mathbf{r}) - m_\pi^2 \overline{\phi}_a(\mathbf{r}) = \frac{f_{\pi NN}}{m_\pi} \sum_{i=1}^{A} \overline{\tau}_{i,a}\, \overline{\boldsymbol{\sigma}}_i \cdot \boldsymbol{\nabla}\delta(\mathbf{r} - \mathbf{r}_i) \ , \quad (3.54)$$

and its solution can be expressed as a superposition of fields $\overline{\phi}_{j,a}$ of single sources $\overline{\boldsymbol{\sigma}}_j$, $\overline{\boldsymbol{\tau}}_j$ at $\mathbf{r}_j$ as for the classical scalar meson or electrostatic field,

$$\overline{\phi}_a(\mathbf{r}) = \sum_{j=1}^{A} \overline{\phi}_{j,a}(\mathbf{r}) \ . \quad (3.55)$$

Each field $\overline{\phi}_{j,a}(\mathbf{r})$ satisfies a partial differential equation identical to Eq. (3.54) except that on the r.h.s. only the source term with $i = j$ is present. It can be easily solved by introducing the Fourier transforms

$$\overline{\phi}_{j,a}(\mathbf{r}) = \int \frac{d^3q}{(2\pi)^3} e^{-i\mathbf{q}\cdot\mathbf{r}} \tilde{\phi}_{j,a}(\mathbf{q}) \ , \tag{3.56}$$

$$\delta(\mathbf{r} - \mathbf{r}_j) = \int \frac{d^3q}{(2\pi)^3} e^{-i\mathbf{q}\cdot(\mathbf{r}-\mathbf{r}_j)} \ . \tag{3.57}$$

We find:

$$\begin{aligned} \overline{\phi}_{j,a}(\mathbf{r}) &= i\frac{f_{\pi NN}}{m_\pi}\overline{\tau}_{j,a}\int \frac{d^3q}{(2\pi)^3}\frac{\overline{\boldsymbol{\sigma}}_j\cdot\mathbf{q}}{q^2+m_\pi^2}\, e^{-i\mathbf{q}\cdot(\mathbf{r}-\mathbf{r}_j)} \\ &= -\frac{f_{\pi NN}}{m_\pi}\overline{\tau}_{j,a}\overline{\boldsymbol{\sigma}}_j\cdot\boldsymbol{\nabla}\frac{e^{-m_\pi|\mathbf{r}-\mathbf{r}_j|}}{4\pi\,|\mathbf{r}-\mathbf{r}_j|} \ . \end{aligned} \tag{3.58}$$

The energy of the static pion field can be simplified as for the scalar field by making use of the Euler-Lagrange equations, namely

$$E_{\overline{\phi}} = -\int d^3r\, \overline{\mathcal{L}}(\overline{\phi}_a, \boldsymbol{\nabla}\overline{\phi}_a) = -\frac{1}{2}\frac{f_{\pi NN}}{m_\pi}\int d^3r \sum_{i=1}^{A}\delta(\mathbf{r}-\mathbf{r}_i)\,\overline{\tau}_{i,a}\,\overline{\boldsymbol{\sigma}}_i\cdot\boldsymbol{\nabla}\overline{\phi}_a \ , \tag{3.59}$$

which can be expressed as

$$\begin{aligned} E_{\overline{\phi}} &= -\frac{1}{2}\frac{f_{\pi NN}^2}{m_\pi^2}\sum_{i,j=1}^{A}\overline{\boldsymbol{\tau}}_i\cdot\overline{\boldsymbol{\tau}}_j\int\frac{d^3q}{(2\pi)^3}\frac{\overline{\boldsymbol{\sigma}}_i\cdot\mathbf{q}\;\overline{\boldsymbol{\sigma}}_j\cdot\mathbf{q}}{q^2+m_\pi^2}e^{-i\mathbf{q}\cdot(\mathbf{r}_i-\mathbf{r}_j)} \\ &= \sum_{i<j=1}^{A}\int\frac{d^3q}{(2\pi)^3}\widetilde{v}_{ij}^{\,\pi}(\mathbf{q}) \ + \ \text{self energy terms} \ . \end{aligned} \tag{3.60}$$

The above $\widetilde{v}_{ij}^{\,\pi}(\mathbf{q})$ is equal to that obtained earlier in Eq. (3.19) with perturbation theory, except for the replacement of the quantum operators $\boldsymbol{\sigma}$ and $\boldsymbol{\tau}$ by the classical vectors $\overline{\boldsymbol{\sigma}}$ and $\overline{\boldsymbol{\tau}}$. Nuclear many-body theory is more challenging due to the presence of these operators in OPEP. For example, in quantum mechanics the Coulomb and the Yukawa potentials, being simple functions of the interparticle distances, commute, namely $[v_{ij}(r_{ij})\,,\, v_{ik}(r_{ik})] = 0$, while OPEP's do not, $[v_{ij}^{\pi}(\mathbf{r}_{ij})\,,\, v_{ik}^{\pi}(\mathbf{r}_{ik}] \neq 0$.

3.7 The Δ-resonance in pion-nucleon scattering

Due to the relatively long life-time of charged pions ($\simeq 2.6\ 10^{-8}$ sec), their scattering by protons can be studied in the laboratory. The observed total and elastic π^+p and π^-p

scattering cross-sections are tabulated by the Particle Data Group and shown in Figs. 3.5 and 3.6 respectively. At lower energies, the $\pi^+ p$ scattering is purely elastic; it becomes inelastic at higher energies due to particle production. For example, reactions such as $\pi^+ + p \to \pi^0 + \pi^+ + p$ contribute to the inelastic $\pi^+ p$ cross-section above their threshold energies. In contrast the charge-exchange reaction $\pi^- + p \to \pi^0 + n$ is allowed at all energies, neglecting the small difference between the masses of the proton and neutron, and between charged and neutral pions. Therefore $\pi^- p$ scattering has elastic and inelastic parts at all energies.

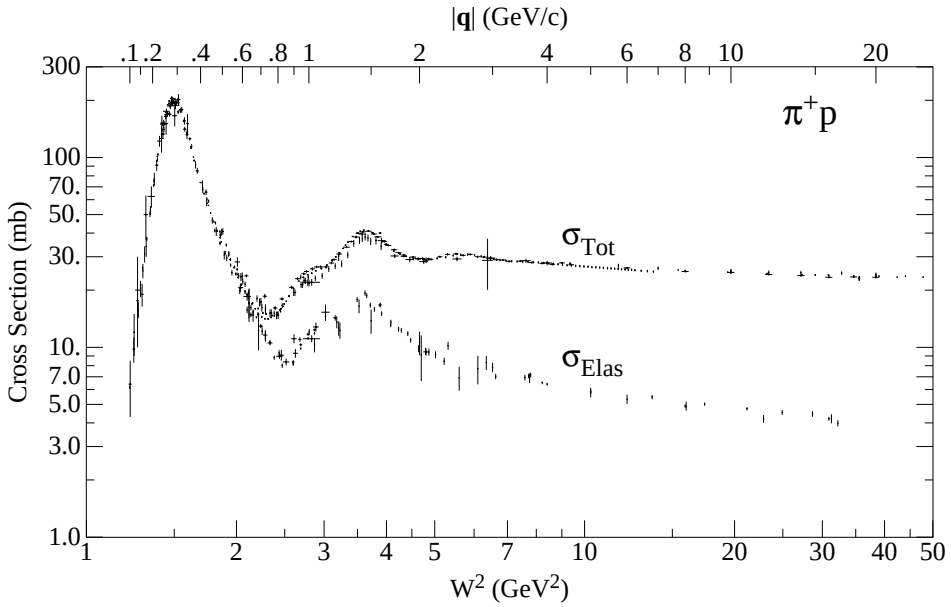

Figure 3.5: The total and elastic $\pi^+ p$ scattering cross sections

In most pion-nucleon scattering experiments the target proton is at rest in the laboratory frame, and its energy-momentum four vector p^μ is $(m_p, 0)$, while the incident pion energy-momentum is $q^\mu = (\omega_q, \mathbf{q})$. The total energy-momentum,

$$P^\mu = p^\mu + q^\mu = (m_p + \omega_q, \mathbf{q}) \ , \tag{3.61}$$

is conserved. The invariant mass of the $\pi + p$ state is denoted by W with

$$W^2 \ = P^\mu P_\mu = \ (m_p + \omega_q)^2 - \mathbf{q}^2 \ , \tag{3.62}$$

and W^2 is also called the Mandelstam variable s. Both the variables, $|\mathbf{q}|$ in the laboratory frame and s, are used in Figs. 3.1 and 3.2.

At energies below $W \simeq 2$ GeV, pion-nucleon scattering is dominated by resonances which occur when the invariant mass W equals the mass of an excited state of the nucleon. They are similar to the resonances seen in the scattering of photons by atoms when the photon

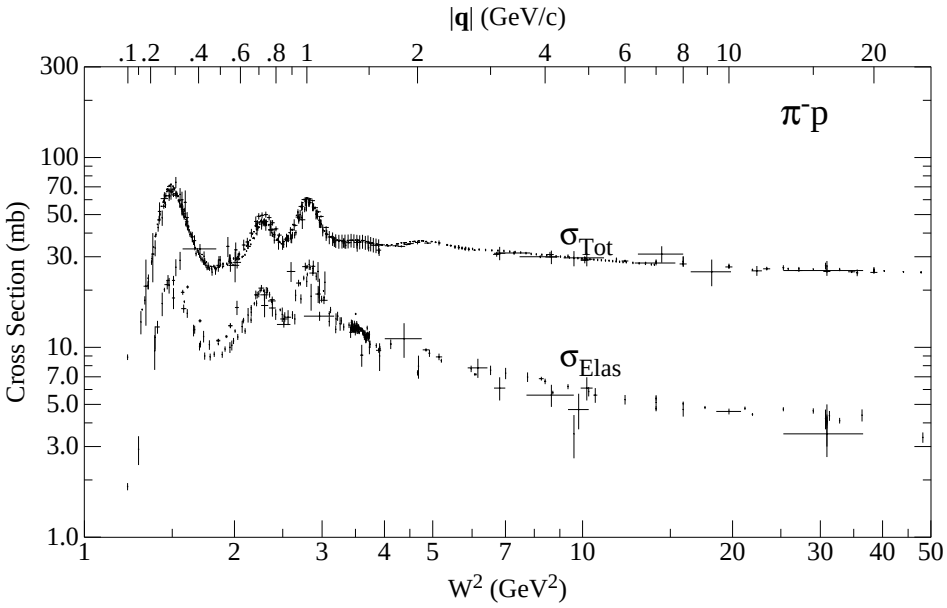

Figure 3.6: The total and elastic $\pi^- p$ scattering cross sections

energy equals the excitation energy of an atomic state. The widths of these resonances are proportional to their decay rates. Due to its large strength and low energy, the Δ-resonance at $W = 1.24$ GeV plays an important role in pion-exchange interactions between nucleons. The spin and isospin of this resonance have values of $3/2$ each, which corresponds to the spin and isospin projections of all the three quarks being parallel in the Δ-state. In the simple constituent quark model, this resonance occurs when the spin and isospin of a quark in the nucleon are flipped by the absorption of the pion of the right energy.

At larger values of W, where $s{=}W^2 > 10$ GeV^2, the total cross-section is mostly inelastic, relatively independent of energy, and nearly the same for $\pi^+ p$ and $\pi^- n$. These features indicate that at very large energies $\pi - N$ scattering may be more easily considered as that of quarks, anti-quarks and gluons inside the pion by those in the nucleon.

Several features of the Δ-resonance can be understood from isospin conservation in strong interactions. Both the $\pi^+ p$ and Δ^{++} states have total isospin $T = 3/2$ and $T_z = 3/2$. The $\pi^+ p$ scattering cross section therefore has a large peak of $\simeq 210$ mb (10^{-3} barns) at the Δ-resonance energy, as can be seen in Fig. 3.5. In contrast to the $\pi^+ p$, the $\pi^- p$ state is not an eigenstate of total isospin T; however, it is an eigenstate of T_z with eigenvalue $-1/2$. The pion-nucleon eigenstates of T and T_z, denoted by $|\pi N; T, T_z\rangle$ are easily obtained by using Clebsch-Gordan coefficients to add the pion and nucleon isospins. The states having $T_z = -1/2$ are:

$$|\pi N; T = 3/2, T_z = -1/2\rangle \;\; = \;\; \sqrt{2/3}\,|\pi^0 n\rangle + \sqrt{1/3}\,|\pi^- p\rangle \;, \tag{3.63}$$

$$|\pi N; T = 1/2, T_z = -1/2\rangle \;\; = \;\; \sqrt{1/3}\,|\pi^0 n\rangle - \sqrt{2/3}\,|\pi^- p\rangle \;, \tag{3.64}$$

and superposing them we obtain:

$$|\pi^- p\rangle = \sqrt{1/3}\,|\pi N; T = 3/2, T_z = -1/2\rangle - \sqrt{2/3}\,|\pi N; T = 1/2, T_z = -1/2\rangle \;. \tag{3.65}$$

Only the $T = 3/2$ part of the $\pi^- p$ state can form the Δ^0-resonance having $T = 3/2, T_z = -1/2$. Therefore the cross-section at the Δ-peak in $\pi^- p$ scattering (Fig. 3.2) is $\simeq 70$ mb, *i.e.* a third of the peak $\pi^+ p$ cross-section (Fig. 3.1). Moreover, the formed Δ^0 decays into the pion-nucleon state $|\pi N; T = 3/2, T_z = -1/2\rangle$ given by Eq. (3.63). In this state the amplitude of the $\pi^0 n$ part is $\sqrt{2}$ times that of the $\pi^- p$ part. Therefore, at the Δ-peak, the charge exchange ($\pi^- p \to \pi^0 n$) reaction cross section is twice as large as the elastic ($\pi^- p \to \pi^- p$) cross section, and the total $\pi^- p$ cross-section at Δ-peak is three times the elastic as shown in Fig. 3.2.

This simple analysis of the relative strengths of $\pi^+ p$ and $\pi^- p$ cross sections is possible in the Δ-peak region because it is a strong and well isolated resonance. The higher energy resonances in pion-nucleon scattering require a more careful treatment because they are weaker and overlapping. Nevertheless it is obvious that those resonances that occur in $\pi^- p$ scattering, but not in $\pi^+ p$, must have $T = 1/2$. The lowest of these has mass $W = 1440$ MeV, and is called the Roper resonance.

3.8 The $\pi N\Delta$ coupling

In the non-relativistic limit the pion-nucleon-Δ Hamiltonian, $H_{\pi N\Delta}$, has the form

$$H_{\pi N\Delta} = -\frac{f_{\pi N\Delta}}{m_\pi}\Big\{\mathbf{S}\cdot\boldsymbol{\nabla}\big[\boldsymbol{\phi}(\mathbf{r})\cdot\mathbf{T}\big] \;+\; \mathbf{S}^\dagger\cdot\big[\boldsymbol{\nabla}\boldsymbol{\phi}(\mathbf{r})\cdot\mathbf{T}^\dagger\big]\Big\} \;. \tag{3.66}$$

Its first term describes the conversion of a nucleon into Δ by the absorption or emission of a pion, while the second describes the reverse conversion of Δ into nucleon. This interaction is a direct generalization of the $H_{\pi NN}$ given by Eq. (3.10); the spin and isospin operators $\boldsymbol{\sigma}$ and $\boldsymbol{\tau}$ in $H_{\pi NN}$ are replaced by the transition spin and isospin operators $\mathbf{S}, \mathbf{S}^\dagger$ and $\mathbf{T}, \mathbf{T}^\dagger$. The operator $\mathbf{S}$ ($\mathbf{T}$) converts a spin 1/2 (isospin 1/2) particle into a spin 3/2 (isospin 3/2) particle. Thus the product $\mathbf{S}\,\mathbf{T}$ changes a nucleon into a Δ, while $\mathbf{S}^\dagger\,\mathbf{T}^\dagger$ does the reverse. This interaction couples the Δ resonance with $J^\pi = (3/2)^+$ to a π-N state having orbital angular momentum $l = 1$. When angular momentum and parity are conserved, this is the only possibility.

The transition spin $\mathbf{S}$ has been defined by Rarita and Schwinger so that it transforms as an axial vector under rotations; then $\mathbf{S}\cdot(\boldsymbol{\nabla}\boldsymbol{\phi}\cdot\mathbf{T})$ is a scalar in both configuration and isospin spaces. The x, y and z components of $\mathbf{S}$ have matrix elements between the four spin

$3/2$ states with projection $m' = -3/2, -1/2, 1/2, 3/2$, and the two spin $1/2$ $m = -1/2, 1/2$ states. The spin-transition operator is thus a set of three 4×2 matrices whose elements are obtained as follows. It is convenient to define the basis:

$$\hat{\boldsymbol{\epsilon}}_{\pm1} \equiv \mp\frac{1}{\sqrt{2}}(\hat{\mathbf{x}} \pm i\hat{\mathbf{y}}) \ , \qquad \hat{\boldsymbol{\epsilon}}_0 \equiv \hat{\mathbf{z}} \ , \tag{3.67}$$

with $\hat{\boldsymbol{\epsilon}}^*_q = (-)^q \, \hat{\boldsymbol{\epsilon}}_{-q}$ and

$$\sum_{q=\pm1,0} (\hat{\boldsymbol{\epsilon}}_q)_a \, (\hat{\boldsymbol{\epsilon}}^*_q)_b = \delta_{a,b} \ . \tag{3.68}$$

The spin-transition operator can be expanded on this basis as

$$\mathbf{S} = \sum_{q=\pm1,0} \hat{\boldsymbol{\epsilon}}_q \left(\hat{\boldsymbol{\epsilon}}^*_q \cdot \mathbf{S}\right) = \sum_{q=\pm1,0} (-)^q \, \hat{\boldsymbol{\epsilon}}_q \, S_{-q} \ , \tag{3.69}$$

where S_q denotes its spherical components, $S_q = \hat{\boldsymbol{\epsilon}}_q \cdot \mathbf{S}$. Matrix elements of these between the $\mid 3/2, m'\rangle$ and $\mid 1/2, m\rangle$ states, denoted simply as $\mid m'\rangle$ and $\mid m\rangle$, are obtained by making use of the Wigner-Eckart theorem:

$$\langle m' \mid S_q \mid m\rangle = \frac{1}{2} \, \langle 3/2 \mid\mid S \mid\mid 1/2\rangle \, \langle 1, 1/2; 3/2, m' \mid 1, q; 1/2, m\rangle \ , \tag{3.70}$$

where the Clebsch-Gordan coefficients combine the spin $1/2$ of the nucleon and the orbital angular momentum 1 of the absorbed or emitted pion to obtain the total spin $3/2$ of the Δ resonance. Choosing the norm of $\mathbf{S}$ such that the reduced matrix element

$$\langle 3/2 \mid\mid S \mid\mid 1/2\rangle = 2 \ , \tag{3.71}$$

leads, via Eqs. (3.69) and (3.70), to

$$\langle m'|\mathbf{S}|m\rangle = \langle 1, 1/2; 3/2, m'|1, m'-m; 1/2, m\rangle \, \hat{\boldsymbol{\epsilon}}^*_{m'-m} \ . \tag{3.72}$$

The isospin-transition operator $\mathbf{T}$ has similar matrix elements between the four isospin $3/2$ states $\Delta^-, \Delta^0, \Delta^+, \Delta^{++}$ and the two isospin $1/2$ states n, p. The operator $\mathbf{S}^\dagger$ is represented by 2×4 matrices, and thus products of $\mathbf{S}^\dagger$ and $\mathbf{S}$ are 2×2 matrices, which can be represented using the Pauli matrices $\boldsymbol{\sigma}$ and the 2×2 unit matrix. The following identities,

$$\mathbf{S}^\dagger \cdot \mathbf{S} \ = \ 2 \ , \tag{3.73}$$

$$\mathbf{S}^\dagger \times \mathbf{S} \ = \ -\frac{2\,i}{3} \, \boldsymbol{\sigma} \ , \tag{3.74}$$

$$\mathbf{S}^\dagger \cdot \mathbf{A} \ \mathbf{S} \cdot \mathbf{B} \ = \ \frac{2}{3}\mathbf{A} \cdot \mathbf{B} - \frac{i}{3} \, \boldsymbol{\sigma} \cdot (\mathbf{A} \times \mathbf{B}) \ , \tag{3.75}$$

are generalizations of the well known identities for products of Pauli matrices, where as in Eq. (3.31) the 2×2 unit matrix is not explicitly indicated. It is often possible to eliminate the transition spin and isospin operators with these identities as illustrated in the next section.

3.9 Pion-nucleon scattering in the Δ-resonance region

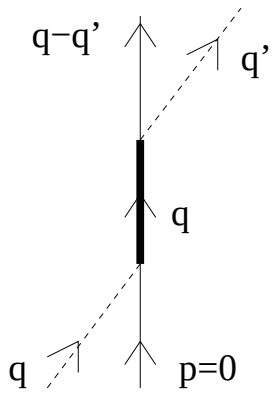

Figure 3.7: The process dominating the pion-nucleon scattering in the region of the Δ resonance. The thick, thin and dashed lines respectively show Δ's, nucleons and pions.

We will now calculate the amplitude for pion-nucleon scattering in the Δ-resonance region where the process shown in Fig. 3.7 is expected to dominate. The initial state has a nucleon at rest with spin-isospin projections $\chi_\sigma\eta_\tau$, and a pion of momentum $\mathbf{q}$ and charge (*i.e.*, isospin projection) α. We denote it by:

$$|i\rangle = |\chi_\sigma\eta_\tau;\mathbf{q},\alpha\rangle \ , \tag{3.76}$$

and similarly the final state by

$$|f\rangle = |\mathbf{q}-\mathbf{q}',\chi'_\sigma\eta'_\tau;\mathbf{q}',\alpha'\rangle \ , \tag{3.77}$$

where $\mathbf{q}-\mathbf{q}'$ is the momentum of the recoiling nucleon.

The spin-isospin projections of the intermediate Δ state are denoted by $\sigma_\Delta\tau_\Delta$. Since the Δ is not observed, we must sum over $\sigma_\Delta\tau_\Delta$. For simplicity, we will neglect the recoil motion of the nucleon (*i.e.*, $\mathbf{q}=\mathbf{q}'$), since it has rather small effects due to the large difference between the nucleon and pion masses ($m_N \simeq 7\,m_\pi$). The second-order scattering amplitude reads

$$A^{(2)}_{fi} = \sum_{\sigma_\Delta\,\tau_\Delta} \frac{\langle f|H_{\pi N\Delta}|\chi_{\sigma_\Delta}\eta_{\sigma_\Delta}\rangle\ \langle\chi_{\sigma_\Delta}\eta_{\sigma_\Delta}|H_{\pi N\Delta}|i\rangle}{\omega_q-\Delta_m} \ , \tag{3.78}$$

where ω_q is the pion eneergy, and Δ_m is simply given by the difference between the nucleon and Δ masses, again neglecting the kinetic energy of the recoiling Δ. Carrying out the sum over the spin-isospin projections leads to

$$A^{(2)}_{fi} = \frac{\langle f|H_{\pi N\Delta}\ H_{\pi N\Delta}|i\rangle}{\omega_q-\Delta_m} = -\frac{f^2_{\pi N\Delta}}{m^2_\pi}\frac{M_\sigma\ M_\tau}{2\,\omega_q(\omega_q-\Delta_m)} \ , \tag{3.79}$$

where the factors M_σ and M_τ give the dependence of the amplitude on the spins and isospins of the interacting nucleons.

Since π-N scattering is due to the strong interaction, many higher order processes neglected here are likely to contribute. Therefore the parameters $f_{\pi N\Delta}$ and Δ_m entering the expression above for the second order amplitude are called effective parameters. They are determined from the observed energy and width of the Δ resonance, and their values contain the effect of the higher order terms not explicitly included here.

We first consider the mass difference Δ_m. The Δ-particle has a short life-time, and therefore a large uncertainty in its energy, as reflected by the width of this resonance. It implies that the mass m_Δ of the Δ-particle is complex:

$$m_\Delta = E_\Delta - i\,\Gamma_\Delta/2\ . \tag{3.80}$$

The time dependent wave function of a Δ at rest is given by

$$\psi_\Delta(t) = e^{-i\ M_\Delta t}\,\chi_{\sigma_\Delta}\,\eta_{\tau_\Delta} = e^{-i\ E_\Delta t}\,e^{-\Gamma_\Delta t/2}\,\chi_{\sigma_\Delta}\,\eta_{\tau_\Delta}\ . \tag{3.81}$$

The probability of finding the Δ in spin-isospin state $\chi_{\sigma_\Delta}\,\eta_{\tau_\Delta}$ decreases as $e^{-\Gamma_\Delta t}$, describing the decay of the Δ with a life-time of $1/\Gamma_\Delta$. The values $E_\Delta = 1232$ and $\Gamma_\Delta = 115$ MeV are obtained from the observed position and width of the Δ-resonance, and hence

$$\Delta_m \simeq (293 - i\,58)\ \text{MeV}\ . \tag{3.82}$$

The dependence of the amplitude on the nucleon spins is contained in the matrix element M_σ,

$$\begin{aligned} M_\sigma &= \langle\chi'_\sigma|\mathbf{S}^\dagger\cdot\mathbf{q}'\ \mathbf{S}\cdot\mathbf{q}|\chi_\sigma\rangle, \\ &= \langle\chi'_\sigma|\left[\frac{2}{3}\mathbf{q}'\cdot\mathbf{q} - \frac{i}{3}\boldsymbol{\sigma}\cdot(\mathbf{q}'\times\mathbf{q})\right]|\chi_\sigma\rangle, \end{aligned} \tag{3.83}$$

using the identity (3.75). The isospin factor M_τ in the scattering amplitude takes into account the contribution of the isospin terms originating from the isoscalar $\boldsymbol{\phi}\cdot\mathbf{T}$ in $H_{\pi N\Delta}$, Eq. (3.66). The absorption of $\pi^{+,0,-}$ with $\alpha = 1, 0, -1$ respectively produces a factor $\mathbf{T}_\alpha = \mathbf{T}\cdot\hat{\mathbf{e}}_\alpha$ in the matrix element $\langle\chi_{\sigma_\Delta}\eta_{\sigma_\Delta}|H_{\pi N\Delta}|i\rangle$. Here the unit vectors $\hat{\mathbf{e}}_\alpha$ are defined as

$$\hat{\mathbf{e}}_{\pm1} = \frac{1}{\sqrt{2}}(\hat{\mathbf{x}} \pm i\,\hat{\mathbf{y}})\ , \qquad \hat{\mathbf{e}}_0 = \hat{\mathbf{z}}\ , \tag{3.84}$$

and differ from the $\hat{\boldsymbol{\epsilon}}_\alpha$ defined in Eq. (3.67) by a phase factor. In a similar way, the pion emission matrix element contains a factor $\mathbf{T}^\dagger\cdot\hat{\mathbf{e}}^*_{\alpha'}$, so that

$$\begin{aligned} M_\tau &= \langle\eta'_\tau|\mathbf{T}^\dagger\cdot\hat{\mathbf{e}}^*_{\alpha'}\ \mathbf{T}\cdot\hat{\mathbf{e}}_\alpha|\eta_\tau\rangle, \\ &= \langle\eta'_\tau|\left[\frac{2}{3}\ \hat{\mathbf{e}}^*_{\alpha'}\cdot\hat{\mathbf{e}}_\alpha - \frac{i}{3}\,\boldsymbol{\tau}\cdot(\hat{\mathbf{e}}^*_{\alpha'}\times\hat{\mathbf{e}}_\alpha)\right]|\eta_\tau\rangle\ . \end{aligned} \tag{3.85}$$

As in Sec. 2.3, the scattering cross section is obtained from

$$\frac{d\sigma}{d\Omega} = 2\pi\,|A_{fi}|^2 \frac{\text{density of final states}}{\text{incident flux}} \ . \tag{3.86}$$

The incident flux equals the velocity of the relativistic pions given by q/ω_q, and the density of final pion states, per unit solid angle, is $\omega_q' q'/(2\pi)^3$. Using these factors and the second-order $A_{fi}^{(2)}$, we get:

$$\frac{d\sigma}{d\Omega} = \frac{1}{(4\pi)^2}\,\frac{f_{\pi N\Delta}^4}{m_\pi^4}\,\frac{q'}{q}\,\frac{|M_\sigma M_\tau|^2}{(E_\Delta - E)^2 + \Gamma_\Delta^2/4} \ , \tag{3.87}$$

where $E = m_N + \omega_q$ is the total energy including m_N, the rest mass of the target nucleon. This cross section obviously peaks at $E{=}E_\Delta$, and the full width of the peak at half maximum value is Γ.

In the last section we showed that the elastic $\pi^+ p$ cross section in the Δ-resonance region is nine times the elastic $\pi^- p$, by adding the isospins of the pion and nucleon to obtain that of the Δ. This relation between the cross sections can also be obtained from the above equation by considering the isospin factor M_τ. It can be easily verified that M_τ equals 1 for $\pi^+ p \to \pi^+ p$ while it is 1/3 for $\pi^- p \to \pi^- p$. The transition isospin (spin) operator automatically adds the pion and nucleon isospins (angular momenta) to obtain the isospin (spin) of the Δ.

3.10 Pion coupling constants

The value of the effective coupling constant $f_{\pi N\Delta}$ can be easily determined from the decay rate Γ_Δ of Δ-particles. This decay rate does not depend upon the spin or isospin of the Δ. For simplicity we study that of Δ^{++} in the spin projection state $\sigma_\Delta = 3/2$. Only π^+-proton final states can occur in this decay, and the proton spin projection can only be $+1/2$ because the P-wave pion carries a unit angular momentum. Thus the amplitude for emission of a pion with momentum $\mathbf{q}$, in the notation of the previous section, is given by

$$\begin{aligned} A_\Delta(\mathbf{q}) &= \langle \chi_{1/2}\,\eta_{1/2}; \mathbf{q}, +|H_{\pi N\Delta}|\chi_{3/2}\,\eta_{3/2}\rangle, \\ &= i\,\frac{f_{\pi N\Delta}}{m_\pi}\,\frac{M_\sigma\,M_\tau}{\sqrt{2\omega_q}} \ , \end{aligned} \tag{3.88}$$

where here the spin and isospin factors are

$$M_\sigma = \langle \chi_{1/2}|\mathbf{S}^\dagger \cdot \mathbf{q}|\chi_{3/2}\rangle = \hat{\boldsymbol{\epsilon}}_{+1} \cdot \mathbf{q} \ , \tag{3.89}$$

$$M_\tau = \langle \eta_{1/2}|\mathbf{T}^\dagger \cdot \hat{\mathbf{e}}_{+1}^*|\eta_{3/2}\rangle = 1 \ . \tag{3.90}$$

The differential decay rate for emission of a pion with momentum $\mathbf{q}$ in a solid angle $d\Omega_q$ follows from

$$d\Gamma_\Delta(\mathbf{q}) = 2\pi\ |A_\Delta(\mathbf{q})|^2 \ (\text{density of final states}) \ . \tag{3.91}$$

Here we will use the correct density of final states taking into account the recoil energy of the nucleon. The emitted pion and the recoiling nucleon have equal and opposite momenta for the decay of a Δ at rest. The magnitude q of their momenta is determined from energy conservation,

$$E_\Delta = \omega_q + E_N \ , \qquad E_N = \sqrt{m_N^2 + q^2} \ , \tag{3.92}$$

from which $q = 227$ MeV for $E_\Delta = 1232$ MeV. The density of final states is also calculated from the above equations, *i.e.*

$$\text{density of final states} = \frac{1}{(2\pi)^3} \left(\frac{dE_\Delta}{dq} \right)^{-1} q^2 \, d\Omega_q = \frac{1}{(2\pi)^3} \, \frac{E_N}{E_\Delta} \, q \, \omega_q \, d\Omega_q \ , \tag{3.93}$$

and the differential rate reads (see Eqs. (3.88)–(3.93))

$$d\Gamma_\Delta(\mathbf{q}) = \frac{1}{(4\pi)^2} \frac{f_{\pi N\Delta}^2}{m_\pi^2} \, q \, (q_x^2 + q_y^2) \, \frac{E_N}{E_\Delta} \, d\Omega_q \ . \tag{3.94}$$

The total rate Γ_Δ of the Δ is obtained by integrating over $d\Omega_q$. Using

$$\int d\Omega_q q_a^2 = \frac{4\pi}{3} \ q^2 \ , \tag{3.95}$$

for $a = x, y, z$, it follows that

$$\Gamma_\Delta = \frac{2}{3} \, \frac{f_{\pi N\Delta}^2}{4\pi} \, \frac{q^3}{m_\pi^2} \, \frac{E_N}{E_\Delta} \ . \tag{3.96}$$

Inserting the observed values in the above equation gives

$$\frac{f_{\pi N\Delta}^2}{4\pi} = 0.36 \ . \tag{3.97}$$

The value of the pion-nucleon coupling constant $f_{\pi NN}$, obtained from fits to the nucleon-nucleon scattering data, is

$$\frac{f_{\pi NN}^2}{4\pi} = 0.075 \ . \tag{3.98}$$

3.11 One pion-exchange transition potentials

The one-pion-exchange $NN \to \Delta\Delta$ and $NN \to N\Delta$ reactions are shown in Fig. 3.8. These processes occur at center of mass energies above $\simeq 300$ MeV, roughly the difference between the energy of the Δ peak and the nucleon mass. At such energies pions are produced in NN collisions, and the description of scattering in terms of NN potentials breaks down. At lower energies, below the pion production threshold, the initial and final states do not contain pions, and the role of virtual pions is absorbed into the potentials.

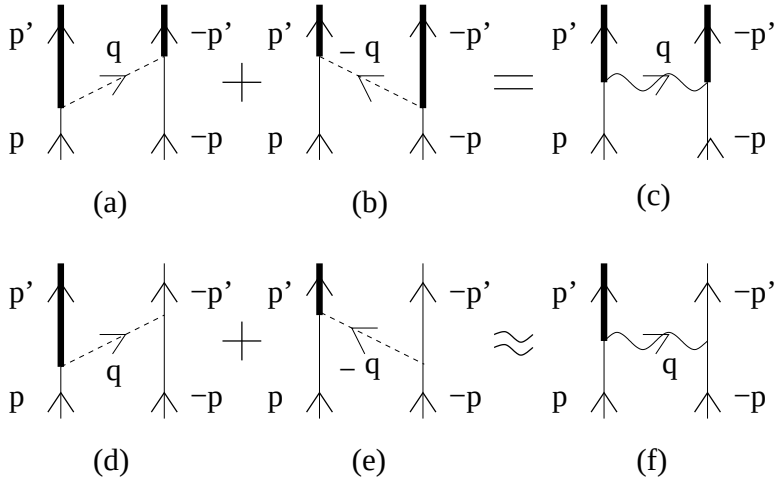

Figure 3.8: The $NN \to \Delta\Delta$ and $NN \to \Delta N$ pion-exchange reactions which make up the one-pion-exchange transition potentials. The thick, thin, dashed, and wavy lines respectively show Δ's, nucleons, pions, and transition potentials.

In this section we describe the $NN \to \Delta\Delta$ and $NN \to \Delta N$ reactions with one-pion-exchange transition potentials (OPETP), which contain only the nucleon and Δ degrees of freedom by eliminating the exchanged virtual pion in Fig. 3.8. Our objective is to use these potentials at energies below the pion production threshold to remove the Δ degrees of freedom from the nuclear Hamiltonian as discussed in the next section. At low energies the Δ particles are virtual, and they cannot decay into real pions and nucleons. The imaginary part of m_Δ in Eq. (3.80), representing this decay, is therefore ignored in this section.

Energy conservation in the center of mass frame implies that

$$\frac{p^2}{2m_N} = \frac{p'^2}{2m_\Delta} + m_\Delta - m_N \ , \tag{3.99}$$

in the $NN \to \Delta\Delta$ processes in Fig. 3.8. The transition amplitude is calculated using Eq. (3.12) with $H_{\pi N\Delta}$ in place of $H_{\pi NN}$. The denominator $E_I - E$ equals the energy ω_q of the exchanged pion in both the processes (a) and (b) in Fig. 3.8, and the total amplitude is

$$A_{NN\to\Delta\Delta}(\mathbf{q}) = -\frac{f^2_{\pi N\Delta}}{m^2_\pi}\frac{1}{\omega^2_q}\,\langle\chi'_{1\Delta},\chi'_{2\Delta}|\mathbf{S}_1\cdot\mathbf{q}\;\mathbf{S}_2\cdot\mathbf{q}\;\mathbf{T}_1\cdot\mathbf{T}_2|\chi_1,\chi_2\rangle \ , \tag{3.100}$$

where $\chi'_{1\Delta}$, $\chi'_{2\Delta}$ are the spin-isospin states of the Δ's in the final state, and χ_1, χ_2 are those of the initial nucleons. The OPETP $\widetilde{v}^\pi_{NN\to\Delta\Delta}$ in momentum space is therefore:

$$\widetilde{v}^\pi_{NN\to\Delta\Delta}(\mathbf{q}) = -\frac{f^2_{\pi N\Delta}}{m^2_\pi}\,\mathbf{T}_1\cdot\mathbf{T}_2\,\frac{\mathbf{S}_1\cdot\mathbf{q}\;\mathbf{S}_2\cdot\mathbf{q}}{q^2+m^2_\pi} \ , \tag{3.101}$$

from which, making use of the methods described in Sec. 3.2, its configuration-space version easily follows as

$$v^{\pi}_{NN\to\Delta\Delta}(\mathbf{r}) = \frac{f^2_{\pi N\Delta}}{4\pi}\frac{m_\pi}{3}\,\mathbf{T}_1\cdot\mathbf{T}_2\left\{T_\pi(r)S^{III}_{12} + \Big[Y_\pi(r) - \frac{4\pi}{m^3_\pi}\,\delta(\mathbf{r})\Big]\mathbf{S}_1\cdot\mathbf{S}_2\right\}, \tag{3.102}$$

where the $NN\to\Delta\Delta$ transition tensor potential S^{III}_{12} is defined as

$$S^{III}_{12} = 3\,\mathbf{S}_1\cdot\hat{\mathbf{r}}\;\mathbf{S}_2\cdot\hat{\mathbf{r}} - \mathbf{S}_1\cdot\mathbf{S}_2\ . \tag{3.103}$$

It contains transition spin operators in place of the Pauli spin operators in the usual tensor operator, Eq. (3.27). The form of this transition potential is very similar to that of $v^{\pi}_{12}(\mathbf{r})$ given by Eq. (3.26). The $NN\to NN$ and $NN\to\Delta\Delta$ one-pion-exchange scattering amplitudes are reproduced by the Born amplitudes of $\widetilde{v}^{\,\pi}$ and $\widetilde{v}^{\pi}_{NN\to\Delta\Delta}$, respectively.

In the $NN\to\Delta N$ processes (d) and (e) shown in Fig. 3.8, energy conservation implies

$$\frac{p^2}{m_N} = \frac{p'^2(m_\Delta+m_N)}{2\,m_\Delta m_N} + m_\Delta - m_N\,, \tag{3.104}$$

and the corresponding transition amplitudes are calculated again using Eq. (3.12) with one of the $H_{\pi NN}$ replaced by $H_{\pi N\Delta}$. The energy denominators in the two processes are

$$E_I - E = \omega_q \pm e\ , \tag{3.105}$$

where e is the energy transfered by the pion from nucleon 2 to 1,

$$e = m_\Delta - m_N + \frac{p'^2}{2m_\Delta} - \frac{p^2}{2m_N}\ . \tag{3.106}$$

The sum of the transition amplitudes (d) and (e) is

$$A_{NN\to\Delta N}(\mathbf{q},\mathbf{p}) = -\,\frac{f_{\pi N\Delta}f_{\pi NN}}{m^2_\pi}\,\frac{1}{\omega^2_q - e^2}\,\langle\chi'_{1\Delta},\chi'_2|\mathbf{S}_1\cdot\mathbf{q}\;\boldsymbol{\sigma}_2\cdot\mathbf{q}\;\mathbf{T}_1\cdot\boldsymbol{\tau}_2|\chi_1,\chi_2\rangle\ . \tag{3.107}$$

The factor $(\omega^2_q - e^2)^{-1}$ in this amplitude is the Feynman propagator for pions of momentum $\mathbf{q}$ and energy $\pm e$. The $NN\to\Delta N$ transition potential obtained from it is nonlocal due to the dependence of the amplitude on e. In the center of mass frame, the exchanged pion does not transfer energy in $NN\to NN$ and $NN\to\Delta\Delta$ processes. Therefore in those cases the OPEP is local.

At low energies near the threshold of Δ production, $\mathbf{p}'\simeq 0$, $\mathbf{q}\simeq\mathbf{p}$ and $p^2\simeq m_N(m_\Delta - m_N)$ from Eq. (3.104), and from these relations it follows that

$$\omega^2_q \simeq m^2_\pi + m_N(m_\Delta - m_N) \gg e^2 \simeq \frac{1}{4}\,(m_\Delta - m_N)^2\ . \tag{3.108}$$

Therefore we may neglect the e^2 factor in the above amplitude. This gives an approximate local $NN \to \Delta N$ transition potential similar in form to the OPEP and the $NN \to \Delta\Delta$ OPETP, in momentum space

$$\tilde{v}^{\pi}_{NN\to\Delta N}(\mathbf{q}) \simeq -\frac{f_{\pi N\Delta} f_{\pi NN}}{m_\pi^2}\,\mathbf{T}_1\cdot\boldsymbol{\tau}_2\,\frac{\mathbf{S}_1\cdot\mathbf{q}\;\boldsymbol{\sigma}_2\cdot\mathbf{q}}{q^2+m_\pi^2}\;, \tag{3.109}$$

and in configuration space

$$v^{\pi}_{NN\to\Delta N}(\mathbf{r}) \simeq \frac{f_{\pi N\Delta} f_{\pi NN}}{4\pi}\frac{m_\pi}{3}\,\mathbf{T}_1\cdot\boldsymbol{\tau}_2\left[T_\pi(r)S^{II}_{12} + \Big[Y_\pi(r) - \frac{4\pi}{m_\pi^3}\delta(\mathbf{r})\Big]\mathbf{S}_1\cdot\boldsymbol{\sigma}_2\right], \tag{3.110}$$

where the $NN \to \Delta N$ transition tensor operator S^{II}_{12} is defined as

$$S^{II}_{12} = 3\,\mathbf{S}_1\cdot\hat{\mathbf{r}}\;\boldsymbol{\sigma}_2\cdot\hat{\mathbf{r}} - \mathbf{S}_1\cdot\boldsymbol{\sigma}_2\;. \tag{3.111}$$

The $NN \to N\Delta$ transition potentials are obtained by interchanging the particle indices 1 and 2 in the above expressions. The potentials $v^{\pi}_{\Delta N\to NN}$ and $v^{\pi}_{\Delta\Delta\to NN}$ converting the ΔN and $\Delta\Delta$ states back into NN states are the adjoints of the $v^{\pi}_{NN\to\Delta N}$ and $v^{\pi}_{NN\to\Delta\Delta}$, respectively. They are easily obtained by replacing the operators $\mathbf{S}$ and $\mathbf{T}$ in the potentials given in Eqs. (3.110) and (3.102) by $\mathbf{S}^\dagger$ and $\mathbf{T}^\dagger$.

3.12 Two pion-exchange two-nucleon potential

There is an infinite number of two-pion-exchange processes that can contribute to the scattering of two nucleons below the pion production threshold energy. These include the twelve processes obtained by replacing the scalar mesons in the diagrams of Fig. 2.2 by pions, and contain four πNN couplings. An additional 36 processes are obtained by replacing either or both the nucleons in the intermediate states by Δ's. They contain either two $\pi N\Delta$ and two πNN or four $\pi N\Delta$ couplings. In addition we can have infinitely many processes in which higher energy nucleon resonances replace the Δ's or nucleons in the intermediate states. In view of the large number of processes that can contribute to it, a complete calculation of the two-pion-exchange potential between nucleons is difficult even in the limit in which nucleons are treated non-relativistically. Our objective here is to study the spin-isospin dependence and the radial shape of the two-pion-exchange interaction, and determine its strengths later by fitting the observed NN scattering data. This way we obtain semi-phenomenological models of nuclear forces.

We expect that the pion-exchange processes with nucleon intermediate states are approximately represented by the second order contributions of the OPEP. However, the processes with Δ-resonances in the intermediate states, are not included in second order OPEP. Their contribution is approximated by the second order OPETP processes illustrated in Fig. 3.9.

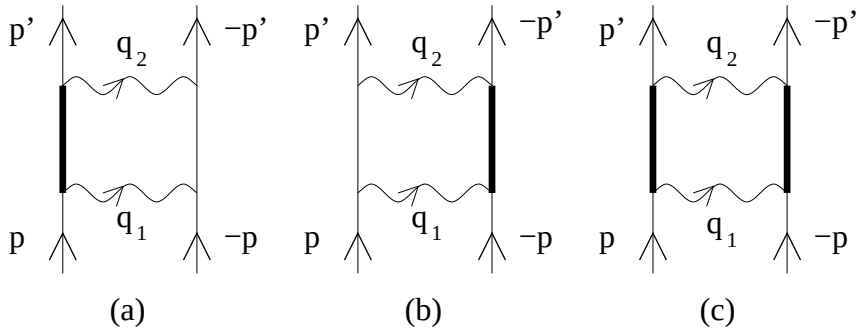

Figure 3.9: The two-pion-exchange two-nucleon interaction via ΔN, $N\Delta$ and $\Delta\Delta$ intermediate states. See caption of Fig. 3.8 for notation.

As mentioned in Sec. 3.5, there is similarity between the strong tensor part of the OPEP and the one-photon exchange interaction between two magnetic dipoles. It is well known that the magnetic field of one of the dipoles can induce a magnetic moment on the other when the interacting bodies are polarizable. The interactions involving the induced moments are described as two-photon exchange potentials. The van der Waals potential between two neutral atoms, due to electrostatic interaction between the induced electric dipole moments of the atoms, is also an example of the two-photon exchange interaction. One can regard the two-pion-exchange interactions shown in Fig. 3.9 in a similar fashion. The pion field of one nucleon polarizes the spins of the quarks in the other nucleon leading to the interaction depicted in diagrams (a) and (b) of Fig. 3.9, while that in diagram (c) is between the two induced polarizations.

The contribution of the 48 two-pion-exchange processes with NN, $N\Delta$, ΔN and $\Delta\Delta$ intermediate states have been calculated explicitly. This calculation is more difficult than that for the simple scalar meson exchange discussed in Sec. 2.5 because the pion-nucleon spin couplings $\boldsymbol{\sigma}_i \cdot \mathbf{q}_1$ and $\boldsymbol{\sigma}_i \cdot \mathbf{q}_2$ do not commute. The isospin, transition-spin and transition-isospin couplings also do not commute. However, taking all the effects together, we find that the sum of the 48 diagrams is well approximated by the sum of the second order contribution of OPEP and OPETP.

The total amplitude due processes (a)-(c) is:

$$\begin{aligned} A^{(2)}_{OPETP} &= 2\sum_{I_1}\langle f|v^{\pi}_{\Delta N\to NN}|I_1\rangle\frac{1}{E-E_{I_1}}\langle I_1|v^{\pi}_{NN\to\Delta N}|i\rangle \\ &+ \sum_{I_2}\langle f|v^{\pi}_{\Delta\Delta\to NN}|I_2\rangle\frac{1}{E-E_{I_2}}\langle I_2|v^{\pi}_{NN\to\Delta\Delta}|i\rangle, \end{aligned} \tag{3.112}$$

where $|I_1\rangle$ and $|I_2\rangle$ are ΔN and $\Delta\Delta$ intermediate states in diagrams (a) and (c), and the first term is doubled to include the contribution of diagram (b) having $N\Delta$ states.

The energy denominators are:

$$E - E_{I_1} = \frac{p^2}{m_N} - (m_\Delta - m_N) - \frac{(m_\Delta + m_N)}{2m_\Delta m_N}(\mathbf{p} - \mathbf{q}_1)^2 , \tag{3.113}$$

$$E - E_{I_2} = \frac{p^2}{m_N} - 2(m_\Delta - m_N) - \frac{(\mathbf{p} - \mathbf{q}_1)^2}{m_\Delta}, \tag{3.114}$$

where $\pm\mathbf{p}$ and $\pm(\mathbf{p} - \mathbf{q}_1)$ are the momenta of the particles in the initial and intermediate state, respectively. Simple estimates are obtained by neglecting the kinetic energies in these denominators so that they become constants equal to $-(m_\Delta - m_N)$ and $-2(m_\Delta - m_N)$. We can then use closure to sum over the intermediate states $|I_1\rangle$ and $|I_2\rangle$ to obtain:

$$\begin{aligned} A^{(2)}_{OPETP} &\simeq \frac{2}{(m_N - m_\Delta)}\langle f|v^\pi_{\Delta N\to NN}v^\pi_{NN\to\Delta N}|i\rangle \\ &+ \frac{1}{2(m_N - m_\Delta)}\langle f|v^\pi_{\Delta\Delta\to NN}v^\pi_{NN\to\Delta\Delta}|i\rangle . \end{aligned} \tag{3.115}$$

The two-pion-exchange potential $v^{2\pi}_\Delta$ is defined so that

$$\langle f|v^{2\pi}_\Delta|i\rangle = A^{(2)}_{OPETP} . \tag{3.116}$$

It reproduces approximately the two-pion-exchange two-nucleon scattering amplitude via intermediate states with one or two Δ-resonances. Comparing the above two equations gives:

$$v^{2\pi}_\Delta(\mathbf{r}) \simeq \frac{2\left[v^\pi_{NN\to\Delta N}(\mathbf{r})\right]^\dagger v^\pi_{NN\to\Delta N}(\mathbf{r})}{m_N - m_\Delta} + \frac{\left[v^\pi_{NN\to\Delta\Delta}(\mathbf{r})\right]^\dagger v^\pi_{NN\to\Delta\Delta}(\mathbf{r})}{2\,(m_N - m_\Delta)} . \tag{3.117}$$

In the OPETP given by Eqs. (3.110) and (3.102) the tensor terms are dominant because the function $T_\pi(r) \gg Y_\pi(r)$ in the region of interest. Keeping only these terms in the OPETP leads to

$$\begin{aligned} v^{2\pi}_\Delta(\mathbf{r}) &= \frac{2}{9}\frac{f^2_{\pi NN}f^2_{\pi N\Delta}}{(4\pi)^2}\frac{m^2_\pi}{(m_N - m_\Delta)}T^2_\pi(r)\,\mathbf{T}^\dagger_1\cdot\boldsymbol{\tau}_2\,\mathbf{T}_1\cdot\boldsymbol{\tau}_2\,\left(S^{II}_{12}\right)^\dagger S^{II}_{12} \\ &+ \frac{1}{18}\frac{f^4_{\pi N\Delta}}{(4\pi)^2}\frac{m^2_\pi}{(m_N - m_\Delta)}T^2_\pi(r)\,\mathbf{T}^\dagger_1\cdot\mathbf{T}^\dagger_2\,\mathbf{T}_1\cdot\mathbf{T}_2\left(S^{III}_{12}\right)^\dagger S^{III}_{12} . \end{aligned} \tag{3.118}$$

Using the identities listed in Eqs. (3.73)–(3.75) gives

$$\mathbf{T}^\dagger_1\cdot\boldsymbol{\tau}_2\;\mathbf{T}_1\cdot\boldsymbol{\tau}_2 = 2 + \frac{2}{3}\boldsymbol{\tau}_1\cdot\boldsymbol{\tau}_2 , \tag{3.119}$$

$$\mathbf{T}^\dagger_1\cdot\mathbf{T}^\dagger_2\;\mathbf{T}_1\cdot\mathbf{T}_2 = \frac{4}{3} - \frac{2}{9}\boldsymbol{\tau}_1\cdot\boldsymbol{\tau}_2 , \tag{3.120}$$

$$\left(S^{II}_{12}\right)^\dagger S^{II}_{12} = 4 - \frac{2}{3}\boldsymbol{\sigma}_1\cdot\boldsymbol{\sigma}_2 + \frac{2}{3}S_{12} , \tag{3.121}$$

$$\left(S^{III}_{12}\right)^\dagger S^{III}_{12} = \frac{10}{3} + \frac{2}{9}\boldsymbol{\sigma}_1\cdot\boldsymbol{\sigma}_2 - \frac{2}{9}S_{12} , \tag{3.122}$$

which, together with the values of the coupling constants given in Sec. 3.10, provide us with an estimate of $v_\Delta^{2\pi}$. It can be conveniently expressed as

$$v_\Delta^{2\pi}(\mathbf{r}) = \sum_{p=1}^{6} I_\Delta^p \, T_\pi^2(r) \, O_{12}^p \ , \tag{3.123}$$

where the six two-body operators O_{12}^p are defined as

$$O_{12}^{p=1,\ldots,6} = 1, \ \boldsymbol{\tau}_1 \cdot \boldsymbol{\tau}_2 \, , \ \boldsymbol{\sigma}_1 \cdot \boldsymbol{\sigma}_2 \, , \ \boldsymbol{\sigma}_1 \cdot \boldsymbol{\sigma}_2 \, \boldsymbol{\tau}_1 \cdot \boldsymbol{\tau}_2 \, , \ S_{12} \, , \ S_{12} \boldsymbol{\tau}_1 \cdot \boldsymbol{\tau}_2 \ . \tag{3.124}$$

The above six operators are also denoted by $O^c, O^\tau, O^\sigma, O^{\sigma\tau}, O^t$ and $O^{t\tau}$ for convenience. The superscript c stands for the central term without spin-isospin dependence, while superscripts τ, σ and t are for $\boldsymbol{\tau}_1 \cdot \boldsymbol{\tau}_2$, $\boldsymbol{\sigma}_1 \cdot \boldsymbol{\sigma}_2$ and tensor terms. Superscripts $\sigma\tau$ and $t\tau$ denote terms that depend on spin as well as isospin.

In the Urbana-Argonne models of the two-nucleon interaction the strengths I^p of the interaction with $T_\pi^2(r)$ radial dependence are obtained by fitting the NN scattering data. Excellent fits to the observed scattering data can be obtained with these models which contain the OPEP, the $I^p \, T_\pi^2(r) \, O_{ij}^P$ terms and a phenomenological short-range core.

Values obtained for the strengths $I_\Delta^{p=1,\ldots,6}$ of the $v_\Delta^{2\pi}$ from Eqs. (3.118)–(3.122) are listed in Table 3.1. This table also reports the strengths $I^{p=1,\ldots,6}$ of the $v^{2\pi}$ in the Argonne v_{18} (AV18) model of the two-nucleon interaction. Some of the differences between the values of I_Δ^p, which take into account only the intermediate states with one or two Δ-resonances, and the I^p determined from experimental data are because the latter includes the contributions of all intermediate states with any resonances. However, a part of the difference is due to the contribution of heavier meson-exchange exchanges. These are not considered explicitly in the AV18, and hence its phenomenological $v^{2\pi}$ part contains their contribution also.

Table 3.1: The strengths of $v_\Delta^{2\pi}$ and $v^{2\pi}$ in the Argonne v_{18} interaction in MeV.

	$v_\Delta^{2\pi}$	$v_{AV18}^{2\pi}$		$v_\Delta^{2\pi}$	$v_{AV18}^{2\pi}$		$v_\Delta^{2\pi}$	$v_{AV18}^{2\pi}$
I^c	-5.20	-8.11	I^σ	$+0.38$	$+0.24$	I^t	-0.38	$+1.18$
I^τ	-0.69	-0.37	$I^{\sigma\tau}$	$+0.20$	$+0.62$	$I^{t\tau}$	-0.20	-0.10

The $v_\Delta^{2\pi}$ accounts for only about 60% of the central potential strength I^c in the phenomenological $v^{2\pi}$. Much of the remaining 40% could come from the attraction due the exchange of a scalar, $T = 0$ meson, which has a large width of 600 to 1000 MeV, and a mass ranging from $\simeq$ 400 to 1200 MeV. In the 2002 compilation of the properties of mesons by the Particle Data Group this meson is denoted by $f_0(600)$ and σ, and it is often considered as a

resonance between two pions which enhances the central component of the two-pion-exchange potential.

The I^t in the Argonne v_{18} is positive, while that in $v_\Delta^{2\pi}$ is small and negative. This difference is likely to be due to the neglect of the one-η-meson exchange in the Argonne model. The η-meson is pseudoscalar, like the pion, but it has a larger mass ($m_\eta = 547$ MeV), and zero isospin. It thus gives rise to a tensor force like the OPEP, but without the $\boldsymbol{\tau}_1 \cdot \boldsymbol{\tau}_2$ isospin dependence, and of shorter range. Most of the $I^t T_\pi^2(r)\ S_{12}$ potential in the AV18 presumably approximates the one-η-meson exchange potential.

Table 3.1 shows that the $v^{2\pi}$ is dominated by an attractive central force, since the I^c is large and negative, while all the other I^p are much smaller in magnitude. However, this is only partly true. The total isospin and spin of two nucleons is denoted by T and S, respectively. Both T and S can have values 0 or 1, giving four two-nucleon isospin-spin states with $TS = 00,\ 01,\ 10$ and 11. Strong interactions conserve T and S, and therefore nuclear forces can also be specified according to TS channels. Interactions in TS states are related to the interaction operator

$$v_{12} = \sum_{p=1}^{6} v^p(r)\ O_{12}^p, \tag{3.125}$$

via the following relations:

$$\begin{aligned} v_{TS} &= v_{TS}^c(r) + \delta_{S,1}\, v_T^t(r)\, S_{12}\,, & (3.126)\\ v_{TS}^c &= v^c + (4T-3)v^\tau + (4S-3)v^\sigma + (4S-3)(4T-3)v^{\sigma\tau}\,, & (3.127)\\ v_T^t &= v^t + (4T-3)v^{t\tau}\ . & (3.128) \end{aligned}$$

The factors $(4S-3)$ and $(4T-3)$ are the eigenvalues of the $\boldsymbol{\sigma}_1 \cdot \boldsymbol{\sigma}_2$ and $\boldsymbol{\tau}_1 \cdot \boldsymbol{\tau}_2$ operators in states with S or $T = 0, 1$, and there is no tensor interaction in $S = 0$ channels according to Eq. (3.39). The seemingly small values of the strengths $I^{p=2,3,4}$ produce a significant channel dependence in the $v_\Delta^{2\pi}$. The values of I_{TS}^c obtained from the I^p for $v_\Delta^{2\pi}$ listed in Table 3.1 are $-2.47, -3.35, -7.63$ and -5.31 MeV for TS =00, 01, 10 and 11, respectively; the corresponding values obtained from the I^p for the AV18 model are $-2.10, -8.63, -11.07$ and -7.63 MeV. The qualitative agreement between the v_{TS}^c obtained from $v_\Delta^{2\pi}$ and the phenomenological $v_{AV18}^{2\pi}$ obtained from the NN scattering data suggests that the former contributes a major part of the two-pion-exchange potential.

In our calculation of the $v_\Delta^{2\pi}$, as well as in the AV18, only terms with the radial shape given by $T_\pi^2(r)$ are included. There are also additional terms with radial shapes $T_\pi(r)\, Y_\pi(r)$ and $Y_\pi^2(r)$. At $r < 1.4$ fm, where the $v^{2\pi}$ becomes important, $T_\pi(r)/Y_\pi(r) > 7$, thus these terms are expected to be smaller. However, more refined models of $v_\Delta^{2\pi}$ should take them into account. The $\delta(\mathbf{r})$-function parts of the OPETP in Eqs. (3.102) and (3.110) are omitted from the calculation of $v_\Delta^{2\pi}$ since the short range part of the interaction between two nucleons

has many other contributions. In semi-phenomenological models it is entirely obtained from fits to two-nucleon scattering data.

The last two decades have witnessed the emergence of chiral effective field theory (χEFT). In χEFT, the symmetries of quantum chromodynamics, in particular its (approximate) chiral symmetry, are used to systematically constrain classes of Lagrangians describing, at low energies, the strong interactions of baryons (nucleons and Δ isobars) with pions (as well as the interactions of these hadrons with electroweak fields). This theory has led to a more fundamental derivation of the two-pion-exchange component of the two-nucleon potential, but will not be discussed in these notes.

3.13 Two pion-exchange three-nucleon P-wave interaction

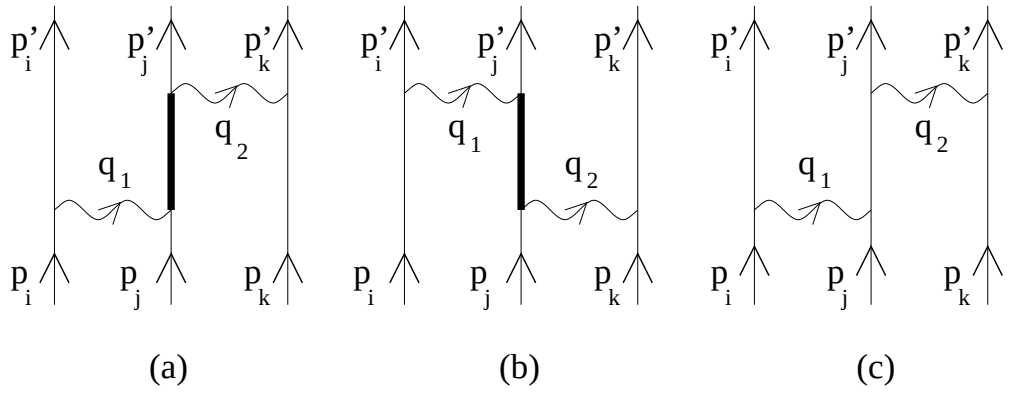

Figure 3.10: The processes (a) and (b) contribute to the two-pion-exchange three-nucleon interaction. The process (c) shows a second order OPEP contribution. See caption of Fig. 3.8 for notation.

The OPETP generate three-nucleon interactions as shown in Fig. 3.10. These were considered by Fujita and Miyazawa (FM) in 1957. They are similar in nature to the three-body force between three magnetic dipoles due to an induced moment on one of them. An other interesting example is the gravitational interaction between the earth, moon and a satellite. In addition to the sum of the three two-body (moon-earth, earth-satellite and satellite-moon) gravitational potentials, it is necessary to consider a three-body potential which depends upon the positions of all the three bodies. It takes into account the change in the gravitational field of the earth due to the polarization of ocean waters via the tides caused by moon's gravity. The three-nucleon potential, denoted by V_{ijk}, is much smaller than the sum $v_{ij} + v_{jk} + v_{ki}$ of pairwise interactions. However, there is a large cancellation

between the positive kinetic energy and the negative pairwise interaction energy of nuclei. Therefore the three-nucleon potentials can give important contributions to nuclear binding, a well known fact by now.

The potential generated by the processes like (a) and (b) in Fig. 3.10 is denoted by $V^{2\pi}_{ijk}(\mathrm{FM})$. It is a part of the two-pion-exchange three-nucleon P-wave interaction, denoted by $V^{2\pi,PW}$, due to the scattering of the pion being exchanged between nucleons i and k by a third nucleon j in the π-N P-wave. The smaller $V^{2\pi,SW}$ due to π-N scattering in relative S-wave is considered in the next section. In the process (c) of Fig. 3.10 the pion is absorbed without excitation by nucleon j and re-emitted. This process is approximately equivalent to v^{π}_{ij} and v^{π}_{jk} acting in succession. To the extent that this is a good approximation, process (c) does not generate a three-nucleon potential.

Figure 3.10 shows only those processes in which nucleon j is excited to the Δ state; other four processes in which nucleons i or k are excited are obtained by cyclic permutation of particle indices $i, j, k \to j, k, i \to k, i, j$. The FM interaction represents the sum of these three cyclic permutations. It is given by

$$\langle f|V^{2\pi}_{ijk}(\mathrm{FM})|i\rangle = \sum_{\mathrm{cyc}}\sum_{I}\Big[\langle f|v^{\pi}_{\Delta N\to NN}(jk)|I\rangle\frac{1}{E-E_I}\langle I|v^{\pi}_{NN\to N\Delta}(ij)|i\rangle + \langle f|v^{\pi}_{\Delta N\to NN}(ji)|I\rangle\frac{1}{E-E_I}\langle I|v^{\pi}_{NN\to N\Delta}(kj)|i\rangle\Big]. \quad (3.129)$$

A simple approximation to $V^{2\pi}_{ijk}(\mathrm{FM})$ is obtained by neglecting the kinetic energies of the particles in the energy denominator $E - E_I$. Without them the denominator is a constant, $m_N - m_\Delta$, and we can use closure to sum over the intermediate states. This leads to

$$V^{2\pi}_{ijk}(\mathrm{FM}) = \sum_{\mathrm{cyc}}\frac{1}{m_N - m_\Delta}\Big[v^{\pi}_{\Delta N\to NN}(jk)v^{\pi}_{NN\to N\Delta}(ij) + v^{\pi}_{\Delta N\to NN}(ji)v^{\pi}_{NN\to N\Delta}(kj)\Big]\ . \quad (3.130)$$

It is convenient to define the following spin-space operators to evaluate the above $V^{2\pi}_{ijk}(\mathrm{FM})$:

$$X_{ij} = T_\pi(r_{ij})\,S_{ij} + Y_\pi(r_{ij})\,\boldsymbol{\sigma}_i\cdot\boldsymbol{\sigma}_j\,, \quad (3.131)$$

$$X^{II}_{ij} = T_\pi(r_{ij})\,S^{II}_{ij} + Y_\pi(r_{ij})\,\mathbf{S}_i\cdot\boldsymbol{\sigma}_j\,, \quad (3.132)$$

where X_{ij} gives the spin-space dependence of the OPEP and X^{II}_{ij} that of OPETP. The $\delta(\mathbf{r})$-function term has been dropped from these operators for reasons mentioned earlier. We obtain:

$$V^{2\pi}_{ijk}(\mathrm{FM}) = -\frac{1}{9}\frac{f^2_{\pi N\Delta}f^2_{\pi NN}}{(4\pi)^2}\frac{m^2_\pi}{m_\Delta - m_N}\sum_{\mathrm{cyc}}\Big(X^{II\dagger}_{jk}\,\mathbf{T}^\dagger_j\cdot\boldsymbol{\tau}_k\,X^{II}_{ji}\,\mathbf{T}_j\cdot\boldsymbol{\tau}_i + X^{II\dagger}_{ji}\,\mathbf{T}^\dagger_j\cdot\boldsymbol{\tau}_i\,X^{II}_{jk}\,\mathbf{T}_j\cdot\boldsymbol{\tau}_k\Big)\,, \quad (3.133)$$

which can be expressed also as

$$V_{ijk}^{2\pi}(\mathrm{FM}) = -\frac{1}{18}\frac{f_{\pi N\Delta}^2 f_{\pi NN}^2}{(4\pi)^2}\frac{m_\pi^2}{m_\Delta - m_N}\sum_{\mathrm{cyc}}\Big[\Big(X_{jk}^{II\dagger}\,X_{ji}^{II} + \mathrm{h.c.}\Big)\Big(\mathbf{T}_j^\dagger\cdot\boldsymbol{\tau}_k\,\mathbf{T}_j\cdot\boldsymbol{\tau}_i + \mathrm{h.c.}\Big) + \Big(X_{jk}^{II\dagger}\,X_{ji}^{II} - \mathrm{h.c.}\Big)\Big(\mathbf{T}_j^\dagger\cdot\boldsymbol{\tau}_k\,\mathbf{T}_j\cdot\boldsymbol{\tau}_i - \mathrm{h.c.}\Big)\Big]\,. \tag{3.134}$$

The transition-spin and -isospin operators can be eliminated from from the $V_{ijk}^{2\pi}(\mathrm{FM})$ using the identities:

$$X_{jk}^{II\dagger}\,X_{ji}^{II} + \mathrm{h.c.} = \frac{2}{3}\Big\{X_{jk}\,,\,X_{ji}\Big\}\,, \tag{3.135}$$

$$X_{jk}^{II\dagger}\,X_{ji}^{II} - \mathrm{h.c.} = -\frac{1}{3}\Big[X_{jk}\,,\,X_{ji}\Big]\,, \tag{3.136}$$

$$\mathbf{T}_j^\dagger\cdot\boldsymbol{\tau}_k\,\mathbf{T}_j\cdot\boldsymbol{\tau}_i + \mathrm{h.c.} = \frac{2}{3}\Big\{\boldsymbol{\tau}_k\cdot\boldsymbol{\tau}_i\,,\,\boldsymbol{\tau}_i\cdot\boldsymbol{\tau}_k\Big\}\,, \tag{3.137}$$

$$\mathbf{T}_j^\dagger\cdot\boldsymbol{\tau}_k\,\mathbf{T}_j\cdot\boldsymbol{\tau}_i - \mathrm{h.c.} = -\frac{1}{3}\Big[\boldsymbol{\tau}_j\cdot\boldsymbol{\tau}_k\,,\,\boldsymbol{\tau}_j\cdot\boldsymbol{\tau}_i\Big]\,, \tag{3.138}$$

derived from Eq. (3.75). This gives the FM potential in the convenient form:

$$V_{ijk}^{2\pi}(\mathrm{FM}) = \sum_{\mathrm{cyc}}\Big[A_{2\pi}^{\mathrm{FM}}\Big\{X_{ij}\,,\,X_{jk}\Big\}\Big\{\boldsymbol{\tau}_i\cdot\boldsymbol{\tau}_j\,,\,\boldsymbol{\tau}_j\cdot\boldsymbol{\tau}_k\Big\} + C_{2\pi}^{\mathrm{FM}}\Big[X_{ij}\,,\,X_{jk}\Big]\Big[\boldsymbol{\tau}_i\cdot\boldsymbol{\tau}_j\,,\,\boldsymbol{\tau}_j\cdot\boldsymbol{\tau}_k\Big]\Big]\,, \tag{3.139}$$

with

$$A_{2\pi}^{\mathrm{FM}} = -\frac{2}{81}\,\frac{f_{\pi N\Delta}^2 f_{\pi NN}^2}{(4\pi)^2}\,\frac{m_\pi^2}{m_\Delta - m_N}\,, \tag{3.140}$$

and

$$C_{2\pi}^{\mathrm{FM}} = \frac{1}{4}\,A_{2\pi}^{\mathrm{FM}}\,. \tag{3.141}$$

Equation (3.140) gives an estimate of $A_{2\pi}^{\mathrm{FM}} = -0.044$ MeV for the strength of the anticommutator part of the FM potential.

The above $V_{jk}^{2\pi}(\mathrm{FM})$ is a part of the $V^{2\pi,PW}$ due to the excitation of nucleon j to the Δ resonance. However, many other π-N P-wave resonances can contribute to the $V^{2\pi,PW}$. We will now show that the total $V^{2\pi,PW}$ retains the form of $V_{ijk}^{2\pi}(\mathrm{FM})$; additional resonances only change the strengths $A_{2\pi}$ and $C_{2\pi}$.

Conservation of angular momentum and isospin implies that the resonance R excited by the capture of a P-wave pion can only have spin $J_R = 1/2$ or $3/2$, and isospin $I_R = 1/2$ or $3/2$. The contribution of the resonance R to the $V^{2\pi,PW}$ can be calculated as in the last section assuming that the πNR coupling has the form

$$H_{\pi NR} = -\frac{f_{\pi NR}}{m_\pi}\Big[\mathbf{S}_R\cdot\Big[\boldsymbol{\nabla}\boldsymbol{\phi}(\mathbf{r})\cdot\mathbf{T}_R\Big] + \mathbf{S}_R^\dagger\cdot\Big[\boldsymbol{\nabla}\boldsymbol{\phi}(\mathbf{r})\cdot\mathbf{T}_R^\dagger\Big]\Big]\,, \tag{3.142}$$

which is the direct generalization of Eqs. (3.10) and (3.66). The operator $\mathbf{S}_R = \boldsymbol{\sigma}$, $\mathbf{S}$ when $J_R = 1/2,\, 3/2$. Similarly $\mathbf{T}_R = \boldsymbol{\tau}$, $\mathbf{T}$ when $I_R = 1/2,\, 3/2$. The interaction generated by a P-wave resonance R has the general form of the FM interaction of Eq. (3.139), *i.e.*

$$V^{2\pi}_{ijk}(\mathrm{R}) = \sum_{\mathrm{cyc}} \left[A^{\mathrm{R}}_{2\pi} \Big\{ X_{ij}\,,\, X_{jk} \Big\} \Big\{ \boldsymbol{\tau}_i \cdot \boldsymbol{\tau}_j\,,\, \boldsymbol{\tau}_j \cdot \boldsymbol{\tau}_k \Big\} + C^{\mathrm{R}}_{2\pi} \Big[X_{ij}\,,\, X_{jk} \Big] \Big[\boldsymbol{\tau}_i \cdot \boldsymbol{\tau}_j\,,\, \boldsymbol{\tau}_j \cdot \boldsymbol{\tau}_k \Big] \right] \,, \quad (3.143)$$

with

$$A^{\mathrm{R}}_{2\pi} = -\frac{1}{18} \frac{f^2_{\pi N\Delta} f^2_{\pi NN}}{(4\pi)^2} \frac{m^2_\pi}{m_\Delta - m_N} \left(\frac{7}{6} - \frac{J_{\mathrm{R}}}{3} \right) \left(\frac{7}{6} - \frac{I_{\mathrm{R}}}{3} \right) \,, \quad (3.144)$$

and

$$C^{\mathrm{R}}_{2\pi} = -\frac{1}{18} \frac{f^2_{\pi N\Delta} f^2_{\pi NN}}{(4\pi)^2} \frac{m^2_\pi}{m_\Delta - m_N} \left(\frac{5}{3} - \frac{4\,J_{\mathrm{R}}}{3} \right) \left(\frac{5}{3} - \frac{4\,I_{\mathrm{R}}}{3} \right) \,. \quad (3.145)$$

The factors $(7/6 - J/3)$ and $(5/3 - 4\,J/3)$ have values 1 each for $J = 1/2$, and they are respectively $2/3$ and $-1/3$ for $J = 3/2$. These factors take into account those in Eqs. (3.135)–(3.138).

The complete $V^{2\pi,PW}$ is just the sum of all the $V^{2\pi}_{ijk}$(PW-R), including the R=Δ of the FM interaction. It obviously has the form

$$V^{2\pi,PW} = \sum_{\mathrm{cyc}} \left[A^{\mathrm{PW}}_{2\pi} \Big\{ X_{ij}\,,\, X_{jk} \Big\} \Big\{ \boldsymbol{\tau}_i \cdot \boldsymbol{\tau}_j\,,\, \boldsymbol{\tau}_j \cdot \boldsymbol{\tau}_k \Big\} + C^{\mathrm{PW}}_{2\pi} \Big[X_{ij}\,,\, X_{jk} \Big] \Big[\boldsymbol{\tau}_i \cdot \boldsymbol{\tau}_j\,,\, \boldsymbol{\tau}_j \cdot \boldsymbol{\tau}_k \Big] \right] \,, \quad (3.146)$$

where the strengths $A^{\mathrm{PW}}_{2\pi}$ and $C^{\mathrm{PW}}_{2\pi}$ are the sums of all P-wave $A^{\mathrm{R}}_{2\pi}$ and $C^{\mathrm{R}}_{2\pi}$, respectively. These strengths have to be determined from experiment. To the extent that the Δ and other $J_R = I_R = 3/2$ resonances dominate $V^{2\pi,PW}$ we may expect $A^{\mathrm{PW}}_{2\pi} \simeq 4\, C^{\mathrm{PW}}_{2\pi}$.

3.13.1 The FM interaction in time-ordered perturbation theory

In this subsection we will recalculate the FM interaction of Eqs. (3.139)–(3.141) using time-ordered perturbation theory instead of the OPETP. When the nucleon and Δ kinetic energies are neglected, we recover the result of the last section justifying the use of OPETP to calculate three-nucleon interactions mediated by N-Δ excitations.

In time-ordered perturbation theory there are 24 diagrams that contribute to the FM interaction. They can be divided into two groups of 12 diagrams, F.1 to F.12 and M.1 to M.12. The diagrams F.1 to F.12 are shown in Fig. 3.11. In these diagrams the pion with momentum $\mathbf{q}_1$ and isospin α—here α specifies the cartesian component of the isospin-one pion field with $\alpha = x, y$ or z rather than its charge state, as in Eq. (3.84)—is either emitted or absorbed by nucleon i. This pion excites the nucleon j to the Δ state. The second pion, $\mathbf{q}_2$, β with $\beta = x, y$ or z de-excites the Δ, and is absorbed or emitted by nucleon k. Let t_1 and t'_1 denote the time when pion "1" interacts with nucleons i and j respectively, while t_2

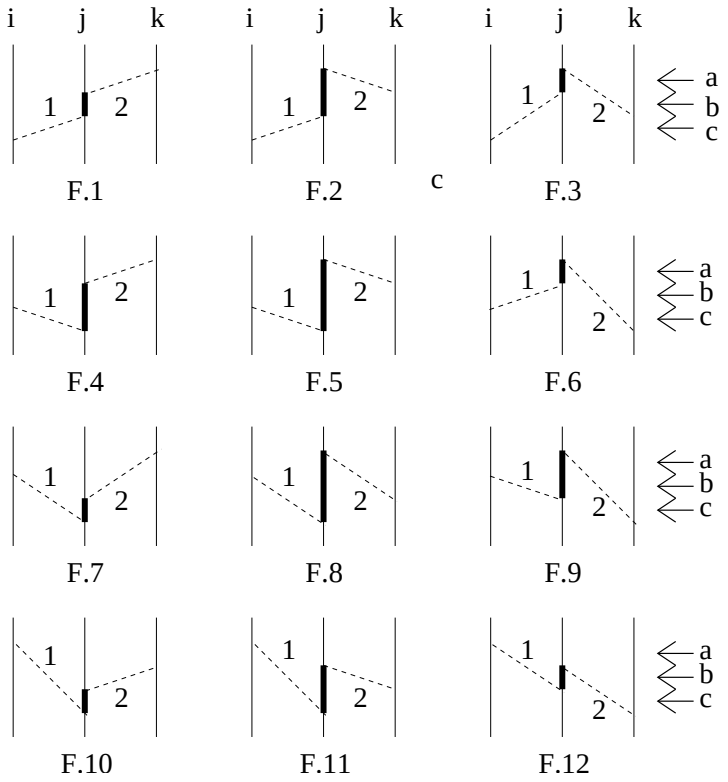

Figure 3.11: The time-ordered diagrams F.I which contribute to the Fujita-Miyazawa interaction. The pion "1" carries a momentum $\mathbf{q}_1$ from nucleon i to j, while "2" carries $\mathbf{q}_2$ from j to k. The positions of the three energy denominators are marked by a, b and c. See caption of Fig. 3.8 for notation.

and t_2' denote the times when pion "2" interacts with nucleons k and j. The 24 diagrams that contribute to the FM interaction are those in which the times t_1, t_1', t_2 and t_2' occur in all possible orders. The 12 F.I diagrams shown in Fig. 3.7 have $t_2' > t_1'$, while the M.I diagrams have $t_1' > t_2'$.

The contributions of diagrams F.1 to F.12 to the three-nucleon scattering amplitude are given by

$$\begin{aligned} A_{3N} &= \sum_{\alpha,\beta} \frac{f_{\pi NN}^2}{m_\pi^2} \frac{f_{\pi N\Delta}^2}{m_\pi^2} \frac{1}{4\,\omega_1\omega_2} \left[\sum_{I=1}^{12} \frac{1}{\text{product } D(\text{F.I})} \right] \langle \chi_k' | \boldsymbol{\sigma}_k \cdot \mathbf{q}_2\, \tau_{k,\beta} | \chi_k \rangle \\ &\times \langle \chi_j' | \mathbf{S}_j^\dagger \cdot \mathbf{q}_2\, \mathbf{S}_j \cdot \mathbf{q}_1 T_{j,\beta}^\dagger\, T_{j,\alpha} | \chi_j \rangle \langle \chi_i' | \boldsymbol{\sigma}_i \cdot \mathbf{q}_1\, \tau_{i,\alpha} | \chi_i \rangle \ , \end{aligned} \tag{3.147}$$

Here $\chi_{i,j,k}$ and $\chi'_{i,j,k}$ denote the initial and final spin-isospin states of nucleons i, j and k, and product D(F.I) is the product of the three energy denominators in diagram F.I. The values of product D(F.I) can be read off the diagrams F.I in Fig. 3.11. They are listed in Table 3.2

neglecting nucleon and Δ kinetic energies and using $m_{\Delta N} \equiv m_\Delta - m_N$. From Table 3.2 we can easily verify that

$$\sum_{I=1}^{12} \frac{1}{\text{product } D(F.I)} = -\frac{4}{\omega_1\,\omega_2 m_{\Delta N}} \ . \tag{3.148}$$

Substituting this in Eq. (3.147) and summing over α, β lead to

$$A_{3N} = -\frac{f_{\pi NN}^2}{m_\pi^2}\frac{f_{\pi N\Delta}^2}{m_\pi^2}\frac{1}{\omega_1^2\,\omega_2^2\,m_{\Delta N}}\langle \chi_k', \chi_j', \chi_i' | \boldsymbol{\sigma}_k \cdot \mathbf{q}_2\, \mathbf{S}_j^\dagger \cdot \mathbf{q}_2\, \mathbf{S}_j \cdot \mathbf{q}_1\, \boldsymbol{\sigma}_i \cdot \mathbf{q}_1 \boldsymbol{\tau}_k \cdot \mathbf{T}_j^\dagger\, \mathbf{T}_j \cdot \boldsymbol{\tau}_i | \chi_k, \chi_j, \chi_i \rangle \ , \tag{3.149}$$

and this equation is identical to that corresponding to diagram (a) of Fig. 3.10 expressing the FM interaction with OPETP. The contribution of all the time ordered diagrams M.I equals that of the diagram (b) of Fig. 3.10, and the sum of F.I and M.I contributions gives the same $V_{ijk}^{2\pi}$(FM) in Eq. (3.139) obtained earlier.

Table 3.2: The values of $-1/[\text{product } D(\text{F.I})]$

I	$-1/[\text{product } D(\text{F.I})$	I	$-1/[\text{product } D(\text{F.I})$
1	$\omega_2\, m_{\Delta N}\, \omega_1$	2	$(m_{\Delta N} + \omega_2)\, m_{\Delta N}\, \omega_1$
3	$(m_{\Delta N} + \omega_2)\, (\omega_1 + \omega_2)\, \omega_1$	4	$\omega_2\, m_{\Delta N}\, (m_{\Delta N} + \omega_1)$
5	$(\omega_2 + m_{\Delta N})\, m_{\Delta N}\, (\omega_1 + m_{\Delta N})$	6	$(\omega_2 + m_{\Delta N})\, (\omega_1 + \omega_2)\, \omega_2$
7	$\omega_2\, (\omega_1 + \omega_2)\, (\omega_1 + m_{\Delta N})$	8	$(\omega_2 + m_{\Delta N})\, (\omega_1 + \omega_2 + m_{\Delta N})\, (\omega_1 + m_{\Delta N})$
9	$(\omega_2 + m_{\Delta N})\, (\omega_1 + \omega_1 + m_{\Delta N})\, \omega_2$	10	$\omega_1\, (\omega_1 + \omega_2)\, (\omega_1 + m_{\Delta N})$
11	$\omega_1\, (\omega_1 + \omega_2 + m_{\Delta N})\, (\omega_1 + m_{\Delta N})$	12	$\omega_1\, (\omega_1 + \omega_2 + m_{\Delta N})\, \omega_2$

3.13.2 The FM interaction using π-N scattering data

The calculation of the $V_{ijk}^{2\pi}$(FM) described above uses the Δ mass and $\pi N\Delta$ coupling constant obtained from the π-N scattering data. It would be more desirable to use the π-N scattering data directly in order to predict the $V_{ijk}^{2\pi}$(FM). Such attempts have been reviewed by Friar in 1999. It is difficult to make a direct connection between the observed π-N scattering data and $V_{ijk}^{2\pi}$(FM), because the former is for real pions, while the pions that generate the FM interaction are virtual. In this subsection we illustrate this problem with a simple model.

The model assumes that π-N scattering is only due to πNN and $\pi N\Delta$ couplings, and that these couplings are weak so that perturbation theory is applicable. The four diagrams that contribute to the π-N scattering amplitude in this model are shown in Fig. 3.12. The processes N.1 and N.2 have only nucleon intermediate states, and they do not contribute

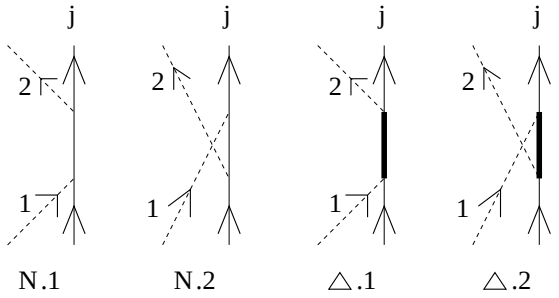

Figure 3.12: The four time-ordered diagrams which contribute to the scattering of low-energy pions by nucleons. See caption of Fig. 3.8 for notation.

to the three-nucleon interaction. The contribution of diagrams $\Delta.1$ and $\Delta.2$ for absorption (emission) of a pion of isospin $\hat{\mathbf{e}}_\alpha$ ($\hat{\mathbf{e}}_\beta$) is given by

$$\begin{aligned} A_{\pi N}(\alpha,\beta) = & -\frac{f^2_{\pi N\Delta}}{m^2_\pi}\frac{1}{m_{\Delta N}-\omega_1}\langle\chi'_j|\mathbf{S}^\dagger_j\cdot\mathbf{q}_2\,\mathbf{S}_j\cdot\mathbf{q}_1\,T^\dagger_{j,\beta}\,T_{j,\alpha}|\chi_j\rangle \\ & -\frac{f^2_{\pi N\Delta}}{m^2_\pi}\frac{1}{m_{\Delta N}+\omega_2}\langle\chi'_j|\mathbf{S}^\dagger_j\cdot\mathbf{q}_1\,\mathbf{S}_j\cdot\mathbf{q}_2\,T^\dagger_{j,\alpha}\,T_{j,\beta}|\chi_j\rangle\ . \end{aligned} \tag{3.150}$$

For the sake of simplicity we consider the amplitude above in the limit $|\mathbf{q}_1|$ and $|\mathbf{q}_2|\to 0$. In this limit $\omega_1\simeq\omega_2\simeq m_\pi$, and the π-N amplitude becomes

$$\begin{aligned} A_{\pi N}(\alpha,\beta) \ = & \ -\frac{8}{9}\frac{f^2_{\pi N\Delta}}{m^2_\pi}\frac{m_{\Delta N}}{m^2_{\Delta N}-m^2_\pi}\langle\chi'_j|\mathbf{q}_1\cdot\mathbf{q}_2\,\hat{\mathbf{e}}_\alpha\cdot\hat{\mathbf{e}}_\beta-\frac{1}{4}\boldsymbol{\sigma}_j\cdot(\mathbf{q}_1\times\mathbf{q}_2)\ \boldsymbol{\tau}_j\cdot(\hat{\mathbf{e}}_\alpha\times\hat{\mathbf{e}}_\beta)\,|\chi_j\rangle \\ & -\ i\frac{4}{9}\frac{f^2_{\pi N\Delta}}{m^2_\pi}\frac{m_\pi}{m^2_{\Delta N}-m^2_\pi}\langle\chi'_j|\boldsymbol{\sigma}_j\cdot(\mathbf{q}_1\times\mathbf{q}_2)\ \hat{\mathbf{e}}_\alpha\cdot\hat{\mathbf{e}}_\beta+\mathbf{q}_1\cdot\mathbf{q}_2\,\boldsymbol{\tau}_j\cdot(\hat{\mathbf{e}}_\alpha\times\hat{\mathbf{e}}_\beta)\,|\chi_j\rangle\ , \end{aligned} \tag{3.151}$$

where $\hat{\mathbf{e}}_\alpha$ are unit vectors along $\alpha=x,y$, or z in isospin space. The second term of the above $A_{\pi N}(\alpha,\beta)$ is odd under the exchange $\mathbf{q}_1,\hat{\mathbf{e}}_\alpha\rightleftharpoons\mathbf{q}_2,\hat{\mathbf{e}}_\beta$ and therefore, after summing over all the time orderings of pions "1" and "2" (see previous section), does not contribute to the three-nucleon interaction. The first term of $A_{\pi N}(\alpha,\beta)$ is denoted by the operator

$$O_{\pi N}(j;\alpha,\beta)=b\ \mathbf{q}_1\cdot\mathbf{q}_2\,\hat{\mathbf{e}}_\alpha\cdot\hat{\mathbf{e}}_\beta-d\ \boldsymbol{\sigma}_j\cdot(\mathbf{q}_1\times\mathbf{q}_2)\ \boldsymbol{\tau}_j\cdot(\hat{\mathbf{e}}_\alpha\times\hat{\mathbf{e}}_\beta)\ , \tag{3.152}$$

where in our model the constants b and d have the values

$$b \ = \ -\frac{8}{9}\frac{f^2_{\pi N\Delta}}{m^2_\pi}\frac{m_{\Delta N}}{m^2_{\Delta N}-m^2_\pi}\ , \tag{3.153}$$

$$d \ = \ -\frac{2}{9}\frac{f^2_{\pi N\Delta}}{m^2_\pi}\frac{m_{\Delta N}}{m^2_{\Delta N}-m^2_\pi}\ . \tag{3.154}$$

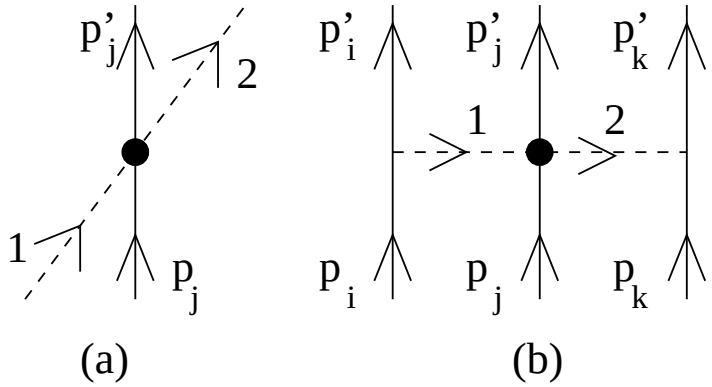

Figure 3.13: Feynman diagram (a) shows the scattering of pion "1" by nucleon j due to S-wave interaction represented by the black dot. The diagram (b) shows the three-nuclon interaction via a similar scattering of the pion being exchanged by nucleons i and k.

The two-pion-exchange three-nucleon interaction obtained by approximating the scattering of the virtual pions by the $O_{\pi N}(j)$ is denoted by $V^{2\pi}(\mathrm{FM};\pi N)$ with

$$V^{2\pi}(\mathrm{FM};\pi N) = \sum_{\alpha,\beta} \frac{f^2_{\pi NN}}{m^2_\pi} \frac{1}{\omega_1^2\,\omega_2^2} \boldsymbol{\sigma}_i \cdot \mathbf{q}_1\, \boldsymbol{\tau}_i \cdot \hat{\mathbf{e}}_\alpha O_{\pi N}(j;\alpha,\beta) \boldsymbol{\sigma}_k \cdot \mathbf{q}_2\, \boldsymbol{\tau}_k \cdot \hat{\mathbf{e}}_\beta \ , \tag{3.155}$$

where the factor $1/(\omega_1^2\,\omega_2^2)$ comes from the pion propagators, and the other factors describe the coupling of the pions to the nucleons i and k. Comparing the $V^{2\pi}(\mathrm{FM};\pi N)$ with the exact $V^{2\pi}(\mathrm{FM})$ we find that the former contains the factor $2m_{\Delta N}/(m^2_{\Delta N} - m^2_\pi)$ instead of $2/m_{\Delta N}$. Since $m_{\Delta N} \simeq 2\,m_\pi$, the $V^{2\pi}(\mathrm{FM};\pi N)$ is too strong by $\simeq 33\%$. The difference comes because the energy denominators in the π-N scattering amplitude (3.150) contain the real pion energies.

Note that the difference between $V^{2\pi}(\mathrm{FM};\pi N)$ and $V^{2\pi}(\mathrm{FM})$ is of order $m^2_\pi/m^2_{\Delta N}$ and will vanish in the so called chiral limit $m_\pi \to 0$. However, in the context of the nuclear many-body problem m_π is not small. The range of OPEP is smaller than the mean inter-nucleon spacing in nuclei, and the energies required to excite nucleons are not much larger than m_π. The pion mass, $\simeq 138$ MeV, is obviously very large compared to nuclear energy scales of few MeV.

3.14 Two pion-exchange three-nucleon S-wave interaction

The S-wave pion-nucleon interaction is believed to be weak and short ranged. It is generally discussed in the framework of chiral perturbation theory. It cannot depend on nucleon spin

since S-wave pions do not have any angular momentum. The scattering amplitude shown in panel (a) of Fig. 3.13 can be parameterized as

$$A_{\pi N}^{\rm SW} = [a_c\,\delta_{\alpha,\beta} + a_{tt}\,\hat{\mathbf{e}}_\alpha{\cdot}\hat{\mathbf{e}}_\beta + i\,a_{tt\tau}\boldsymbol{\tau}_j\cdot(\hat{\mathbf{e}}_\alpha\times\hat{\mathbf{e}}_\beta)]\ , \tag{3.156}$$

where the coefficients a_c, a_{tt} and $a_{tt\tau}$ can depend upon the momentum of the pion, and approach constant values at small momenta. Here we neglect the momentum dependence of these coefficients. All the π-N S-wave interactions are represented by the "dot" in Fig. 3.13. These include the direct and crossed pion scattering via S-wave resonances as well as boson exchange interactions between pions and nucleons.

In the last subsection we argued that it is difficult to calculate the strength of the large $V_{ijk}^{2\pi}$(PW) from the π-N scattering data, and that it is better to determine it from nuclear data. This is mainly due to the fact that m_π is not much smaller than $m_\Delta - m_N$. In contrast, the $V_{ijk}^{2\pi,SW}$ has been calculated approximately from the π-N scattering data for the following two reasons. The first is that the nucleon resonances that can contribute to π-N S-wave scattering must have spin-parity $1/2^-$. Their masses $m^*_{1/2^-}$ are in excess of 1500 MeV, and so

$$\frac{m_\pi^2}{(m^*_{1/2^-}-m_N)^2} < 0.07\ . \tag{3.157}$$

Therefore the $m_\pi \to 0$ limit is more accurate for the $V_{ijk}^{2\pi}$(SW).

The second reason is that $V_{ijk}^{2\pi}$(SW) is very weak, and has little effect on nuclear binding energies. It is difficult to determine its strength from nuclear data.

The $A_{\pi N}^{\rm SW}$ contributes to the three-nucleon scattering amplitude via the Feynman diagram (b) shown in Fig. 3.13. It includes the sum of all time orderings. The contribution of the first term is given by:

$$\begin{aligned} A_{3N}^{\rm SW}(a_c) &= 2\,\frac{f_{\pi NN}^2}{m_\pi^2}\,a_c\sum_{\alpha,\beta}\frac{\boldsymbol{\sigma}_k\cdot\mathbf{q}_2}{m_\pi^2+q_2^2}\,\boldsymbol{\tau}_k\cdot\hat{\mathbf{e}}_\beta\,\delta_{\beta,\alpha}\,\hat{\mathbf{e}}_\alpha\cdot\boldsymbol{\tau}_i\frac{\boldsymbol{\sigma}_i\cdot\mathbf{q}_1}{m_\pi^2+q_1^2}\ , \\ &= 2\,\frac{f_{\pi NN}^2}{m_\pi^2}\,a_c\,\boldsymbol{\tau}_k\cdot\boldsymbol{\tau}_i\,\frac{\boldsymbol{\sigma}_k\cdot\mathbf{q}_2}{m_\pi^2+q_2^2}\,\frac{\boldsymbol{\sigma}_i\cdot\mathbf{q}_1}{m_\pi^2+q_1^2}\ . \end{aligned} \tag{3.158}$$

Let the $\mathbf{p}_{i,j,k}$ denote the initial and $\mathbf{p}'_{i,j,k}$ the final momenta of the nucleons i,j and k. The pion momenta are given by:

$$\mathbf{q}_1 = \mathbf{p}_i - \mathbf{p}'_i\ , \qquad \mathbf{q}_2 = \mathbf{p}'_k - \mathbf{p}_k\ , \tag{3.159}$$

and

$$\mathbf{p}_j - \mathbf{p}'_j = \mathbf{q}_2 - \mathbf{q}_1\ . \tag{3.160}$$

The three-nucleon potential due to the a_c term in the S-wave amplitude is the Fourier transform of $A_{3N}(a_c)$:

$$V_{ijk}^{2\pi}({\rm SW};a_c) = \sum_{\rm cyc}\int\frac{d^3q_1}{(2\pi)^3}\frac{d^3q_2}{(2\pi)^3}e^{-i\mathbf{q}_1\cdot\mathbf{r}_{ij}}e^{-i\mathbf{q}_2\cdot\mathbf{r}_{jk}}\,A_{3N}(a_c)\ . \tag{3.161}$$

We note that:

$$\int \frac{d^3q}{(2\pi)^3}\,\boldsymbol{\sigma}\cdot\mathbf{q}\,\frac{e^{-i\mathbf{q}\cdot\mathbf{r}}}{m_\pi^2+q^2} = \frac{i}{4\pi}\,m_\pi\,\boldsymbol{\sigma}\cdot\boldsymbol{\nabla}\,Y_\pi(r) = -\frac{i}{4\pi}\,m_\pi^2\,\boldsymbol{\sigma}\cdot\hat{\mathbf{r}}\,Z(r)\ , \tag{3.162}$$

where the function $Z(r)$ is defined as

$$Z(r) = \left(1+\frac{1}{m_\pi r}\right)Y_\pi(r)\ , \tag{3.163}$$

so that

$$V_{ijk}^{2\pi}(\mathrm{SW};a_c) = -2\,\frac{f_{\pi NN}^2}{(4\pi)^2}\,a_c\,m_\pi^2\sum_{\mathrm{cyc}} Z(r_{ij})\,Z(r_{jk})\,\boldsymbol{\tau}_i\cdot\boldsymbol{\tau}_k\,\boldsymbol{\sigma}_i\cdot\hat{\mathbf{r}}_{ij}\,\boldsymbol{\sigma}_k\cdot\hat{\mathbf{r}}_{jk}\ . \tag{3.164}$$

The isospin dependence of the $V_{ijk}^{2\pi}(\mathrm{SW};a_{tt})$ due to the a_{tt} term in the $A_{\pi N}^{\mathrm{SW}}$, Eq. (3.156), is the same as that of $V^{2\pi,SW}(a_c)$, since

$$\sum_{\alpha,\beta}\boldsymbol{\tau}_k\cdot\hat{\mathbf{e}}_\beta\,\hat{\mathbf{e}}_\beta\cdot\hat{\mathbf{e}}_\alpha\,\hat{\mathbf{e}}_\alpha\cdot\boldsymbol{\tau}_i = \boldsymbol{\tau}_k\cdot\boldsymbol{\tau}_i\ , \tag{3.165}$$

and therefore the sum of $V_{ijk}^{2\pi}(\mathrm{SW};a_c)+V_{ijk}^{2\pi}(\mathrm{SW};a_{tt})$ is obtained simply by replacing the a_c by a_c+a_{tt} in Eq. (3.164).

The contributions of the $a_{\tau tt}$ term contain equal and apposite parts with isospin factors $\boldsymbol{\tau}_j\cdot(\boldsymbol{\tau}_i\times\boldsymbol{\tau}_k)$ and $\boldsymbol{\tau}_j\cdot(\boldsymbol{\tau}_k\times\boldsymbol{\tau}_i)$ which cancel out. Therefore the total $V^{2\pi,SW}$ can be expressed as

$$V^{2\pi,SW} = -\frac{f_{\pi NN}^2}{(4\pi)^2}a'\,m_\pi^2\sum_{\mathrm{cyc}} Z(r_{ij})\,Z(r_{jk})\,\boldsymbol{\tau}_i\cdot\boldsymbol{\tau}_k\,\boldsymbol{\sigma}_i\cdot\hat{\mathbf{r}}_{ij}\,\boldsymbol{\sigma}_k\cdot\hat{\mathbf{r}}_{jk}\ . \tag{3.166}$$

with $a'=2(a_c+a_{tt})$. Ideally the strength parameter a' should be determined from three-nucleon scattering data or nuclear binding energies. However, as mentioned earlier, this interaction is very small compared with the $V^{2\pi,PW}$, and it is difficult to obtain its strength from nuclear binding energies. The parameter a' has been extracted from low-energy π-N scattering data. Present estimates give

$$A_{2\pi}^{SW} = \frac{f_{\pi NN}^2}{(4\pi)^2}a'\,m_\pi^2 \simeq -1\,\mathrm{MeV}\ . \tag{3.167}$$

3.15 Three pion-exchange three-nucleon interaction

The various three-pion-exchange processes that can contribute to the three-nucleon interaction are shown in Fig. 3.14. Here we consider only the $N\to\Delta$ excitations because Δ is the strongest resonance in π-N scattering. Our objective is to study the spin-isospin dependence

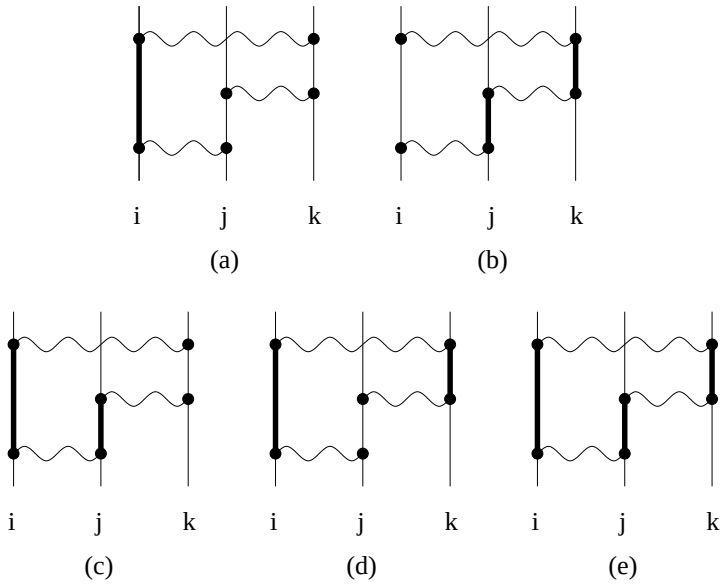

Figure 3.14: Three-pion-exchange ring diagrams with pion-exchange transition potentials.

of this interaction, and find a useful approximation. The full interaction has a very complex structure.

The processes (a) and (b) of Fig. 3.14 are pion-exchange ring diagrams with one Δ excitation at a time. We will estimate their contribution in this section. The pion-exchange rings (c), (d) and (e) have two Δ's at a time and are not considered in detail. All the ring diagrams lead to interactions of range of order $\exp[-m_\pi(r_{ij}+r_{jk}+r_{ki})]$.

The potentials generated by diagrams of type (a) and (b) are respectively denoted by $V_1^{3\pi,\Delta R}$ and $V_2^{3\pi,\Delta R}$, and their sum $V^{3\pi,\Delta R}$ gives the contribution of ring diagrams with one Δ at each time. After neglecting the kinetic energies of the nucleons and the Δ in the intermediate states, diagram (a) gives:

$$V_{1,ijk}^{3\pi,\Delta R} = \sum_{\rm cyc} \frac{1}{(m_\Delta - m_N)^2} \left[v^\pi_{\Delta N\to NN}(ik)\; v^\pi_{jk}\; v^\pi_{NN\to\Delta N}(ij) \;+\; j \rightleftharpoons k \right] \;, \tag{3.168}$$

where $j \rightleftharpoons k$ denotes the term obtained by interchanging j and k in the previous term. The above $V_1^{3\pi,\Delta R}$ can be reduced to a three-nucleon operator by eliminating the transition spin and isospin operators in the OPETP using Eqs. (3.73)–(3.75). It is useful to reduce the $V_1^{3\pi,\Delta R}$ further by eliminating all the terms quadratic in either $\boldsymbol{\tau}_l$ or $\boldsymbol{\sigma}_l$ ($l = i,j,k$) with the Pauli identity, Eq. (3.31). The resulting $V_1^{3\pi,\Delta R}$ contains very many terms which can be organized in the following way:

$$V_{1,ijk}^{3\pi,\Delta R} = A_{3\pi}^{\Delta R}\, O_{1,ijk}^{3\pi,\Delta R} \;, \tag{3.169}$$

where

$$A_{3\pi}^{\Delta R} = \frac{1}{27}\frac{f_{\pi NN}^6}{(4\pi)^3}\frac{f_{\pi N\Delta}^2}{f_{\pi NN}^2}\ \frac{m_\pi^3}{(m_\Delta - m_N)^2}\ , \tag{3.170}$$

and

$$O_{1,ijk}^{3\pi,\Delta R} = 6\left(S_\tau^I S_\sigma^I + A_\tau^I A_\sigma^I\right) + 2\sum_{\rm cyc}\left(S_\sigma^I S_{\tau,ijk}^D + S_\tau^I S_{\sigma,ijk}^D + A_\tau^I A_{\sigma,ijk}^D + S_{\tau,ijk}^D S_{\sigma,ijk}^D\right)\ . \tag{3.171}$$

The letters S and A denote operators that are symmetric and antisymmetric under the exchange of j with k. Subscripts τ and σ label operators containing isospin and spin-space parts respectively, while superscripts I and D indicate operators that are independent or dependent on the cyclic permutation of ijk. The interaction $V_1^{3\pi,\Delta R}$ has to be symmetric under the exchange of i, j, and k, therefore products of S- and A-type operators are not allowed.

The permutation-independent isospin operators are:

$$S_\tau^I = 2 + \frac{2}{3}\left(\boldsymbol{\tau}_i\cdot\boldsymbol{\tau}_j + \boldsymbol{\tau}_j\cdot\boldsymbol{\tau}_k + \boldsymbol{\tau}_k\cdot\boldsymbol{\tau}_i\right) = 4P_{T=3/2}\ , \tag{3.172}$$

$$A_\tau^I = \frac{i}{3}\,\boldsymbol{\tau}_i\cdot\boldsymbol{\tau}_j\times\boldsymbol{\tau}_k = \frac{1}{6}\left[\boldsymbol{\tau}_i\cdot\boldsymbol{\tau}_j\ ,\ \boldsymbol{\tau}_i\cdot\boldsymbol{\tau}_k\right]\ . \tag{3.173}$$

They occur in all the three cyclic permutations of diagram (a) as well as in those obtained by interchanging j and k in diagram (a). Therefore their contribution gets multiplied by six in Eq. (3.171). In Eq. (3.172) we have indicated that S_τ^I is a projection operator for the isospin 3/2 state of three nucleons. Therefore the $V^{3\pi,\Delta R}$ interaction is much stronger in isospin 3/2 triplets, and one can identify its presence in nuclei. The A_τ^I, Eq. (3.173), also occurs in the commutator part of $V_{ijk}^{2\pi}$(FM) in Eq. (3.139).

The permutation-dependent isospin operators are:

$$S_{\tau,ijk}^D = \frac{2}{3}\boldsymbol{\tau}_j\cdot\boldsymbol{\tau}_k\ , \tag{3.174}$$

$$A_{\tau,ijk}^D = 0\ . \tag{3.175}$$

The spin-space operators have many terms, and explicit expression for them, obtained after a long but straightforward calculation starting from Eq. (3.168), are listed in the original paper [Pieper *et al.*, PRC**64**, 014001 (2001)].

The $V_{2,ijk}^{3\pi,\Delta R}$ obtained from diagram (b) in Fig. 3.14, after neglecting the kinetic energies, is given by

$$V_{2,ijk}^{3\pi,\Delta R} = \sum_{\rm cyc}\frac{1}{(m_\Delta - m_N)^2}\left[v_{N\Delta\to NN}^\pi(ik)\ v_{\Delta N\to N\Delta}^\pi(jk)\ v_{NN\to N\Delta}^\pi(ij)\ +\ j\rightleftharpoons k\right]\ . \tag{3.176}$$

After appropriate reductions, it can be cast in the form of $V_{1,ijk}^{3\pi,\Delta R}$ as follows

$$V_{2,ijk}^{3\pi,\Delta R} = A_{2,3\pi}^{\Delta R}\, O_{2,ijk}^{3\pi,\Delta R} \ , \tag{3.177}$$

with

$$A_{2,3\pi}^{\Delta R} = A_{3\pi}^{\Delta R} \frac{f_{\pi N\Delta}^2}{f_{\pi NN}^2} \ , \tag{3.178}$$

and

$$O_{2,ijk}^{3\pi,\Delta R} = \frac{8}{3} S_\tau^I S_\sigma^I + \frac{2}{3} A_\tau^I A_\sigma^I - \frac{4}{9} \sum_{\rm cyc} \left(S_\sigma^I S_{\tau,ijk}^D + S_\tau^I S_{\sigma,ijk}^D + A_\tau^I A_{\sigma,ijk}^D - \frac{1}{2} S_{\tau,ijk}^D S_{\sigma,ijk}^D \right) \ . \tag{3.179}$$

The $V_{1,ijk}^{3\pi,\Delta R}$ and $V_{2,ijk}^{3\pi,\Delta R}$ may be approximately combined using $f_{\pi N\Delta}^2 \sim 4\, f_{\pi NN}^2$ to obtain

$$V_{ijk}^{3\pi,\Delta R} = A_{3\pi}^{\Delta R} \left(O_{1,ijk}^{3\pi,\Delta R} + 4\, O_{2,ijk}^{3\pi,\Delta R} \right) = A_{3\pi}^{\Delta R} O_{ijk}^{3\pi,\Delta R} \ , \tag{3.180}$$

where

$$O_{ijk}^{3\pi,\Delta R} = \frac{50}{3} S_\tau^I S_\sigma^I + \frac{26}{3} A_\tau^I A_\sigma^I + \frac{2}{9} \sum_{\rm cyc} \left(S_\sigma^I S_{\tau,ijk}^D + S_\tau^I S_{\sigma,ijk}^D + A_\tau^I A_{\sigma,ijk}^D - 13\ S_{\tau,ijk}^D S_{\sigma,ijk}^D \right) \ . \tag{3.181}$$

The strengths of the terms independent of cyclic permutations are larger than those which depend upon them. Therefore we may use the simpler $V_{ijk}^{3\pi,\Delta R}$ obtained by neglecting them, *i.e.* with the approximate operator

$$O_{ijk}^{3\pi,\Delta R} \simeq \frac{50}{3} S_\tau^I S_\sigma^I + \frac{26}{3} A_\tau^I A_\sigma^I \ . \tag{3.182}$$

The value of $A_{3\pi}^{\Delta R}$ estimated from the observed values of the constants is $\simeq 0.002$ MeV. However, this estimate is not robust due to neglect of diagrams (c), (d) and (e) of Fig. 3.14, of π-N resonances other than the Δ, and of the kinetic energies in the energy denominators. In practice $A_{3\pi}^{\Delta R}$ is determined from nuclear data.

3.16 Isotensor components of the one pion-exchange potential

The small difference between the masses $m_\pi^\pm$ of the charged pions, and m_π^0 of the neutral pion have been neglected so far in our calculations of the one pion-exchange potential. We also considered isoscalar πNN coupling in Eq. (3.10) invariant under rotations in the isospin space. The OPEP calculated within these approximations is naturally isoscalar.

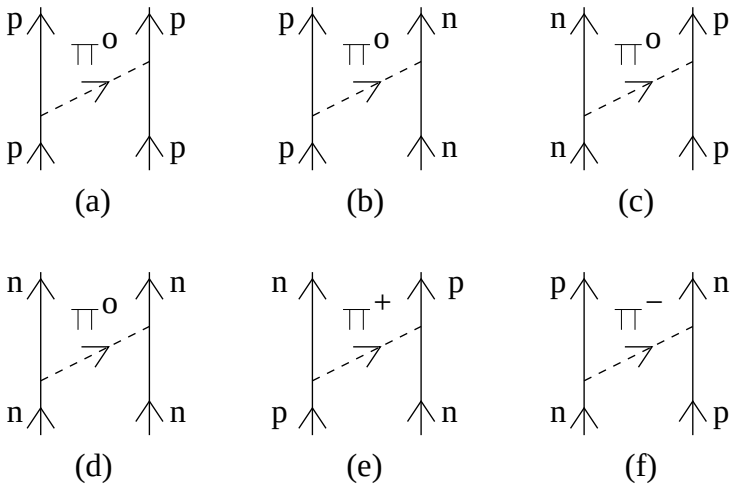

Figure 3.15: Neutral and charged pion-exchange interactions. Vertical lines labeled p and n denote protons and neutrons, and dashed lines labeled $\pi^{0,+,-}$ denote the charged pions.

In general there can be four independent pion-nucleon coupling constants $f_{\pi^0 pp}$, $f_{\pi^0 nn}$, $f_{\pi^+ np}$, and $f_{\pi^- pn}$, describing the emission and absorption of neutral and charged pions by nucleons. The available pion-nucleon and nucleon-nucleon scattering data is consistent with the pion-nucleon coupling being isoscalar, *i.e.*

$$f_{\pi^0 pp} = -f_{\pi^0 nn} = f_{\pi^+ np} = f_{\pi^- pn} = f_{\pi NN}. \tag{3.183}$$

The $f_{\pi^0 nn}$ has a minus sign because the neutral pion field ϕ_0 couples to the isospin projection τ_z of the nucleon, see Eq. (3.7). Assuming these relations between the coupling constants, only the mass difference between the charged and neutral pions can be responsible for the breaking of the isospin symmetry of the OPEP given by Eq. (3.19).

The OPEP between two protons can only be mediated by neutral pions as shown in panels (a) and (b) of Fig. 3.11. Using the interaction Hamiltonian

$$H_{\pi^0 pp} = -\frac{f_{\pi^0 pp}}{m_{\pi,s}} \boldsymbol{\sigma} \cdot \boldsymbol{\nabla} \hat{\phi}_0(\mathbf{r}) = -\frac{f_{\pi NN}}{m_{\pi,s}} \boldsymbol{\sigma} \cdot \boldsymbol{\nabla} \hat{\phi}_0(\mathbf{r}) \ , \tag{3.184}$$

the OPEP between two protons can be easily derived by methods described in Sec. 3.2:

$$\begin{aligned} v^{\pi}_{pp\to pp}(\mathbf{r}) &= v^{\pi^0}(\mathbf{r}) \\ &= \frac{f^2_{\pi NN}}{4\pi} \frac{m^0_\pi}{3} \left(\frac{m^0_\pi}{m_{\pi,s}}\right)^2 \left\{ T_{\pi^0}(r) S_{12} + \Big[Y_{\pi^0}(r) - \frac{4\pi}{m^3_{\pi^0}} \delta(\mathbf{r}) \Big] \boldsymbol{\sigma}_1 \cdot \boldsymbol{\sigma}_2 \right\} , \end{aligned} \tag{3.185}$$

where $m_{\pi,s}$ is a mass scale, often chosen equal to the charged pion mass m_{π^+}, to make the coupling constant $f_{\pi NN}$ dimensionless, and $Y_{\pi^0}(r)$ and $T_{\pi^0}(r)$ are dimensionless functions of

$m_{\pi^0} r$ defined in Eqs. (3.28) and (3.29). Similarly, from the interaction Hamiltonian

$$H_{\pi^0 nn} = -\frac{f_{\pi^0 nn}}{m_{\pi,s}} \boldsymbol{\sigma} \cdot \boldsymbol{\nabla} \hat{\phi}_0(\mathbf{r}) = \frac{f_{\pi NN}}{m_{\pi,s}} \boldsymbol{\sigma} \cdot \boldsymbol{\nabla} \hat{\phi}_0(\mathbf{r}) \ , \tag{3.186}$$

we obtain

$$v^{\pi}_{nn\to nn}(\mathbf{r}) = v^{\pi}_{pp\to pp}(\mathbf{r}) = v^{\pi^0}(\mathbf{r}). \tag{3.187}$$

The OPEP between a neutron-proton pair can either be mediated by π^0, giving $v^{\pi}_{np\to np}$ and $v^{\pi}_{pn\to pn}$ illustrated in panels (c) and (d) of Fig. 3.15, or by charged pions giving $v^{\pi}_{np\to pn}$ and $v^{\pi}_{pn\to np}$, panels (e) and (f) of Fig. 3.15 (e). The π^0-mediated potentials are:

$$v^{\pi}_{np\to np}(\mathbf{r}) = v^{\pi}_{pn\to pn}(\mathbf{r}) = -v^{\pi^0}(\mathbf{r}) \ , \tag{3.188}$$

and the minus sign stems from the sign difference between $H_{\pi^0 pp}$ and $H_{\pi^0 nn}$, or equivalently between the τ_z of the neutron and the proton. The potentials mediated by the charged pions come from the interaction Hamiltonian

$$H_{\pi^{+,-}NN} = -\frac{f_{\pi NN}}{m_{\pi,s}} \boldsymbol{\sigma} \cdot \boldsymbol{\nabla} \left[\hat{\phi}_+(\mathbf{r}) \tau_- + \hat{\phi}_-(\mathbf{r}) \tau_+ \right] \ , \tag{3.189}$$

having charged pion fields given by Eq. (3.3) and nucleon isospin raising/lowering operators defined in Eq. (3.8). We obtain:

$$v^{\pi}_{np\to pn}(\mathbf{r}) \ = \ v^{\pi}_{pn\to np}(\mathbf{r}) = 2\, v^{\pi^{\pm}}(\mathbf{r}), \tag{3.190}$$

$$v^{\pi^{\pm}}(\mathbf{r}) \ = \ \frac{f^2_{\pi NN}}{4\pi} \frac{m_{\pi^{\pm}}}{3} \left(\frac{m_{\pi^{\pm}}}{m_{\pi,s}} \right)^2 \left\{ T_{\pi^{\pm}}(r) S_{12} + \left[Y_{\pi^{\pm}}(r) - \frac{4\pi}{m^3_{\pi^{\pm}}} \delta(\mathbf{r}) \right] \boldsymbol{\sigma}_1 \cdot \boldsymbol{\sigma}_2 \right\} , \tag{3.191}$$

where $T_{\pi^{\pm}}(r)$ and $Y_{\pi^{\pm}}(r)$ are functions of $m_{\pi^{\pm}} r$. These charge exchange potentials contain the product of nucleon isospin matrix elements:

$$\langle n|\tau_-|p\rangle \langle p|\tau_+|n\rangle = 2 \ , \tag{3.192}$$

and are therefore twice the $v^{\pi^{\pm}}$ defined such that

$$v^{\pi^0} = v^{\pi^{\pm}} \quad \text{when} \quad m_{\pi^0} = m_{\pi^{\pm}} \ . \tag{3.193}$$

The isospin symmetry is violated by the difference between v^{π^0} and $v^{\pi^{\pm}}$ caused by that between $m_{\pi^{\pm}}$ and m_{π^0}.

The total OPEP can be written as a sum of isoscalar (IS) and isotensor (IT) terms as follows

$$v^{\pi}_{\rm TOT}(\mathbf{r}) = v^{\pi}_{\rm IS}(\mathbf{r})\, \boldsymbol{\tau}_1 \cdot \boldsymbol{\tau}_2 + v^{\pi}_{\rm IT}(\mathbf{r})\, T_{ij} \ , \tag{3.194}$$

where T_{ij} is the tensor operator in isospin space defined by

$$T_{ij} = 3\,\tau_{z,i}\,\tau_{z,j} - \boldsymbol{\tau}_i \cdot \boldsymbol{\tau}_j \ , \tag{3.195}$$

similar to the more familiar S_{ij} in configuration space, and

$$v^\pi_{IS} = \frac{1}{3}\left[2v^{\pi^\pm}(\mathbf{r}) + v^{\pi^0}(\mathbf{r})\right] \ , \tag{3.196}$$

$$v^\pi_{IT} = \frac{1}{3}\left[v^{\pi^0}(\mathbf{r}) - v^{\pi^\pm}(\mathbf{r})\right] \ . \tag{3.197}$$

Equations (3.187), (3.188) and (3.190) can be easily obtained from the above by means of the identity

$$\boldsymbol{\tau}_i \cdot \boldsymbol{\tau}_j = 2\,P^\tau_{ij} - 1, \tag{3.198}$$

where P^τ_{ij} exchanges the isospins of i and j. Historically, the $v^\pi_{\rm IS}$ is called the charge independent part, while the $v^\pi_{\rm IT}$ is the charge dependent part of OPEP. Just as the tensor operator S_{ij} is zero in states with spin $S = 0$, the isotensor operator is zero in states with isospin $T = 0$. Therefore only the IS part of OPEP contributes to the interaction of two nucleons in the $T = 0$ state.

In principle the two- and three-pion-exchange interactions discussed in Secs. 3.12 to 3.15 should also have isospin symmetry breaking terms. However, as indicated in those sections, it is difficult to calculate these interactions exactly, and their strengths have to be determined from experimental data.

3.17 Finite size effects

Thus far we have considered nucleons as point particles coupled to pion fields. However, they are in fact finite objects made up of quarks and gluons. The interaction of a pion field $\boldsymbol{\phi}(\mathbf{r})$ with a nucleon having its center of mass at $\mathbf{r}$, and a density distribution given by $\rho(\mathbf{r}' - \mathbf{r})$, is described with the interaction Hamiltonian

$$H^{\rm FS}_{\pi NN} = -\frac{f_{\pi NN}}{m_\pi}\int d^3r'\,\rho(\mathbf{r}' - \mathbf{r})\,\boldsymbol{\sigma} \cdot \left[\boldsymbol{\nabla}'\hat{\boldsymbol{\phi}}(\mathbf{r}') \cdot \boldsymbol{\tau}\right] \ , \tag{3.199}$$

whose superscript FS stands for finite size. The nucleon density distribution is conveniently normalized such that

$$\int d^3r'\,\rho(\mathbf{r}' - \mathbf{r}) = 1. \tag{3.200}$$

Equation (3.10) for the coupling of point nucleons with the pion field follows from Eq. (3.199) by using $\delta(\mathbf{r}' - \mathbf{r})$ to describe the nucleon density distribution.

The OPEP is obtained from the pion emission and absorption matrix elements in Sec. 3.2. We want to recalculate these matrix elements for the above $H^{\rm FS}_{\pi NN}$. Consider the first matrix element, given by Eq. (3.15), describing the emission of a pion by nucleon 1. It becomes:

$$\begin{aligned}\langle I|H^{\rm FS}_{\pi NN}|i\rangle &= i\frac{f_{\pi NN}}{m_\pi}\frac{1}{\sqrt{2\omega_q}}\langle\chi'_1|\boldsymbol{\sigma}_1\cdot\mathbf{q}\;\tau_{1,-\alpha}|\chi_1\rangle\int d^3r\;d^3r'\;\rho(\mathbf{r}'-\mathbf{r})\;e^{i(\mathbf{p}-\mathbf{p}')\cdot\mathbf{r}}\;e^{-i\mathbf{q}\cdot\mathbf{r}'}\\ &= \langle I|H_{\pi NN}|i\rangle\;F_{\pi NN}(q)\;,\end{aligned}\tag{3.201}$$

where

$$F_{\pi NN}(q)=\int d^3r\;\rho(r)e^{-i\mathbf{q}\cdot\mathbf{r}}\;,\tag{3.202}$$

since $\mathbf{p}-\mathbf{p}'=\mathbf{q}$. The matrix element for point nucleons $\langle I|H_{\pi NN}|i\rangle$, given by Eq. (3.15), contains everything except the Fourier transform $F_{\pi NN}(q)$ in the matrix element of $H^{\rm FS}_{\pi NN}$. When the nucleon density distribution $\rho(\mathbf{r}'-\mathbf{r})$ is spherically symmetric $F_{\pi NN}(q)$, called the πNN vertex form factor, is real and depends only on the magnitude q of the momentum of the emitted pion.

The results obtained for the point nucleon $H_{\pi NN}$ can be easily generalized for the $H^{\rm FS}_{\pi NN}$ by adding a factor $F_{\pi NN}(q)$ for every emitted or absorbed pion, *i.e.* at every πNN vertex in the time-ordered diagrams describing the process. In particular the OPEP in momentum space, given by Eq. (3.19), becomes:

$$\tilde v^\pi_{12}(\mathbf{q})=-\frac{f^2_{\pi NN}}{m^2_\pi}\frac{F^2_{\pi NN}(q)}{q^2+{m_\pi}^2}\boldsymbol{\tau}_1\cdot\boldsymbol{\tau}_2\,\boldsymbol{\sigma}_1\cdot\mathbf{q}\;\boldsymbol{\sigma}_2\cdot\mathbf{q}\;.\tag{3.203}$$

The configuration space $v^\pi_{12}(\mathbf{r})$ is obtained by using the Yukawa function $y^{\rm FS}_\pi(r)$ including form factors, namely

$$y^{\rm FS}_\pi(r)=\int\frac{d^3q}{(2\pi)^3}\,\frac{F^2_{\pi NN}(q)}{q^2+{m_\pi}^2}\,e^{-i\mathbf{q}\cdot\mathbf{r}},\tag{3.204}$$

in Eq. (3.20). Effects of the finite sizes of both the nucleon and Δ can be included by calculating the OPETP from the modified Yukawa functions containing an $F_{\pi N\Delta}(q)$ for each $\pi N\Delta$ vertex and an $F_{\pi NN}(q)$ for each πNN vertex in their integrand.

Pions, being made up of quarks, anti-quarks and gluons, also have a finite size. In principle its effects are included in the phenomenological vertex form factors. The fundamental theory of quantum chromodynamics (QCD) describing pion-nucleon interactions has not yet advanced sufficiently to allow theoretical calculations of the pion-nucleon coupling constants and form factors. Thus $F_{\pi NN}(q)$ and $F_{\pi N\Delta}(q)$ have to be experimentally determined together with $f_{\pi NN}$ and $f_{\pi N\Delta}$. Note that pion-nucleon scattering does not give direct information of the pion-nucleon form factors because a nucleon cannot absorb a real pion conserving energy and momentum. The πNN vertex in OPEP must always have a virtual pion. For the same reason charge distributions of finite systems like nuclei are generally studied by

electron-nucleus scattering, in which the photon exchanged between the electron and the nucleus is virtual, rather than from interactions of nuclei with real photons.

The form factor

$$F^2_{\pi NN}(q) = \frac{\Lambda^2}{\Lambda^2 + q^2} \tag{3.205}$$

is very simple to use. It is unity in the limit $q \to 0$, as required by the normalization in Eq. (3.200), and goes to zero for $q^2 \gg \Lambda^2$. The size of the nucleon is of the order of 1 fm, and hence we expect $F_{\pi NN}$ to become small when the pion wavelength $\lambda = 2\pi/q \sim 1$ fm, *i.e.* $q \sim 2\pi$ fm^{-1}. Therefore $\Lambda \sim 1$ GeV is typically used. The Yukawa function modified by this form-factor is given by

$$y^{\rm FS}_\pi(r) = \int \frac{d^3q}{(2\pi)^3} \frac{\Lambda^2}{\Lambda^2 + q^2} \frac{1}{q^2 + m_\pi^2} e^{-i\mathbf{q}\cdot\mathbf{r}} = \frac{\Lambda^2}{\Lambda^2 - m_\pi^2} \left(\frac{e^{-m_\pi r}}{4\pi\, r} - \frac{e^{-\Lambda r}}{4\pi\, r} \right) \ . \tag{3.206}$$

It is just the difference between two Yukawa functions with range parameters m_π and Λ. The first term of this modified Yukawa function corresponds to the OPEP for point nucleons, given by Eq. (3.26) but renormalized by the factor $\Lambda^2/(\Lambda^2 - m_\pi^2)$, while the second term gives a one-pion-exchange-like potential with range parameter Λ and strength renormalized by an additional factor Λ^3/m_π^3. From their difference the following OPEP, including the finite size effects implied by the form factor in Eq. (3.205), results:

$$v^{\pi,{\rm FS}}_{12}(\mathbf{r}) = \frac{f^2_{\pi NN}}{4\pi} \frac{m_\pi}{3} \ \boldsymbol{\tau}_1 \cdot \boldsymbol{\tau}_2 \ \left[T^{\rm FS}_\pi(r)\, S_{12} + Y^{\rm FS}_\pi(r)\, \boldsymbol{\sigma}_1 \cdot \boldsymbol{\sigma}_2 \right] \ , \tag{3.207}$$

with

$$Y^{\rm FS}_\pi(r) = \frac{\Lambda^2}{\Lambda^2 - m_\pi^2} \left[Y_\pi(r) - \frac{\Lambda^3}{m_\pi^3}\, Y_\Lambda(r) \right] \ , \tag{3.208}$$

$$T^{\rm FS}_\pi(r) = \frac{\Lambda^2}{\Lambda^2 - m_\pi^2} \left[T_\pi(r) - \frac{\Lambda^3}{m_\pi^3}\, T_\Lambda(r) \right] \ , \tag{3.209}$$

where $Y_\Lambda(r)$ and $T_\Lambda(r)$ are dimensionless functions of Λr defined by Eqs. (3.28) and (3.29).

The point particle $v^\pi_{12}(\mathbf{r})$ is very singular at the origin: it contains a $\delta(\mathbf{r})$ function, and the $T_\pi(r)$ diverges as $1/r^3$. In contrast, the $v^{\pi,{\rm FS}}_{12}(\mathbf{r})$ obtained from the simple πNN form factor in Eq. (3.205) is much less singular. The $\delta(\mathbf{r})$ is replaced by $(\Lambda/m_\pi)^3\ Y_\Lambda(r)$ which is proportional to $1/r$ at small r. The $T^{\rm FS}_\pi(r)$ and $Y^{\rm FS}_\pi(r)$ obtained with this form factor also have $1/r$ behavior at small r. The various dimensionless Y_π and T_π functions are shown in Figs. 3.12 and 3.13.

In nonrelativistic mechanics, the nucleon density distribution $\rho(r)$ can be easily calculated from the form factor by inverting the Fourier transform in Eq. (3.202):

$$\rho(r) = \int \frac{d^3q}{(2\pi)^3} F_{\pi NN}(q) e^{i\mathbf{q}\cdot\mathbf{r}} = \frac{1}{2\pi^2\, r} \int dq\, q\, F_{\pi NN}(q) \sin(qr) \ . \tag{3.210}$$

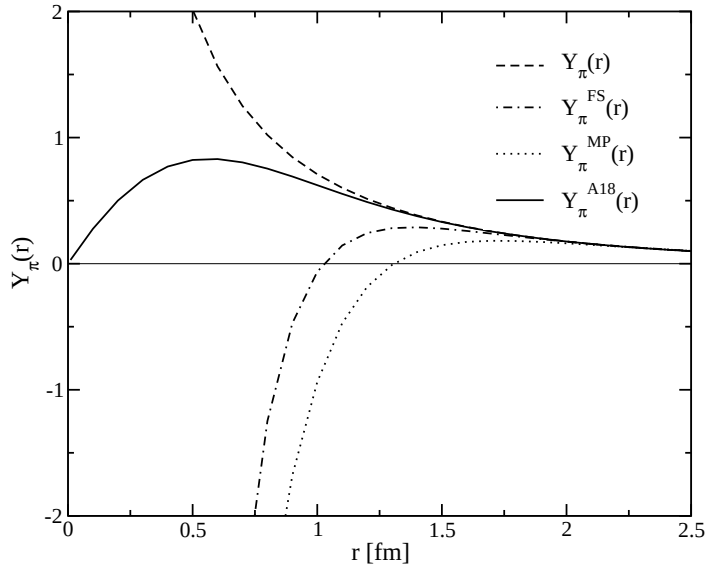

Figure 3.16: The dimensionless $Y_\pi(r)$ functions without and with various short range cutoffs. The $Y_\pi^{\rm FS}$ and $Y_\pi^{\rm MP}$ are with $\Lambda = 6\,m_\pi$, and the A18 potential has $c = 2.1$ fm^{-2}.

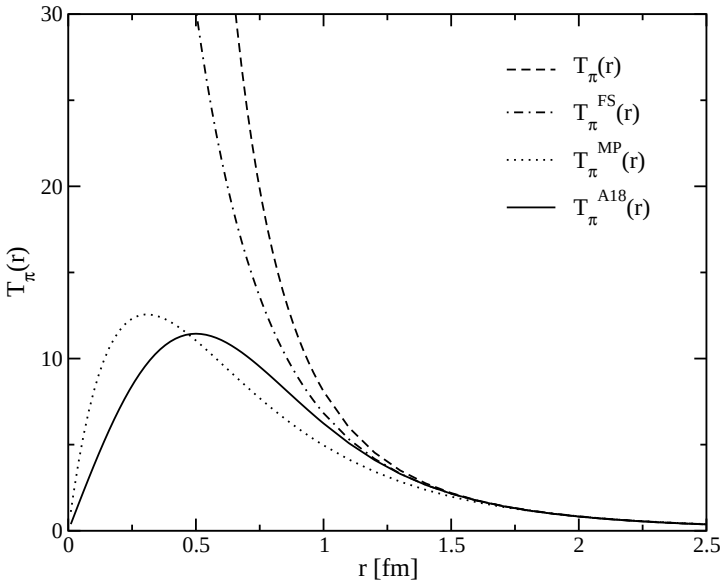

Figure 3.17: The dimensionless $T_\pi(r)$ functions without and with various short range cutoffs. The $T_\pi^{\rm FS}$ and $T_\pi^{\rm MP}$ are with $\Lambda = 6\,m_\pi$, and the A18 potential has $c = 2.1$ fm^{-2}.

The simple form factor of Eq. (3.205) decreases very slowly as $1/q$ at large q. Therefore the $\rho(r)$ obtained from it is singular at the origin, and consequently the $v^{\pi,{\rm FS}}(\mathbf{r})$ has a $1/r$

behavior. The class of form factors

$$F_{\pi NN}(q) = \frac{\Lambda^{2n}}{(\Lambda^2 + q^2)^n} \ , \tag{3.211}$$

has been used with various values of n. The simple form factor considered above has $n = 1/2$, and for historical reasons those having $n = 1, 2$ are called monopole and dipole form factors, respectively. The density distributions corresponding to these form factors are:

$$\text{monopole} \quad \rho(r) = \frac{\Lambda^3}{4\pi} \, Y_\Lambda(r) \ , \tag{3.212}$$

$$\text{dipole} \quad \rho(r) = \frac{\Lambda^3}{8\pi} \, e^{-\Lambda r} \ . \tag{3.213}$$

The charge density of a proton is approximately given by the exponential distribution corresponding to the dipole form factor. However, the nucleon density to which the pion field couples may not have the distribution of proton charge because virtual pions in the proton contribute to proton charge distribution.

The Yukawa function modified by the monopole form factor, labeled with superscript MP, can be easily calculated by differentiating the $y_\pi^{\rm FS}(r)$ with Λ^2. It is given by

$$y_\pi^{\rm MP}(r) = \frac{\Lambda^4}{(\Lambda^2 - m_\pi^2)^2} \left[\frac{e^{-m_\pi r}}{4\pi \, r} - \frac{e^{-\Lambda r}}{4\pi \, r} - \frac{1}{8\pi \, \Lambda} (\Lambda^2 - m_\pi^2) e^{-\Lambda r} \right] \ , \tag{3.214}$$

and the dimensionless Y and T functions in the modified OPEP of Eq. (3.207) become in this case:

$$Y_\pi^{\rm MP}(r) = \frac{\Lambda^4}{(\Lambda^2 - m_\pi^2)^2} \left[Y_\pi(r) - \frac{\Lambda^3}{m_\pi^3} \, Y_\Lambda(r) + \left(\frac{\Lambda^2}{m_\pi^2} - 1 \right) \left(\frac{1}{m_\pi r} - \frac{\Lambda}{2m_\pi} \right) e^{-\Lambda r} \right] \ , \tag{3.215}$$

and

$$T_\pi^{\rm MP}(r) = \frac{\Lambda^4}{(\Lambda^2 - m_\pi^2)^2} \left[T_\pi(r) - \frac{\Lambda^3}{m_\pi^3} \, T_\Lambda(r) - \frac{1}{2} \left(\frac{\Lambda^2}{m_\pi^2} - 1 \right) \left(\frac{1}{m_\pi r} + \frac{\Lambda}{m_\pi} \right) e^{-\Lambda r} \right] \ , \tag{3.216}$$

they are shown in Figs. 3.16 and 3.17. The $Y_\pi^{\rm MP}(r = 0)$ is finite, while $T_\pi^{\rm MP}(r = 0) = 0$. The $\delta(\mathbf{r})$ term in the point particle OPEP, Eq. (3.26), spreads out and acquires a size proportional to the nucleon density distribution. It dominates the $Y_\pi^{\rm MP}$ at small r where it is negative.

In realistic models of the NN interaction it is convenient to absorb the smeared δ-function part of OPEP in the phenomenological short range part. Algebraic cutoffs are used to make $Y_\pi(r), T_\pi(r) \to 0$ as $r \to 0$. For example, the functions used in the Urbana-Argonne models of the NN interaction are:

$$Y_\pi^{\rm UA}(r) = \frac{e^{-m_\pi r}}{m_\pi r} \left(1 - e^{-cr^2} \right) \ , \tag{3.217}$$

$$T_\pi^{\rm UA}(r) = \left(\frac{3}{m_\pi^2 r^2} + \frac{3}{m_\pi r} + 1 \right) \frac{e^{-m_\pi r}}{m_\pi r} \left(1 - e^{-cr^2} \right)^2 \ . \tag{3.218}$$

The value of the cutoff parameter c is adjusted to reproduce the observed NN scattering data. These functions are also shown in Figs. 3.16 and 3.17.

The OPEP used in realistic models of the two-nucleon interaction always includes nucleon finite size effects. For brevity, from now on we will assume that these are contained in the functions $Y_\pi(r)$ and $T_\pi(r)$ and omit the superscripts, such as MP or UA, specifying the cutoffs of these functions. The isotensor parts of v^π (Sec. 3.16) are also obtained including the finite size effects. The functions $Y_{\pi^{\pm,0}}(r)$ and $T_{\pi^{\pm,0}}(r)$ use the physical pion masses $m_\pi^{\pm,0}$ and include cutoffs. The charge dependent OPEP's in Eqs. (3.185) and (3.191) are given by

$$v^{\pi^{\pm,0}} = \frac{f_{\pi NN}^2}{4\pi}\frac{m_\pi^{\pm,0}}{3}\left(\frac{m_{\pi^{\pm,0}}}{m_{\pi,s}}\right)^2 \left[Y_{\pi^{\pm,0}}(r)\boldsymbol{\sigma}_1\cdot\boldsymbol{\sigma}_2 + T_{\pi^{\pm,0}}(r)S_{12}\right] \ , \tag{3.219}$$

and the $v^\pi_{nn\to nn}$, $v^\pi_{pp\to pp}$, $v^\pi_{np\to np}$ and $v^\pi_{np\rightleftharpoons pn}$ are obtained from them using Eqs. (3.187), (3.188) and (3.190). The isoscalar and isotensor parts are projected out with Eqs. (3.194)–(3.197).

3.18 Momentum distribution of exchanged pions

Consider a system of A nucleons in state $|A\rangle$. In absence of the pion-nucleon coupling, Eq. (3.10), this state will have no pions in it. It is an eigenstate of a Hamiltonian H_0 which contains only nucleon degrees of freedom. We treat the pion-nucleon interaction $H_{\pi NN}$ as a small perturbation. In first order perturbation theory, the amplitude of the state $|I;\mathbf{k},\alpha\rangle$ having a pion with momentum $\mathbf{k}$ and charge state α, and the nucleons in the state $|I\rangle$ mixed with the unperturbed state $|A\rangle$, is given by

$$\begin{aligned} A(I;\mathbf{k},\alpha) &= \frac{\langle I;\mathbf{k},\alpha|H_{\pi NN}|A\rangle}{E_A - E_I - \omega_k} \\ &= -i\frac{f_{\pi NN}}{m_\pi}\sum_{i=1}^{A}\frac{1}{\omega_k\sqrt{2\omega_k}}\langle I|\boldsymbol{\sigma}_i\cdot\mathbf{k}\ \tau_{i,-\alpha}\ e^{-i\mathbf{k}\cdot\mathbf{r}_i}|A\rangle \ , \end{aligned} \tag{3.220}$$

where we have neglected the nucleon kinetic energies and approximated the energy denominator $E_A - E_I - \omega_k$ by $-\omega_k$.

The probability of the system having a pion of momentum $\mathbf{k}$ is generally expressed as the expectation value of the pion number operator $n^\pi(\mathbf{k})$. In the Hilbert space of nuclear wave functions this operator is represented by

$$\begin{aligned} \langle A|n^\pi(\mathbf{k})|A\rangle &= \sum_{\alpha=\pm,0}\sum_I |A(I;\mathbf{k},\alpha)|^2 \\ &= \frac{f_{\pi NN}^2}{m_\pi^2}\frac{1}{2\,\omega_k^3}\sum_{i,j=1}^{A}\langle A|\boldsymbol{\sigma}_i\cdot\mathbf{k}\,\boldsymbol{\sigma}_j\cdot\mathbf{k}\,\boldsymbol{\tau}_i\cdot\boldsymbol{\tau}_j\,e^{-i\mathbf{k}\cdot(\mathbf{r}_i-\mathbf{r}_j)}|A\rangle \ . \end{aligned} \tag{3.221}$$

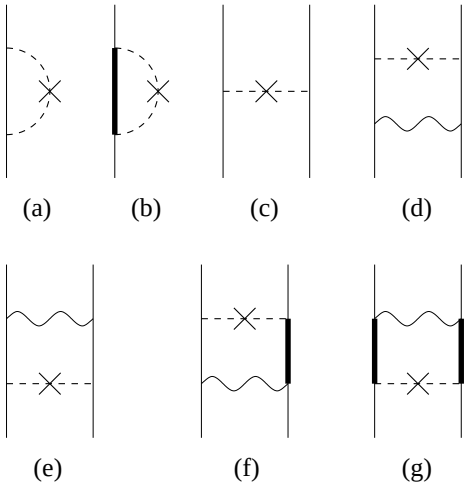

Figure 3.18: Examples of first and second order diagrams that contribute to the pion number in nuclei. The dashed line with an "x" denotes the pion number operator, the thin and thick vertical lines show propagating nucleons and Δ's, and the wavy lines represent realistic $NN \to NN$ and transition potentials. The self energy pions shown in diagrams (a) and (b) are not counted by the operators of Eqs. (3.223) and (3.224). Contributions of second order diagrams like (d) and (e) are included along with higher order corrections when eigenfuctions of realistic nuclear Hamiltonian are used to calculate the expectation values. Diagrams such as (f) and (g) containing *Delta* excitations are included via the operator in Eq. (3.224).

The terms in the above expectation value with $i = j$ occur in isolated nucleons, include the self energy pions as illustrated in Fig. 3.18. Omitting these, the expectation value of the number of exchanged pions is given by

$$\begin{aligned} \langle A|\delta n^\pi(\mathbf{k})|A\rangle &= \frac{f_{\pi NN}^2}{m_\pi^2}\frac{1}{\omega_k^3}\sum_{i<j=1}^{A}\langle A|\boldsymbol{\sigma}_i\cdot\mathbf{k}\;\boldsymbol{\sigma}_j\cdot\mathbf{k}\;\boldsymbol{\tau}_i\cdot\boldsymbol{\tau}_j\;e^{-i\mathbf{k}\cdot(\mathbf{r}_i-\mathbf{r}_j)}|A\rangle \\ &= \langle A|\sum_{i<j=1}^{A}-\frac{e^{-i\mathbf{k}\cdot(\mathbf{r}_i-\mathbf{r}_j)}}{\omega_k}\;\widetilde{v}_{ij}^{\pi}(\mathbf{k})\;|A\rangle\;, \end{aligned} \tag{3.222}$$

where $\tilde{v}_{ij}^{\pi}(\mathbf{k})$ is the momentum space OPEP of Eq. (3.19). The number operator $\delta n^\pi(\mathbf{k})$ for the pions being exchanged by nucleons is related to OPEP, *i.e.*

$$\delta n^\pi(\mathbf{k}) = \sum_{i<j=1}^{A}-\frac{e^{-i\mathbf{k}\cdot(\mathbf{r}_i-\mathbf{r}_j)}}{\omega_k}\;\tilde{v}_{ij}^{\pi}(\mathbf{k})\;. \tag{3.223}$$

Expectation values of this operator have been calculated in light nuclei with quantum Monte Carlo methods to estimate the momentum distribution of pions being exchanged by nucleons in nuclei.

When $|A\rangle$ is a state of noninteracting nucleons, the expectation value of Eq. (3.222) provides just the contribution of first order in $\widetilde{v}^{\,\pi}$ to the $\langle\delta n^\pi(\mathbf{k})\rangle$, shown by diagram (c) in Fig. 3.18. However, the $\widetilde{v}^{\,\pi}$ is strong, and the contributions of all orders need to be considered. When $|A\rangle$ is the eigenstate of a realistic nuclear Hamiltonian, then the expectation value above, Eq. (3.222), includes diagrams with all orders of v_{NN}. Those with one v_{NN} are shown by (d) and (e) in Fig. 3.18. Since v_{NN} contains v^π this expectation value contains contributions of all orders in v^π.

The $\pi N\Delta$ coupling is strong and produces a significant fraction of the pions in nuclei. Including it leads to

$$\delta n^\pi(\mathbf{k}) = \sum_{i<j=1}^{A} \delta n^\pi_{ij}(\mathbf{k}) \ , \tag{3.224}$$

with

$$\begin{aligned}\delta n^\pi_{ij}(\mathbf{k}) = -\frac{e^{-i\mathbf{k}\cdot(\mathbf{r}_i-\mathbf{r}_j)}}{\omega_k}\Big[\widetilde{v}^\pi_{ij,NN\to NN}(\mathbf{k}) \ &+ \ \widetilde{v}^\pi_{ij,NN\rightleftharpoons N\Delta}(\mathbf{k}) + \widetilde{v}^\pi_{ij,NN\rightleftharpoons \Delta N}(\mathbf{k}) \\ &+ \ \widetilde{v}^\pi_{ij,NN\rightleftharpoons \Delta\Delta}(\mathbf{k}) + \widetilde{v}^\pi_{ij,N\Delta\rightleftharpoons \Delta N}(\mathbf{k})\Big] \ , \end{aligned} \tag{3.225}$$

where $\widetilde{v}^\pi_{XY\rightleftharpoons X'Y'}(\mathbf{k})$ are the OPETP discussed in Sec. 3.11. In order to sum the higher order contributions, the above operator must be used with eigenfunctions of the Hamiltonian

$$\begin{aligned} H = &\sum_{i=1}^{A}\left[P_i^N\left(m_N - \frac{1}{2\,m_N}\nabla_i^2\right) + P_i^\Delta\left(m_\Delta - \frac{1}{2\,m_\Delta}\nabla_i^2\right)\right] \\ &+ \sum_{i<j=1}^{A}\Big[v_{ij,NN\to NN} + v_{ij,NN\rightleftharpoons N\Delta} + v_{ij,NN\rightleftharpoons\Delta N} + v_{ij,NN\rightleftharpoons\Delta\Delta} + v_{ij,N\Delta\rightleftharpoons\Delta N}\Big] \ , \end{aligned} \tag{3.226}$$

where P_i^N and P_i^Δ are nucleon and Δ projection operators. The interactions $v_{ij,XY\to X'Y'}$ must contain the $v^\pi_{ij,XY\to X'Y'}$ in the pion number operator, and also fit the NN scattering data. Such interactions were first studied by von Hipple and Sugawara, and methods to calculate the eigenfunctions of the above Hamiltonian were developed by Sauer and collaborators for $A = 3$. Approximations for $A > 3$ were described in papers by the present authors and collaborators.

The results for the momentum distribution

$$\delta N^\pi(k) \equiv \frac{k^2}{2\pi^2 A}\langle A|\delta n^\pi(\mathbf{k})|A\rangle \ , \tag{3.227}$$

of exchanged pions per nucleon in few-body nuclei and nuclear matter are shown in Fig. 3.19. These are obtained with the Argonne v_{28} interaction containing OPEP and OPETP. At small values of k the $\delta N_\pi(k)$ is negative indicating that nucleons bound in nuclei have fewer low momentum pions than free nucleons. Self energy processes shown in diagram (A) of Fig. 3.18

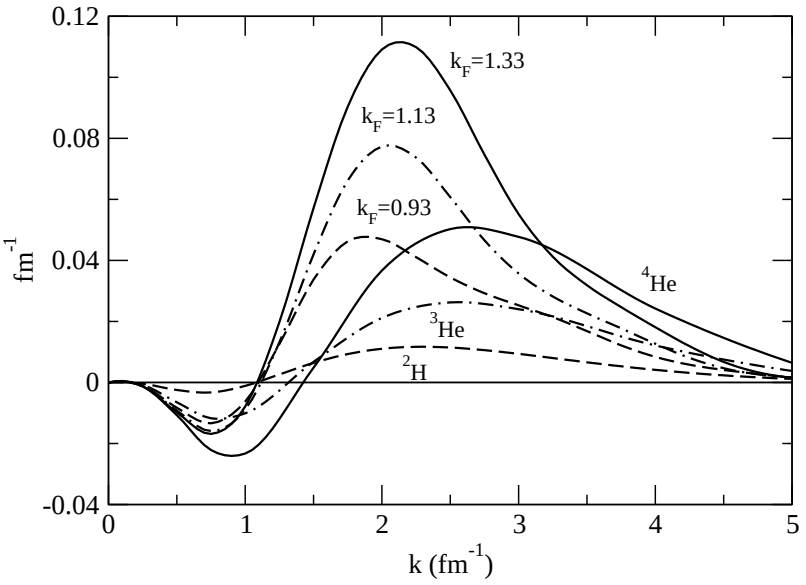

Figure 3.19: The momentum distribution of excess pions in few-body nuclei and nuclear matter.

are suppressed in nuclei due to the Pauli blocking of the nucleon in the intermediate state, when k is small. This leads to negative $\delta N_\pi(k)$ at small k.

The peak in $\delta N_\pi(k)$ is between 2 and 3 fm^{-1} with the Argonne v_{28} interaction. The position of this peak is sensitive to the short range cutoffs of the OPEP and OPETP and the repulsive core in the interaction model. Nevertheless such theoretical calculations indicate that most of the attraction from OPEP and OPETP comes from pions with momenta in the 1 to 4 fm^{-1} range.

After emitting a pion of momentum $\simeq 2.5$ fm^{-1} the nucleon will also obtain a momentum of that order, and a kinetic energy of $\simeq 130$ MeV. This energy is not very small compared to $m_\Delta - m_n \simeq 300$ MeV. Therefore the estimates of the strengths of two-pion-exchange two- and three-nucleon interactions, and of three-pion-exchange three-nucleon interaction given in Table 3.1 and Eqs. (3.140) and (3.169), neglecting nucleon kinetic energies, are not expected to be very accurate.

The integral

$$\delta N^\pi_{\rm TOT} = \int_0^\infty dk\ \delta N^\pi(k)\ , \tag{3.228}$$

gives the number of excess pions in nuclei, per nucleon, relative to that in free nucleons. The estimated values of $\delta N^\pi_{\rm TOT}$ in ^{2}H, ^{3}H, ^{4}He and nuclear matter at equilibrium density are respectively 0.024, 0.05, 0.09 and 0.18. They suggest, for example, that the ^{4}He nucleus has a pion being exchanged about a third of the time.

A great deal of effort has been made to measure the $\delta N^\pi(k)$ in nuclei. One can hope to knock out the pions in light nuclei by high energy electrons. In heavier nuclei, the knocked

out pions are estimated to have significant "final state interactions" on their way out of the nucleus. The experimental data on light nuclei confirms the negative dip in $\delta N^\pi(k)$ at small k, but not the positive peak. The relation between the pion-exchange potential and the δN^π operator–see Eqs. (3.223) and (3.224)–is simple and direct. However, the interpretation of the pion knock out experiments is complex, particularly because the exchanged pions are not free, and do not have a unique energy determined by their momentum. Nevertheless, an experimental verification of the height and position of the peak of $\delta N^\pi(k)$ is important.

3.19 Summary

In the nonrelativistic limit the OPEP can be calculated exactly including differences between pion masses. It gives a major part of the two-nucleon interaction, and thus helps put nuclear physics on at least a semi quantitative footing. However, the two-pion exchange two-nucleon interaction cannot yet be calculated exactly. It can be easily shown that it contains all the six isoscalar static operators O^p listed in Eq. (3.124). The strengths of these and the momentum dependent parts of $v_{NN}^{2\pi}$ have to be obtained from data.

The spin-isospin dependence and the spatial structure of the two-pion exchange three-nucleon interaction can also be derived from theory for general S- and P-wave π-N interactions. However, the strengths of these interactions cannot yet be calculated exactly. It is likely that three-pion-exchange three-nucleon interactions are important in nuclear physics due to their unique isospin dependence. Their general form can be calculated assuming that they are mediated by $N \to \Delta$ excitations.

It is necessary to include pion and nucleon finite size effects in the pion-exchange interactions. They modify the OPEP and OPETP at small distances, and are difficult to determine due to the unknown nature of nuclear forces at small distances.

Chapter 4

Electromagnetic Interactions

The longest range part of the interaction between nucleons is given by electromagnetic (EM) forces mediated by the massless photon. The largest of these is the Coulomb interaction between protons. It is responsible for the neutron excess and fission instability of heavy nuclei, and has a large effect on the structure of neutron stars. The magnetic dipole-dipole interaction between nucleons is small and it has been neglected in most of the past studies. However, we can now calculate properties of light nuclei with over 99% accuracy. At this level the magnetic interactions must be included. For example, they give a contribution of $\sim$18 keV to the $-2.224575(9)$ MeV ground-state energy of the deuteron, which corresponds to 0.8%. In addition, the scattering of two protons has been most precisely measured. The electromagnetic magnetic forces have a large effect on this scattering, and as has been stressed by the Nijmegen group, it is essential to include corrections of order α^2 in the partial wave analysis of the precise *p*-*p* scattering data.

The EM interactions inherently break the isospin symmetry of the strong interactions. It is therefore simpler to discuss them as $v^\gamma_{NN'}$ where $NN' = pp\ , pn,\ np$ and nn. Since the photon has zero charge, there is no charge exchange interaction:

$$v^\gamma(np \rightleftharpoons pn) = 0\ . \tag{4.1}$$

The isospin dependence of the v^γ can be expressed as:

$$v^\gamma = v^\gamma_1 + v^\gamma_\tau\, \boldsymbol{\tau}_i \cdot \boldsymbol{\tau}_j + v^\gamma_{IV}\,(\tau_{z,i} + \tau_{z,j}) + v^\gamma_{IT}\, T_{ij} + \dots\ , \tag{4.2}$$

where T_{ij} is the isotensor (IT) operator in Eq. (3.195) and $\tau_{z,i} + \tau_{z,j}$ is an isovector (IV) operator. The smaller spin-orbit parts of v^γ have additional, so called class-4 terms listed in Sec. 4.2, and denoted by the $\dots$ in the above equation. The various isospin terms of v^γ can be easily extracted from the $v^\gamma_{NN'}$. We obtain:

$$v^\gamma_1 \ = \ \frac{1}{4}\left(v^\gamma_{pp} + 2\, v^\gamma_{pn} + v^\gamma_{nn}\right)\ , \tag{4.3}$$

$$v^\gamma_{IV} = \frac{1}{4}\left(v^\gamma_{pp} - v^\gamma_{nn}\right) , \tag{4.4}$$

$$v^\gamma_{IT} = v^\gamma_\tau = \frac{1}{12}\left(v^\gamma_{pp} - 2v^\gamma_{pn} + v^\gamma_{nn}\right) , \tag{4.5}$$

Note that Eq. (4.1) requires that the complete v^γ does not have any $\boldsymbol{\tau}_i \cdot \boldsymbol{\tau}_j$ part. In fact, the v^γ_τ term in v^γ is canceled by the $\boldsymbol{\tau}_i \cdot \boldsymbol{\tau}_j$ part of $v^\gamma_{IV}\, T_{ij}$.

The calculation of the EM interactions is well described in standard texts. We will describe the v^γ in the recent Nijmegen and Argonne models to establish the notation. The v^γ depends upon the distribution of charge and magnetization in proton and neutron. The EM form factors of the nucleon have been measured by electron-nucleon and electron-deuteron scattering. The commonly used Sacks form factors are normalized such that the electric form factors denoted by $G^N_E(q)$ equal the total nucleon charge at momentum transfer $q = 0$, while the the magnetic, $G^N_M(q)$ equal the nucleon magnetic moment μ_N. They are more convenient because they contain the observed magnetic moments of the nucleons. The $q = 0$ values corresponding to this normalization are:

$$G^p_E(q=0) = \frac{G^p_M(q=0)}{\mu_p} = \frac{G^n_M(q=0)}{\mu_n} = 1 , \qquad \text{and } G^n_E(q=0) = 0 . \tag{4.6}$$

Empirically it is known that the first three are well approximated by the dipole form:

$$G^p_E(q) = \frac{G^p_M(q)}{\mu_p} = \frac{G^n_M(q)}{\mu_n} = \left(1 + \frac{q^2}{b^2}\right)^{-2} , \tag{4.7}$$

where $b = 4.27$ fm^{-1}; and the $G^n_E(q)$ by

$$G^n_E(q) = \beta_n\, q^2 \left(1 + \frac{q^2}{b^2}\right)^{-3} . \tag{4.8}$$

Here β_n denotes the slope of G^n_E at $q^2 = 0$. From electron-neutron scattering experiments we obtain:

$$\beta_n = \left[\frac{G^n_E(q)}{dq^2}\right]_{q=0} = 0.0189 \text{ fm}^2 . \tag{4.9}$$

However, recent experiments indicate deviations from the above dipole forms at large values of q. Dipole forms are assumed in the Argonne v_{18} model and the following sections mainly because they provide a good approximation, and lead to analytic expressions.

4.1 The $v^\gamma(pp)$

The $v^\gamma(pp)$ is expressed as a sum of six terms:

$$v^\gamma(pp) = v_{C1}(pp) + v_{DF}(pp) + v_{C2}(pp) + v_{VP}(pp) + v_{DD}(pp) + v_{LS}(pp) . \tag{4.10}$$

The $v^\gamma_{C1}(pp)$ contains the leading Coulomb interaction between protons:

$$v^\gamma_{C1}(pp) \;=\; \alpha' \frac{F_C(r)}{r} \;, \tag{4.11}$$

$$F_C(r) \;=\; 1 - \left(1 + \frac{11}{16}x + \frac{3}{16}x^2 + \frac{1}{48}x^3\right) e^{-x} \;, \tag{4.12}$$

where $x = b\,r$ and

$$\alpha' = \alpha\,\frac{2\,k}{m_p\,v_{\rm lab}} \tag{4.13}$$

The function $F_C(r)$ takes into account the size of the proton charge distribution in the dipole approximation. In general it is given by the Fourier transform:

$$F_C(r) = 4\pi \int d^3q\,\frac{e^{i\mathbf{q}\cdot\mathbf{r}}}{q^2}\,[G^p_E(q)]^2 \;. \tag{4.14}$$

When $r \to \infty$ $F_C(r) \to 1$, and $F_C(r = 1\ {\rm fm}) = 0.874$. The Coulomb potential v^γ_{C1} is shown in Fig. 4.1 for the empirical value $b = 4.27\ {\rm fm}^{-1}$ along with the other EM terms in $v^\gamma_{NN'}$.

The α', derived by Breit in 1955, takes into account the energy dependence of the Coulomb interaction via relativistic effects. Here k is the relative momentum in the center of mass (COM) frame, m_p is the proton mass and $v_{\rm lab}$ is the proton velocity in the laboratory frame. It is simple to derive α' in the COM frame, as a function of the velocity $v_{\rm cm}$ of the protons in that frame. We have:

$$k = \frac{m_p v_{\rm cm}}{\sqrt{1 - v^2_{\rm cm}}} \;, \qquad v_{\rm lab} = \frac{2\,v_{\rm cm}}{1 + v^2_{\rm cm}} \;, \qquad \alpha' = \alpha \frac{1 + v^2_{\rm cm}}{\sqrt{1 - v^2_{\rm cm}}} \simeq \alpha\left(1 + \frac{3}{2}v^2_{\rm cm} + \ldots\right) \;. \tag{4.15}$$

The kinematical relativistic corrections can be easily studied using the "relativistic Hamiltonian":

$$H_R = \sum_i \sqrt{m^2 + \mathbf{p}_i^2} + \sum_{i<j} v_{ij} + \ldots \;, \tag{4.16}$$

which retains only the nucleon degrees of freedom. It is obviously correct for non interacting nucleons, and the interactions v_{ij}, V_{ijk}, ... are assumed to contain relativistic effects. These interactions depend on the velocities of the interacting particles. The Schrödinger equation $H_R\,\Psi = E\,\Psi$ is called the "relativistic Schrödinger equation". It neglects the antiparticle degrees of freedom.

The Coulomb interaction between two point protons in the COM frame, including the current-current part, is given by $\alpha\,(1 + v^2_{\rm cm})/r$, and the relativistic pp Schrödinger equation in the COM frame reads:

$$\left[2\sqrt{m_p^2 - \boldsymbol{\nabla}^2} + \alpha(1 + v^2_{\rm cm})\frac{1}{r}\right]\psi(\mathbf{r}) = 2\sqrt{m_p^2 + k^2}\,\psi(\mathbf{r}) \;. \tag{4.17}$$

The strong pp interaction is neglected in the above equation because most of the Coulomb contribution comes from large r. Since the Coulomb potential is small, the above equation implies:

$$-\boldsymbol{\nabla}^2\,\psi(\mathbf{r}) \simeq k^2\,\psi(\mathbf{r})\ . \tag{4.18}$$

Therefore we rewrite it as:

$$\left[2\sqrt{m_p^2+k^2-k^2-\boldsymbol{\nabla}^2}+\alpha(1+v_{\rm cm}^2)\frac{1}{r}\right]\psi(\mathbf{r}) = 2\sqrt{m_p^2+k^2}\,\psi(\mathbf{r})\ , \tag{4.19}$$

and expand in powers of $(k^2+\mathbf{p}^2)/(m_p^2+k^2)$. Keeping only the term of the lowest order gives the "nonrelativistic" Schrödinger equation:

$$\left(-\frac{\boldsymbol{\nabla}^2}{m_p}+\alpha'\frac{1}{r}\right)\psi(\mathbf{r}) = \frac{k^2}{m_p}\,\psi(\mathbf{r})\ , \tag{4.20}$$

with Breit's α' given by Eqs. (4.13) or (4.15). Note that at $E_{\rm lab}\simeq 200$ MeV, $\alpha'\sim 1.16\,\alpha$ and the correction is significant. However, it is mostly of order $v_{\rm cm}^2$.

4.1.1 Corrections to pp Coulomb interaction

The v_{DF} in Eq. (4.10) is the Darwin-Foldy relativistic correction to the Coulomb interaction, while the v_{C2} and v_{VP} are the second order Coulomb and vacuum polarization corrections, both of order α^2. These corrections are rather small, as can be seen in Fig. 4.1, but it is necessary to include them in order to use the high precision data on pp scattering at small energies for modeling the strong NN interaction. We obtain:

$$v_{DF}(pp) = -\frac{\alpha}{4m_p^2}F_\delta(r) \tag{4.21}$$

$$F_\delta(r) = -\boldsymbol{\nabla}^2\left[F_C(r)/r\right] = b^3\left(1+x+\frac{x^2}{3}\right)\frac{e^{-x}}{16}\ , \tag{4.22}$$

for the dipole form factor. For point charges $F_C=1$, the Darwin-Foldy term has zero range. The proton finite size removes the δ-function singularity, and gives a v_{DF} of range $\sim 1/b$.

The $v_{C2}(pp)$ correction is given by

$$v_{C2}(pp) = -\frac{\alpha}{2\,m_p^2}\left[(\boldsymbol{\nabla}^2+k^2)\frac{F_c(r)}{r}+\frac{F_c(r)}{r}(\boldsymbol{\nabla}^2+k^2)\right] \approx -\frac{\alpha\alpha'}{m_p}\left[\frac{F_C(r)}{r}\right]^2\ , \tag{4.23}$$

The approximation is based on the two-body Schrödinger equation

$$\left[-\frac{\boldsymbol{\nabla}^2}{m_p}+v_{pp}(r)\right]\psi(r) = \frac{k^2}{m_p}\psi(r)\ . \tag{4.24}$$

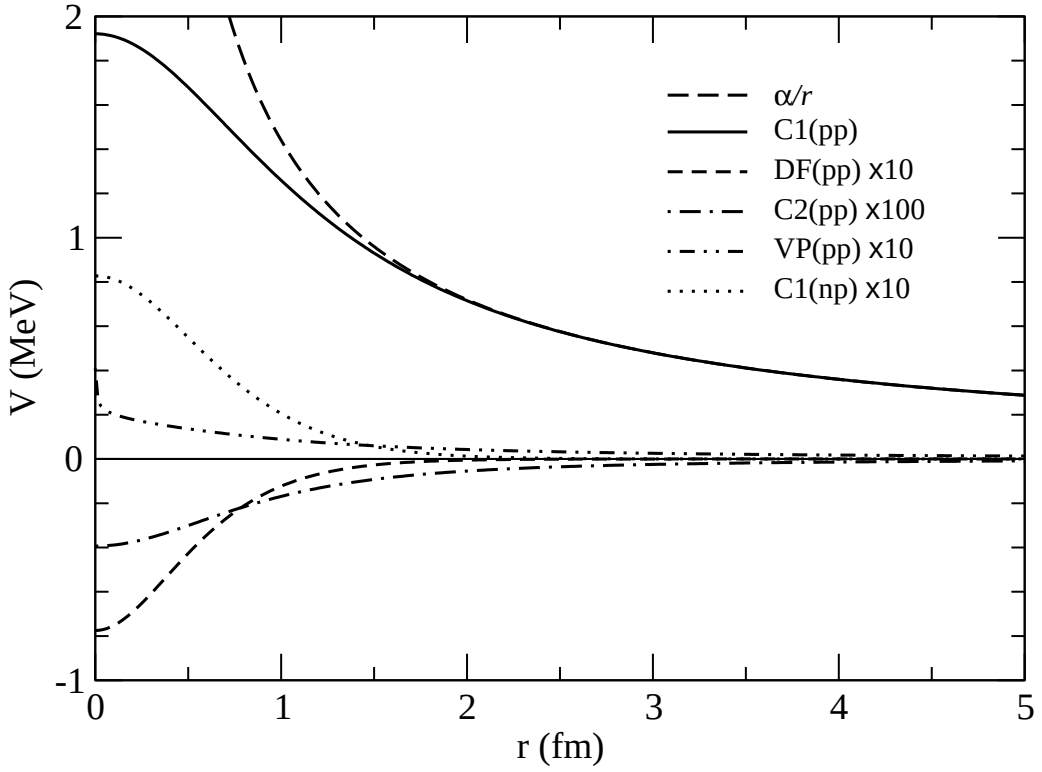

Figure 4.1: The *pp* and *np* Coulomb potentials along with the corrections to the *pp* Coulomb potential. The Coulomb potential between static point protons is shown by the long dashed line α/r.

It is valid at large values of $m_\pi\, r$) where the strong part of v_{pp} becomes negligible, and its leading term becomes $v_{C1}(pp)$. In this important region the Schrödinger equation gives

$$(\nabla^2 + k^2) \simeq v_{C1}(pp) = \alpha' \, \frac{F_C(r)}{r} \ . \tag{4.25}$$

The use of $F_C^2(r)$ in the expression for $v_{C2}(pp)$ Eq. (4.23) removes the $1/r^2$ singularity approximately.

Finally, the $v_{VP}(pp)$ correction is given by:

$$v_{VP}(pp) = \frac{2\alpha\alpha'}{3\pi} \frac{F_C(r)}{r} \int_1^\infty dy \, \mathrm{e}^{-(2\, m_e\, r)\, y} \left[1 + \frac{1}{2y^2}\right] \frac{\sqrt{y^2-1}}{y^2} \ . \tag{4.26}$$

In the above equation, the $F_C(r)$ approximately represents the proton size effect. In fact this effect has been treated exactly, but the simple approximation is fairly accurate.

4.1.2 Magnetic interactions in $v^\gamma(pp)$

The magnetic dipole-dipole interaction in $v^\gamma(pp)$ in Eq. (4.10) is given by

$$v_{DD}(pp) = -\frac{\alpha}{4m_p^2}\mu_p^2\left[\frac{2}{3}F_\delta(r)\,\boldsymbol{\sigma}_i\cdot\boldsymbol{\sigma}_j + \frac{F_t(r)}{r^3}\,S_{ij}\right], \tag{4.27}$$

$$F_t(r) = 1-\left(1+x+\frac{1}{2}x^2+\frac{1}{6}x^3+\frac{1}{24}x^4+\frac{1}{144}x^5\right)e^{-x}, \tag{4.28}$$

for the dipole approximation. In the above equation, μ_p is in units of nuclear magnetons. Thus the magnetic moment of proton, $\mu = \mu_p(e/2\,m_p)$, and the strength of $v_{DD}(pp)$ is given by $\mu^2/4\pi = \alpha\,\mu_p^2/(4m_p^2)$ as per Eq. (3.52). We can easily verify that the $v_{DD}(pp)$ for point protons is given by Eq. (3.52) apart from proton size effects. Note that there are no magnetic Darwin-Foldy terms when Sachs form factors are used. The magnetic dipole-dipole interactions between nucleons are shown in Fig. 4.2.

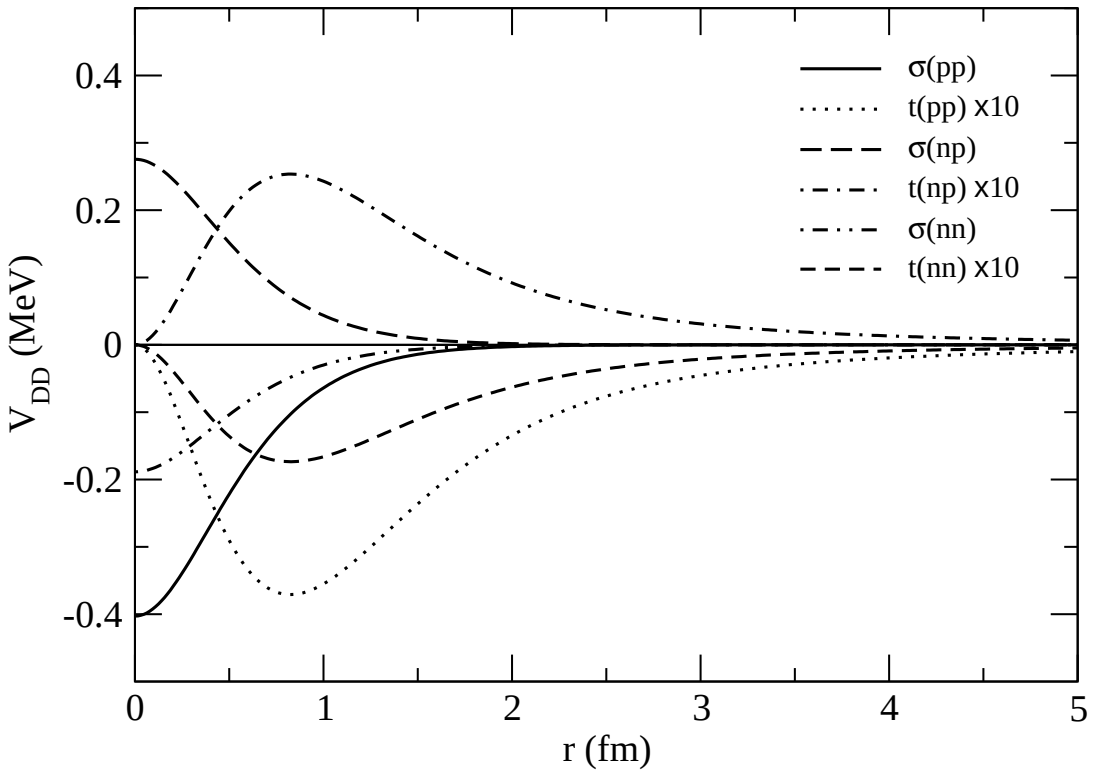

Figure 4.2: The pp, np and nn magnetic dipole-dipole interactions. The curves labeled $\sigma(pp)$, $\sigma(np)$ and $\sigma(nn)$ give the $\boldsymbol{\sigma}_i\cdot\boldsymbol{\sigma}_j$ parts, while those labeled $t(pp)$, $t(np)$ and $t(nn)$ give the tensor parts.

Finally, the spin-orbit $v_{LS}(pp)$ correction between the spin and orbital magnetic moments is given by

$$v_{LS}(pp) = -\frac{\alpha}{2\,m_p^2}(4\,\mu_p - 1)\frac{F_{ls}(r)}{r^3}\mathbf{L}\cdot\mathbf{S}\ , \tag{4.29}$$

$$F_{ls}(r) = = 1 - \left(1 + x + \frac{1}{2}x^2 + \frac{7}{48}x^3 + \frac{1}{48}x^4\right)e^{-x}\ , \tag{4.30}$$

for dipole form factors. It originates from the interaction of one of the protons magnetic moments with the magnetic field generated by the orbital motion of the other proton. The spin-orbit corrections are shown in Fiq. 4.3.

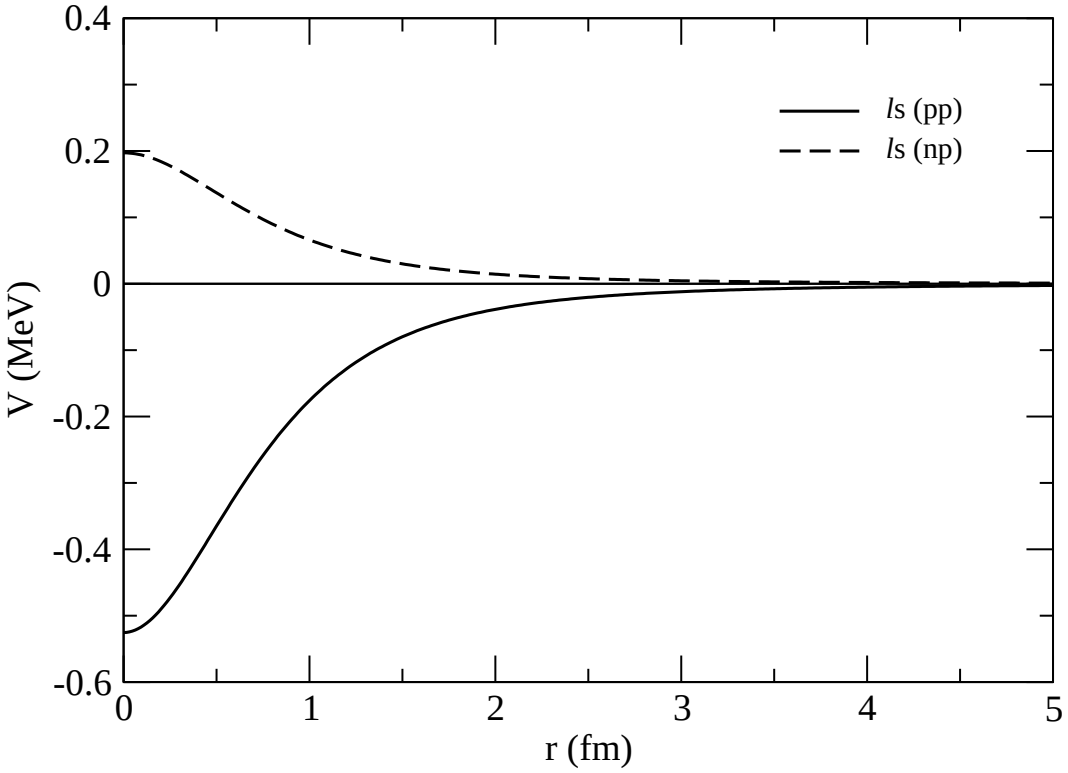

Figure 4.3: The pp and np electromagnetic spin-orbit interactions.

4.2 The $v^\gamma(pn)$

The pn EM interaction is expressed as

$$v^\gamma(pn) = v_{C1}(pn) + v_{DD}(pn) + v_{LS}(pn) + \dots\ . \tag{4.31}$$

The Coulomb interaction due to the neutron charge distribution is given by

$$v_{C1}(pn) = \alpha\beta_n \frac{F_{pn}(r)}{r} , \tag{4.32}$$

$$F_{pn}(r) = b^2 \left(15\,x + 15\,x^2 + 6\,x^3 + x^4\right) \frac{e^{-x}}{384} , \tag{4.33}$$

for the dipole form factors. The $v_{C1}(pn) \ll v_{C1}(pp)$. It peaks at $r \simeq 1$ fm, where it is less than 1% of $v_{C1}(pp)$ (see Fig. 4.1).

The $v_{DD}(pn)$ correction is obtained by replacing a $\mu_p/(2m_p)$ by the neutron magnetic moment, $\mu_n/(2m_n)$, in the strength of $v_{DD}(pp)$ of Eq. (4.27) to obtain

$$v_{DD}(pn) = -\frac{\alpha}{4m_n m_p}\mu_p\,\mu_n \left[\frac{2}{3}F_\delta(r)\,\boldsymbol{\sigma}_i\cdot\boldsymbol{\sigma}_j + \frac{F_t(r)}{r^3}\,S_{ij}\right] . \tag{4.34}$$

This correction is positive since μ_n is negative (see Fig. 4.2).

The EM spin-orbit interaction between protons and neutrons is due to that of the neutron magnetic moment with protons orbital magnetic moment. It is therefore given by

$$v_{LS}(pn) = -\frac{\alpha}{2\,m_n m_r}\mu_n \frac{F_{ls}(r)}{r^3}\mathbf{L}\cdot\boldsymbol{\sigma}_n . \tag{4.35}$$

Here $m_r = m_p m_n/(m_p + m_n)$ is the pn reduced mass. The $\mathbf{L}\cdot\boldsymbol{\sigma}_n$ operator can be written as

$$\mathbf{L}\cdot\boldsymbol{\sigma}_n = \mathbf{L}\cdot\mathbf{S} \mp \mathbf{L}\cdot\mathbf{A} , \qquad \mathbf{A} = \frac{1}{2}(\boldsymbol{\sigma}_i - \boldsymbol{\sigma}_j) , \tag{4.36}$$

where the upper/lower sign applies for pn/np interaction. The new operator $\mathbf{A}$ is antisymmetric so that $v_{LS}(pn) = v_{LS}(np)$. The $\mathbf{A}$ term is known as the class-4 charge asymmetric force. It is very small, but it mixes the spin singlet and triplet np states and affects the magnetic moment scattering amplitude.

4.3 The $v^\gamma(nn)$

In the present context the Coulomb interaction between neutrons is extremely small, and is neglected. There is also no spin-orbit contribution, and therefore

$$v^\gamma(nn) \simeq v_{DD}(nn) = -\frac{\alpha}{4m_n^2}\mu_n^2 \left[\frac{2}{3}F_\delta(r)\,\boldsymbol{\sigma}_i\cdot\boldsymbol{\sigma}_j + \frac{F_t(r)}{r^3}\,S_{ij}\right] , \tag{4.37}$$

by trivial changes in Eq. (4.27). It is compared with the pp and pn dipole-dipole interaction corrections in Fig. 4.2.

Chapter 5

Electromagnetic Current of Nucleons and Nuclei

The interaction of an external electromagnetic (EM) field with a nucleus is given by

$$\begin{aligned} H_{EM} &= e \int d\mathbf{x}\, A^\mu(\mathbf{x})\, j_\mu(\mathbf{x}) \\ &= e \int d\mathbf{r} \left[\phi^0(\mathbf{x})\, \rho_c(\mathbf{x}) - \mathbf{A}(\mathbf{x}) \cdot \mathbf{j}(\mathbf{x}) \right] \ . \end{aligned} \tag{5.1}$$

Here $A^\mu(\mathbf{x})$ is the four-vector EM field acting on the nucleus, and $j^\mu(\mathbf{x})$ is the nuclear four-current density operator with the proton charge $e > 0$ factored out. The $A^\mu(\mathbf{x})$ has components consisting of the electrostatic potential, $\phi^0(\mathbf{x})$ and the vector potential $\mathbf{A}(\mathbf{x})$, while the components of the four-current density j^μ are the charge density $\rho_c(\mathbf{x})$ and the vector current $\mathbf{j}(\mathbf{x})$ (hereafter, the superscript μ from A^μ and j^μ is dropped unless necessary).

The interaction of the nucleus with the EM field determines the EM moments of nuclei and the radiative capture and decay rates. The interaction in electron-nucleus scattering processes can be regarded as that of the EM field of the virtual photon emitted by the scattered electron with the nuclear EM current.

The EM field is quantized, and the field operator $A(\mathbf{x})$ either annihilates or creates a photon. Thus it is useful to classify the terms in the nuclear current operator according to the process induced by the photon as illustrated in Fig. 5.1 and described below. Few of the many possible processes are shown just to illustrate the classification, and a photon can also be emitted in these same processes.

- **One-body currents**: Individual nucleons in nuclei as well as in vacuum can absorb photons via their charges and magnetic moments. These terms are illustrated by diagram (1) in Fig. 5.1, and are included in the one-body current $j_1(i)$, where the label i runs over nucleons $1, \ldots, A$ in the nucleus.

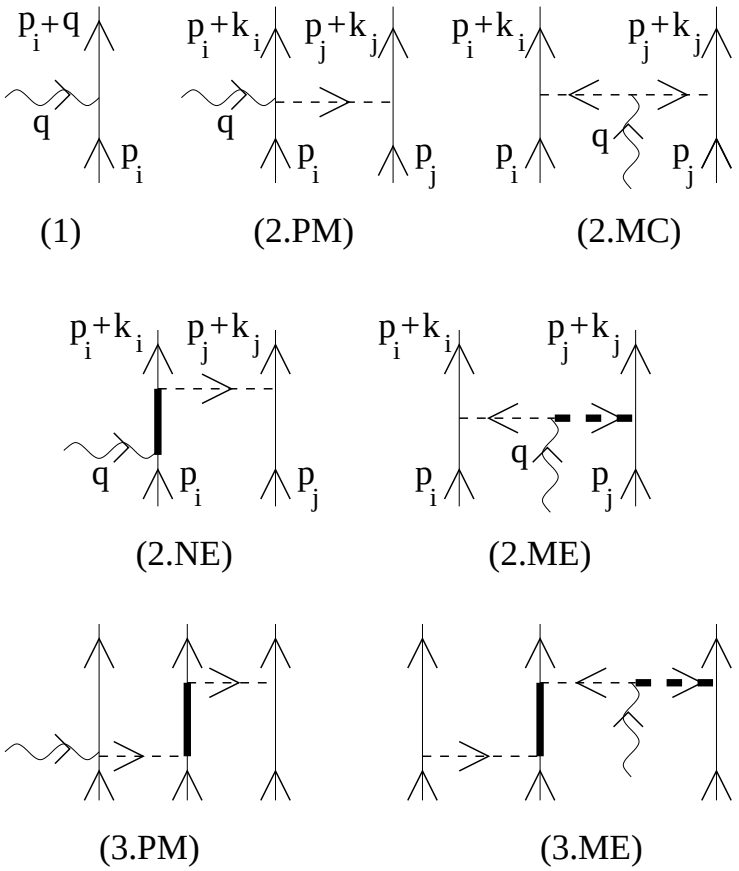

Figure 5.1: Feynman diagrams illustrating the classification of terms in the nuclear four-current operator. Thin and thick vertical lines denote nucleons and deltas, while thin dashed lines represent pions and the wavy line shows the absorbed photon. The thick dashed line denotes heavier mesons such as ρ and ω. Only one diagram per class is shown for brevity. Many more diagrams contribute to each of the classes. Momentum labels are omitted from three-body current diagrams to avoid clutter.

Only one nucleon absorbs all the momentum of the photon via one-body current. However, that nucleon can later share the absorbed momentum with other nucleons via two- and three-nucleon interactions. These interactions determine the final state of the nucleus, and are not a part of the current operator. They are often called final state interactions in approaches based on perturbation theory. Interactions between nucleons that take place before the absorption of the photon are called initial state interactions. Non-perturbative approaches use eigenstates of the nuclear Hamiltonian as initial and final states, and treat only the interaction of the external photon, real or virtual, as a weak perturbation. The nuclear eigenstates contain all the effects of

nuclear forces including those of the EM interaction between nucleons in the nucleus.

- **Photo-meson (PM) currents**: In the process illustrated in diagram (2.PM) the photon produces a meson by hitting a nucleon. The meson is virtual, and has to be absorbed by an other nucleon in all low-energy processes and most electron-nucleus interactions. We denote currents associated with such processes by $j_2^{PM}(ij)$.

- **Meson currents (MC)**: The photon can be absorbed by the current of a charged meson being exchanged by nucleons i and j as in diagram (2.MC). The mesons are virtual, and the the associated two-nucleon currents are denoted by $j_2^{MC}(ij)$.

- **Nucleon excitation (NE) currents**: In these processes, illustrated by diagram (2.NE), the photon excites the nucleon it hits. The most common excitation is from N to Δ. The excited nucleon de-excites by emitting or absorbing a virtual meson absorbed or emitted by an other nucleon. We denote these currents by $j_2^{NE}(ij)$.

- **Meson excitation (ME) currents**: The photon can excite a pion, or any other meson being exchanged by nucleons i and j to an other mesonic state such as ω or ρ. Such processes, shown in diagram (2.ME), generate the $j_2^{ME}(ij)$ currents.

Two-body currents: These include all possible two-nucleon currents, and are denoted by $j_2(ij)$. According to the above classification:

$$j_2(ij) = j_2^{PM}(ij) + j_2^{MC}(ij) + j_2^{NE}(ij) + j_2^{ME}(ij) \ . \tag{5.2}$$

Three-body currents: All the processes that contribute to two-body currents can as well contribute to three-body currents. The three-body analogues of photo-meson and meson excitation currents are illustrated in diagrams (3.PM) and (3.ME) of Fig. 5.1. The total three-body current is denoted by $j_3(ijk)$.

Full current operator: The total EM current of the nucleus is expanded as:

$$j = \sum_{1\le i\le A} j_1(i) + \sum_{1\le i<j\le A} j_2(ij) + \sum_{1\le i<j<k\le A} j_3(ijk) + \dots \ . \tag{5.3}$$

An n-body current allows the photon momentum to be shared by n nucleons. When the photon has small momentum, the above series converges rapidly with the j_1 current giving the dominant contribution. However, there are interesting exceptions. For example, when j_1 is suppressed by symmetry requirements, then the $j_2(ij)$ current gives the leading contribution. A classic example of these effects is provided by the thermal neutron capture cross sections by deuterons and ^{3}He nuclei.

In contrast, when the photon momentum is large, the two-body currents can give large contributions to the elastic electron-nucleus scattering, exceeding those of j_1. In this case it

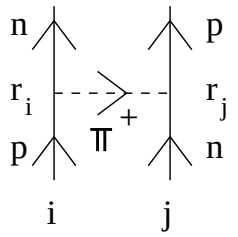

Figure 5.2: One of the Feynman diagrams contributing to the charge exchange interaction between two nucleons.

is simpler to keep the nucleus bound when the large momentum transfer is divided among the two nucleons, than when given to only one.

The dominant pair current occurs when a proton (neutron) i at $\mathbf{r}_i$ changes into a neutron (proton) by a charge-exchange interaction with a neutron (proton) j at $\mathbf{r}_j$ as illustrated in Fig. 5.2. It is necessary if the current carried by protons in nuclei is to be conserved. Since the charge exchange interaction is mediated by the two-nucleon interaction v_{ij}, the pair current $j_2(ij)$ depends on it. Parts of the three-body current are related the three-nucleon interaction V_{ijk}. Since $\langle V_{ijk}\rangle \ll \langle v_{ij}\rangle$ in light nuclei and presumably in nuclear matter too, the contributions of $j_3(ijk)$ may be expected to be smaller than those of $j_2(ij)$. At present n-body interactions and currents with $n \geq 4$ are neglected in most approaches.

The continuity equation provides a complicated relation between the two- and three-nucleon interactions and the corresponding currents. This relation is not sufficient to determine the currents from the interactions. However, its validity provides a test of the approximations used in their construction.

5.1 Nonrelativistic one-body current

The photon gives its momentum $\mathbf{q}$ to the nucleon that absorbs it. Therefore it is convenient to consider the Fourier transform of the nuclear current density defined in Eq. (5.1),

$$j(\mathbf{q}) = \int d\mathbf{x}\, \mathrm{e}^{i\mathbf{q}\cdot\mathbf{x}}\, j(\mathbf{x}) \ . \tag{5.4}$$

In classical physics, a charge e at position $\mathbf{r}$ leads to a charge density $e\,\delta(\mathbf{x}-\mathbf{r})$. Therefore, for point protons—their charge $e > 0$ has been factored out as in Eq. (5.1)—and point neutrons of zero charge, the one-body charge operator $\rho_{c,1}(\mathbf{q})$ reads

$$\rho_{c,1}(\mathbf{q}) = \sum_{1\leq i\leq A} \mathrm{e}^{i\mathbf{q}\cdot\mathbf{r}_i} \frac{1+\tau_{z,i}}{2} \ . \tag{5.5}$$

It gives the interaction of a nucleus made up of point nucleons with an external Coulomb field $e^{i\mathbf{q}\cdot\mathbf{r}}$. Including the effects of the finite size of the nucleons we obtain

$$\begin{aligned}\rho_{c,1}(\mathbf{q}) &= \sum_{1\le i\le A} \mathrm{e}^{i\mathbf{q}\cdot\mathbf{r}_i}\left[G_E^p(q)\,\frac{1+\tau_{z,i}}{2}+G_E^n(q)\,\frac{1-\tau_{z,i}}{2}\right]\\ &= \sum_{1\le i\le A} \mathrm{e}^{i\mathbf{q}\cdot\mathbf{r}_i}\,\frac{1}{2}\left[G_E^S(q)+G_E^V(q)\,\tau_{z,i}\right]\ ,\end{aligned} \tag{5.6}$$

where the following isoscalar and isovector combinations of the nucleon Sachs form factors discussed in Chapter 4 have been introduced

$$G_E^S(q)=G_E^p(q)+G_E^n(q)\ ,\qquad G_E^V(q)=G_E^p(q)-G_E^n(q)\ , \tag{5.7}$$

with the normalization $G_E^S(0)=G_E^V(0)=1$.

Classically, a moving charge of mass m produces a convection current density given by $\delta(\mathbf{x}-\mathbf{r})\,\mathbf{p}/m$, where $\mathbf{r}$ is the position of the charge and $\mathbf{p}/m$ is its velocity. Therefore, in quantum mechanics $\mathbf{j}_{c,1}(\mathbf{q})$ is obtained as

$$\mathbf{j}_{c,1}(\mathbf{q})=\sum_{1\le i\le A}\frac{1}{4\,m_N}\left\{\mathrm{e}^{i\mathbf{q}\cdot\mathbf{r}_i}\ ,\ \mathbf{p}_i\right\}\left[G_E^S(q)+G_E^V(q)\tau_{z,i}\right]\ . \tag{5.8}$$

The last term in the nonrelativistic j_1 operator, denoted by $\mathbf{j}_{m,1}$, is from the magnetic moment $\mu\,e/(2\,m_N)$ of the nucleon. It interacts with the magnetic field $\mathbf{B}$ of the photon via

$$-\mu\,\frac{e}{2\,m_N}\boldsymbol{\sigma}\cdot\mathbf{B}=-i\,\mu\,\frac{e}{2\,m_N}\,\boldsymbol{\sigma}\times\mathbf{q}\cdot\mathbf{A}\ , \tag{5.9}$$

corresponding to the current $i\,(\mu/2\,m_N)\,\boldsymbol{\sigma}\times\mathbf{q}$ after factoring out e. Taking into account the difference in the magnetic moments of the proton and the neutron, we obtain

$$\mathbf{j}_{m,1}(\mathbf{q})=\sum_{1\le i\le A}\mathrm{e}^{i\mathbf{q}\cdot\mathbf{r}_i}\frac{i}{4\,m_N}\,\boldsymbol{\sigma}_i\times\mathbf{q}\left[G_M^S(q)+G_M^V(q)\,\tau_{z,i}\right]\ , \tag{5.10}$$

where isoscalar and isovector magnetic Sachs form factors are defined as

$$G_M^S(q)=G_M^p(q)+G_M^n(q)\ ,\qquad G_M^V(q)=G_M^p(q)-G_M^n(q)\ . \tag{5.11}$$

These form factors at $q=0$ are related to the proton and neutron magnetic moments via Eqs. (4.6).

5.2 Photo-pion current and charge operators

In the nonrelativistic limit the coupling of a charged pion to the nucleon involves a gradient operator, see Eq. (3.10). By minimal substitution in the terms of $H_{\pi NN}$ involving absorption or emission of charged pions, we find

$$-\frac{f_{\pi NN}}{m_\pi}\,\boldsymbol{\sigma}\cdot[\boldsymbol{\nabla}\pm i\,\mathbf{A}(\mathbf{r})]\,\hat{\phi}_\pm(\mathbf{r})\,\tau_\mp\ , \tag{5.12}$$

where the charged pion fields are as defined in Eq. (3.3) and use has been made of Eq. (3.7) for $\hat{\boldsymbol{\phi}}(\mathbf{r})\cdot\boldsymbol{\tau}$. The upper and lower signs are for the positive and negative pion fields $\hat{\phi}_+$ and $\hat{\phi}_-$, respectively. Neutral pions cannot be photo-produced in first order of $f_{\pi NN}$. However, they can be produced in higher order by charge exchange πN scattering, for example via $\gamma+n\to\Delta^0\to n+\pi^0$. We will neglect here these higher order contributions and derive the photo-pion current $\mathbf{j}_2^{PM}(ij)$ in the leading order proportional to $f^2_{\pi NN}$.

The photo-pion currents come from the term containing $\mathbf{A}$ in Hamiltonian (5.12), which can be written as

$$-i\,\frac{f_{\pi NN}}{m_\pi}\,\boldsymbol{\sigma}\cdot\mathbf{A}(\mathbf{r})\left[\hat{\phi}_+(\mathbf{r})\,\tau_- - \hat{\phi}_-(\mathbf{r})\,\tau_+\right]=\frac{f_{\pi NN}}{m_\pi}\,\boldsymbol{\sigma}\cdot\mathbf{A}(\mathbf{r})\,\epsilon_{abz}\,\tau_a\,\hat{\phi}_b(\mathbf{r})\ , \tag{5.13}$$

where a and b denote components x, y, and z in isospin space, and a sum over repeated indices is understood. In the interaction shown in diagram (2.PM) of Fig. 5.1 the photo-pion is produced by nucleon i. A part of the photon momentum, denoted by $\mathbf{k}_i$ is taken by nucleon i, and $\mathbf{k}_j$ by nucleon j. We must have

$$\mathbf{q}=\mathbf{k}_i+\mathbf{k}_j\ . \tag{5.14}$$

The calculation of this interaction proceeds as that of v^π_{ij} given in Sec. 3.2. However, the current is derived in the static limit, *i.e.* neglecting the nucleon kinetic energies as well as the energy ω_q injected by the external EM field. Equation (5.1) is then used to identify the photo-pion current off nucleon i, which (in momentum space) reads

$$\mathbf{j}_i^{PM,\pi}(\mathbf{k}_i,\mathbf{k}_j)=-i\,\frac{f^2_{\pi NN}}{m^2_\pi}\,(\boldsymbol{\tau}_i\times\boldsymbol{\tau}_j)_z\,\frac{1}{m^2_\pi+k^2_j}\,\boldsymbol{\sigma}_i\,\boldsymbol{\sigma}_j\cdot\mathbf{k}_j\ . \tag{5.15}$$

The $\langle i(\boldsymbol{\tau}_i\times\boldsymbol{\tau}_j)_z\rangle=1$ when initially the nucleons i and j are respectively proton and neutron and finally they become neutron and proton. In this case the current flows from i to j. When i,j are initially n,p and become p,n, the $\langle i(\boldsymbol{\tau}_i\times\boldsymbol{\tau}_j)_z\rangle=-1$ and the current flows from j to i. The $\langle i(\boldsymbol{\tau}_i\times\boldsymbol{\tau}_j)_z\rangle=0$ when there is no charge exchanged between i and j. The $\mathbf{j}_j^{PM,\pi}(\mathbf{k}_i,\mathbf{k}_j)$ current has a similar expression with $i\rightleftharpoons j$. Combining both we get the total photo-pion current as

$$\mathbf{j}_2^{PM,\pi}(\mathbf{k}_i,\mathbf{k}_j)=-i\,\frac{f^2_{\pi NN}}{m^2_\pi}(\boldsymbol{\tau}_i\times\boldsymbol{\tau}_j)_z\left(\frac{1}{m^2_\pi+k^2_j}\,\boldsymbol{\sigma}_i\,\boldsymbol{\sigma}_j\cdot\mathbf{k}_j-\frac{1}{m^2_\pi+k^2_i}\,\boldsymbol{\sigma}_j\,\boldsymbol{\sigma}_i\cdot\mathbf{k}_i\right)\ , \tag{5.16}$$

for point nucleons and pions. Our derivation of photo-pion current ignores the finite size effects on the coupling of the photon to the nucleon, and gives the above equations without the isovector nucleon electric form factor $G_E^V(q)$. At small values of q the $G_E^V(q) \to 1$, and the equation for the current is exact. At larger value of q it is important to include $G_E^V(q)$ to satisfy current conservation as discussed in Sec. 5.4.

The one pion exchange also contributes to a coupling of the scalar potential $\phi^0(\mathbf{r})$ to the nucleon via the interaction Hamiltonian given by

$$-\frac{1}{2\,m_N}\,\frac{f_{\pi NN}}{m_\pi}\,\left[\boldsymbol{\tau}\cdot\hat{\boldsymbol{\phi}}(\mathbf{r})+\hat{\phi}_z(\mathbf{r})\right]\boldsymbol{\sigma}\cdot\boldsymbol{\nabla}\phi^0(\mathbf{r})\ . \tag{5.17}$$

It vanishes in the static limit ($m_N \to \infty$), and can be regarded as a relativistic correction. A similar analysis to that carried out above for the one pion-exchange two-body current leads to a corresponding charge operator (for point nucleon and pions) of the form

$$\begin{aligned}\rho_{c,2}^{PM,\pi}(\mathbf{k}_i,\mathbf{k}_j) &= \frac{1}{2\,m_N}\,\frac{f_{\pi NN}^2}{m_\pi^2}\left[(\boldsymbol{\tau}_i\cdot\boldsymbol{\tau}_j+\tau_{z,j})\,\frac{1}{m_\pi^2+k_j^2}\,\boldsymbol{\sigma}_i\cdot\mathbf{q}\;\boldsymbol{\sigma}_j\cdot\mathbf{k}_j\right.\\ &\left.+(\boldsymbol{\tau}_i\cdot\boldsymbol{\tau}_j+\tau_{z,i})\,\frac{1}{m_\pi^2+k_i^2}\,\boldsymbol{\sigma}_i\cdot\mathbf{k}_i\;\boldsymbol{\sigma}_j\cdot\mathbf{q}\right]\ .\end{aligned} \tag{5.18}$$

Finite size effects on the nucleon-photon coupling are accounted for by multiplying the isoscalar part proportional to $\boldsymbol{\tau}_i\cdot\boldsymbol{\tau}_j$ by $G_E^S(q)$ and the isovector part proportional to $\tau_{z,i}$ or $\tau_{z,j}$ by $G_E^V(q)$. This operator gives important contributions to the longitudinal form factors of light nuclei, in particular to the deuteron A structure function and tensor polarization observable, and ^{3}He/^{3}H and ^{4}He charge form factors, measured in elastic electron scattering at low and moderate values of the momentum transfer.

The two-body operators in Eqs. (5.16) and (5.18) are in momentum space, and coordinate-space expressions follow from

$$\mathbf{j}_2^{PM,\pi}(\mathbf{q};ij)=\int\frac{d\mathbf{k}_i}{(2\pi)^3}\,\frac{d\mathbf{k}_j}{(2\pi)^3}\,\mathrm{e}^{i\mathbf{k}_i\cdot\mathbf{r}_i}\,\mathrm{e}^{i\mathbf{k}_j\cdot\mathbf{r}_j}\,(2\pi)^3\,\delta(\mathbf{k}_i+\mathbf{k}_j-\mathbf{q})\,\mathbf{j}_2^{PM,\pi}(\mathbf{k}_i,\mathbf{k}_j)\ , \tag{5.19}$$

and similarly for $\rho_{c,2}^{PM,\pi}(\mathbf{q};ij)$.

5.3 Pion current and charge operators

Half of the time ordered diagrams that contribute to the pion current are shown in Fig. 5.3. In all of them nucleon i gets momentum $\mathbf{k}_i$, and the rest is taken by nucleon j. The pions interact with nucleons i and j respectively with the $\hat{\phi}_+$ and $\hat{\phi}_-$ field operators, and convert them from p,n to n,p. In the remaining six processes, not shown in Fig. 5.3, i and j are converted from n,p to p,n.

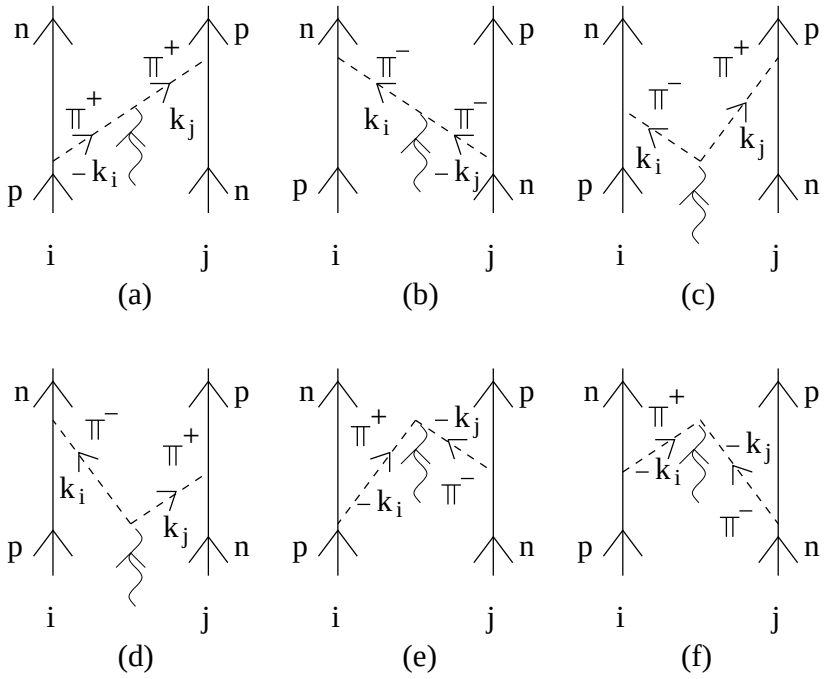

Figure 5.3: Time ordered diagrams contributing to the π-meson current. See caption of Fig. 5.1 for notation.

The coupling of the charged pion field to the EM field is given by minimal substitution in the pion kinetic energy density

$$\frac{1}{2}\left[\boldsymbol{\nabla}\hat{\phi}_x\cdot\boldsymbol{\nabla}\hat{\phi}_x+\boldsymbol{\nabla}\hat{\phi}_y\cdot\boldsymbol{\nabla}\hat{\phi}_y\right]=\boldsymbol{\nabla}\hat{\phi}_+\cdot\boldsymbol{\nabla}\hat{\phi}_-\rightarrow(\boldsymbol{\nabla}-i\mathbf{A})\hat{\phi}_-\cdot(\boldsymbol{\nabla}+i\mathbf{A})\hat{\phi}_+\ , \tag{5.20}$$

which leads to the following $\gamma\pi\pi$ interaction

$$-\epsilon_{abz}\int d^3r\,\mathbf{A}(\mathbf{r})\cdot\left[\boldsymbol{\nabla}\hat{\phi}_a(\mathbf{r})\right]\hat{\phi}_b(\mathbf{r}) \tag{5.21}$$

and to the corresponding vertex

$$i\,\frac{\epsilon_{abz}}{\sqrt{4\,\omega_{k_i}\omega_{k_j}}}\mathbf{A}\cdot(\mathbf{k}_i-\mathbf{k}_j) \tag{5.22}$$

in all the six diagrams of Fig. 5.3, where the pions have momenta $\mathbf{k}_i$ and $\mathbf{k}_j$ and isospin components a and b, respectively. The pion-nucleon vertices in these six diagrams give an additional factor of

$$-\frac{f^2_{\pi NN}}{m^2_\pi}\,\frac{1}{\sqrt{4\,\omega_{k_i}\omega_{k_j}}}\,\tau_{a,i}\,\tau_{b,j}\,\boldsymbol{\sigma}_i\cdot\mathbf{k}_i\;\boldsymbol{\sigma}_j\cdot\mathbf{k}_j\ . \tag{5.23}$$

In the above equations $\omega_k = \sqrt{m_\pi^2 + k^2}$ is the free pion energy and form factors have been included at the pion-nucleon vertices to account for finite size effects.

In time ordered perturbation theory, neglecting nucleon kinetic energies and the energy ω_q injected by the external EM field, the diagrams (a) and (b) have a factor $1/(\omega_{k_i}\,\omega_{k_j})$ from the two energy denominators, while (c) and (f), and (d) and (e), have respectively

$$\frac{1}{(\omega_{k_i} + \omega_{k_j})\,\omega_{k_j}} \qquad \text{and} \qquad \frac{1}{(\omega_{k_i} + \omega_{k_j})\,\omega_{k_i}} \ . \tag{5.24}$$

Adding the contributions of all the six diagrams, we obtain the pion current

$$\mathbf{j}_2^{MC,\pi}(\mathbf{k}_i, \mathbf{k}_j) = i\,\frac{f_{\pi NN}^2}{m_\pi^2}\,G_E^V(q)\,(\boldsymbol{\tau}_i \times \boldsymbol{\tau}_j)_z\,(\mathbf{k}_i - \mathbf{k}_j)\,\frac{\boldsymbol{\sigma}_i \cdot \mathbf{k}_i\ \boldsymbol{\sigma}_j \cdot \mathbf{k}_j}{(m_\pi^2 + k_i^2)(m_\pi^2 + k_j^2)}\ , \tag{5.25}$$

where inclusion of the isovector electric form factor of the nucleon ensures that $\mathbf{j}_2^{PM,\pi} + \mathbf{j}_2^{MC,\pi}$ is conserved, as discussed in the next section.

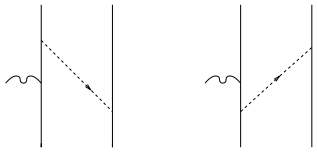

Figure 5.4: Some of the time ordered diagrams contributing to the π-meson charge operator. See caption of Fig. 5.1 for notation.

There is also a coupling of the pion field to the scalar potential ϕ^0 which leads to the following vertex

$$-i\,\frac{\epsilon_{abz}}{\sqrt{4\,\omega_{k_i}\omega_{k_j}}}\phi^0\,(\omega_{k_i} - \omega_{k_j}) \tag{5.26}$$

for emission of pions with momenta $\mathbf{k}_i$ and $\mathbf{k}_j$, energies ω_{k_i} and ω_{k_j}, and isospin components a and b, respectively. In the static limit, in which the external field energy and the nucleon kinetic energies are neglected, we find that, after summing over the six possible time orderings, the two-body pion charge operator vanishes. However, a careful analysis of non-static corrections of the diagrams in Fig. 5.3 as well as of those in Fig. 5.4 leads to the operator (for point nucleons and pions)

$$\begin{aligned}\rho_{c,2}^{MC,\pi}(\mathbf{k}_i, \mathbf{k}_j) \ &= \ \frac{i}{m_N}\,\frac{f_{\pi NN}^2}{m_\pi^2}\,(\boldsymbol{\tau}_i \times \boldsymbol{\tau}_j)_z \left[\frac{\boldsymbol{\sigma}_i \cdot \mathbf{k}_i\ \boldsymbol{\sigma}_j \cdot \mathbf{k}_j}{(m_\pi^2 + k_i^2)\,(m_\pi^2 + k_j^2)}\,\mathbf{k}_i \cdot \mathbf{K}_i\right. \\ &\left. -\frac{\boldsymbol{\sigma}_i \cdot \mathbf{k}_j\,\boldsymbol{\sigma}_j \cdot \mathbf{k}_j}{(m_\pi^2 + k_j^2)^{\,2}}\,\mathbf{k}_j \cdot \mathbf{K}_j\right] + (i \rightleftharpoons j)\ ,\end{aligned} \tag{5.27}$$

where the momentum $\mathbf{K}_i = \mathbf{p}_i + \mathbf{k}_i/2$ referring to diagram (2.MC) in Fig. 5.1. We should note that the operator $\rho_2^{MC,\pi}(\mathbf{k}_i, \mathbf{k}_j)$ above corresponds to a specific choice of non-static corrections to the one pion-exchange potential. Different choices for these, otherwise arbitrary, corrections lead to different charge operators $\rho_2^{MC,\pi}(\mathbf{k}_i, \mathbf{k}_j)$. However, it can be shown that the different (non-static) one pion-exchange potentials and corresponding charge operators are related to each other by a unitary transformation. Therefore, their lack of uniqueness has no consequence on the predictions of physical observables.

5.4 Charge conservation

The total charge operator is given by

$$\begin{aligned} \int d\mathbf{x}\, \rho_c(\mathbf{x}) &= \rho_c(\mathbf{q}=0) \\ &= \rho_{c,1}(\mathbf{q}=0) + \rho_{c,2}(\mathbf{q}=0) + \rho_{c,3}(\mathbf{q}=0) + \dots \ , \end{aligned} \tag{5.28}$$

where $\rho_{c,n}(\mathbf{q}=0)$ are the one-body, two-body, three-body, and so on, charge operators, defined in Eq. (5.3). In a nucleus A^Z (with Z protons), (global) charge conservation demands that

$$\langle A^Z \,|\, \int d\mathbf{x}\, \rho_c(\mathbf{x}) \,|\, A^Z \rangle = Z \ , \tag{5.29}$$

in units of the proton charge e. This condition is satisfied by $\rho_{c,1}(\mathbf{q}=0)$, since

$$\rho_{c,1}(\mathbf{q}=0) = \sum_i \frac{1+\tau_{z,i}}{2} \qquad \text{and} \qquad \langle A^Z \,|\, \rho_{c,1}(\mathbf{q}=0) \,|\, A^Z \rangle = Z \ . \tag{5.30}$$

Therefore it follows that

$$\langle A^Z \,|\, \rho_{c,2}(\mathbf{q}=0) + \rho_{c,3}(\mathbf{q}=0) + \dots \,|\, A^Z \rangle = 0 \ . \tag{5.31}$$

The photo-pion charge operator in Eq. (5.18) obviously satisfies this requirement, since it vanishes at $\mathbf{q}=0$. It is also satisfied by the pion charge operator in Eq. (5.27), since $\mathbf{q}=0$ implies $\mathbf{k}_i = -\mathbf{k}_j$, and hence $\rho_{c,2}^{MC,\pi}(\mathbf{k}_i, -\mathbf{k}_i) = 0$.

Locally charge conservation requires

$$\boldsymbol{\nabla} \cdot \mathbf{j}(\mathbf{x}) + \frac{\partial \rho_c(\mathbf{x})}{\partial t} = 0 \ , \tag{5.32}$$

where the time derivative of the Schrödinger picture operator $\rho_c(\mathbf{x})$ is defined as

$$\frac{\partial \rho_c(\mathbf{x})}{\partial t} \equiv i\, [H\,,\, \rho_c(\mathbf{x})] \ , \tag{5.33}$$

and H is the nuclear Hamiltonian. In terms of the Fourier transforms $\mathbf{j}(\mathbf{q})$ and $\rho_c(\mathbf{q})$ local charge conservation then implies

$$\mathbf{q}\cdot\mathbf{j}(\mathbf{q}) = [H\,,\,\rho_c(\mathbf{q})]\ , \tag{5.34}$$

which establishes a complicated relation between many-body interactions and currents. It is interesting to show that it is satisfied for the photo-pion and pion currents derived in the previous sections. To lowest order in $1/m_N$, Eq. (5.34) separates into

$$\mathbf{q}\cdot\mathbf{j}_1(\mathbf{q};i) = \left[\frac{\mathbf{p}_i^2}{2\,m_N}\,,\,\rho_{c,1}(\mathbf{q};i)\right]\ , \tag{5.35}$$

$$\mathbf{q}\cdot\left[\mathbf{j}_2^{PM,\pi}(\mathbf{q};ij)+\mathbf{j}_2^{MC,\pi}(\mathbf{q};ij)\right] = \left[v_{ij}^{\pi}\,,\,\rho_{c,1}(\mathbf{q};i)+\rho_{c,1}(\mathbf{q};j)\right]\ , \tag{5.36}$$

where $v_{ij}^{\pi}\equiv\overline{v}_{ij}^{\pi}\,\boldsymbol{\tau}_i\cdot\boldsymbol{\tau}_j$ is the one pion-exchange potential. By evaluating the commutators on the r.h.s. of the above equations, we easily find

$$\left[\frac{\mathbf{p}_i^2}{2\,m_N}\,,\,\rho_{c,1}(\mathbf{q};i)\right] = \frac{1}{4\,m_N}\left(\mathrm{e}^{i\mathbf{q}\cdot\mathbf{r}_i}\,\mathbf{q}\cdot\mathbf{p}_i+\mathbf{p}_i\cdot\mathbf{q}\,\mathrm{e}^{i\mathbf{q}\cdot\mathbf{r}_i}\right)\left[G_E^S(q)+G_E^V(q)\tau_{z,i}\right]\ , \tag{5.37}$$

$$\left[v_{ij}^{\pi}\,,\,\rho_{c,1}(\mathbf{q};i)+\rho_{c,1}(\mathbf{q};j)\right] = i\,G_E^V(q)(\boldsymbol{\tau}_i\times\boldsymbol{\tau}_j)_z\,\overline{v}_{ij}^{\pi}\left(\mathrm{e}^{i\mathbf{q}\cdot\mathbf{r}_i}-\mathrm{e}^{i\mathbf{q}\cdot\mathbf{r}_j}\right)\ . \tag{5.38}$$

Equation (5.35) is obviously satisfied by $\mathbf{j}_{c,1}(\mathbf{q};i)$ in Eq. (5.8), while $\mathbf{q}\cdot\mathbf{j}_{m,1}(\mathbf{q};i)$ in Eq. (5.10) vanishes identically. The l.h.s. of Eq. (5.36) gives

$$\begin{aligned}\text{l.h.s} = -i\,G_E^V(q)\,\frac{f_{\pi NN}^2}{m_\pi^2}\,(\boldsymbol{\tau}_i\times\boldsymbol{\tau}_j)_z\int\frac{d\mathbf{k}_i}{(2\pi)^3}\,\frac{d\mathbf{k}_j}{(2\pi)^3}\,\mathrm{e}^{i\mathbf{k}_i\cdot\mathbf{r}_i}\,\mathrm{e}^{i\mathbf{k}_j\cdot\mathbf{r}_j}\,(2\pi)^3\,\delta(\mathbf{k}_i+\mathbf{k}_j-\mathbf{q})\\ \left[\frac{(\mathbf{k}_i+\mathbf{k}_j)\cdot\boldsymbol{\sigma}_i\;\boldsymbol{\sigma}_j\cdot\mathbf{k}_j}{m_\pi^2+k_j^2}\;-\frac{(\mathbf{k}_i+\mathbf{k}_j)\cdot\boldsymbol{\sigma}_j\;\boldsymbol{\sigma}_i\cdot\mathbf{k}_i}{m_\pi^2+k_i^2}-\frac{k_i^2-k_j^2}{(m_\pi^2+k_i^2)(m_\pi^2+k_j^2)}\,\boldsymbol{\sigma}_i\cdot\mathbf{k}_i\;\boldsymbol{\sigma}_j\cdot\mathbf{k}_j\right]\end{aligned}$$

and the last term in the square bracket can be written as

$$-\frac{k_i^2-k_j^2}{(m_\pi^2+k_i^2)(m_\pi^2+k_j^2)} = \frac{1}{m_\pi^2+k_i^2}-\frac{1}{m_\pi^2+k_j^2}\ .$$

Combining terms and carrying out the integrations over $\mathbf{k}_i$ and $\mathbf{k}_j$, the r.h.s. of Eq. (5.38) is obtained.

The finite size effects in $H_{\pi NN}$ are included via vertex factors $F_{\pi NN}(k)$ as discussed in Sec. 3.17. Including these, the one pion-exchange potential is as given in Eq. (3.203). These finite size effects can be accounted for in the photo-pion and pion currents by defining

$$\mathbf{j}_2^{PM,\pi}(\mathbf{k}_i,\mathbf{k}_j) = -i\,G_E^V(q)\,\frac{f_{\pi NN}^2}{m_\pi^2}(\boldsymbol{\tau}_i\times\boldsymbol{\tau}_j)_z\left[\frac{F_{\pi NN}^2(k_j)}{m_\pi^2+k_j^2}\,\boldsymbol{\sigma}_i\;\boldsymbol{\sigma}_j\cdot\mathbf{k}_j-\frac{F_{\pi NN}^2(k_i)}{m_\pi^2+k_i^2}\,\boldsymbol{\sigma}_j\;\boldsymbol{\sigma}_i\cdot\mathbf{k}_i\right]\ , \tag{5.39}$$

$$\mathbf{j}_2^{MC,\pi}(\mathbf{k}_i,\mathbf{k}_j) = i\,\frac{f_{\pi NN}^2}{m_\pi^2}\,G_E^V(q)\,(\boldsymbol{\tau}_i\times\boldsymbol{\tau}_j)_z\,\frac{\mathbf{k}_i-\mathbf{k}_j}{k_i^2-k_j^2}\boldsymbol{\sigma}_i\cdot\mathbf{k}_i\;\boldsymbol{\sigma}_j\cdot\mathbf{k}_j\left[\frac{F_{\pi NN}^2(k_j)}{m_\pi^2+k_j^2}-\frac{F_{\pi NN}^2(k_i)}{m_\pi^2+k_i^2}\right]\,. \tag{5.40}$$

These currents are conserved. However, in this context it is worthwhile noting that the relation Eq. (5.34) constrains only the longitudinal (along $\mathbf{q}$) component of the current. In the case of the photo-pion and pion currents above, in particular, this constraint imposes that the nucleon electromagnetic form factor $G_E^V(q)$ be used in their longitudinal components. However, it poses no restrictions on their transverse components. Ignoring this ambiguity, the choice in Eqs. (5.39) and (5.40) satisfies the "minimal" requirement of current conservation.

5.5 The nucleon excitation currents

The $N \rightleftharpoons \Delta$ transition currents are believed to be the leading currents due to the excitation of nucleons by the photon. In the quark model, the spins of valance quarks are coupled to a total spin 1/2 and 3/2 in the N and Δ states respectively. The photon can flip the spin of a quark by a magnetic dipole transition and convert $N \rightleftharpoons \Delta$. This leads to the $\gamma N\Delta$ coupling

$$H_{\gamma N\Delta} = -\frac{\mu_{\gamma N\Delta}}{2\,m_N}\left[T_z\,\mathbf{S}\times\boldsymbol{\nabla} + T_z^\dagger\,\mathbf{S}^\dagger\times\boldsymbol{\nabla}\right]\cdot\mathbf{A}\;, \tag{5.41}$$

where $\mathbf{S}$ and $\mathbf{T}$ are respectively $N\to\Delta$ transition spin and isospin. This coupling is a generalization of the $-\mu\,\boldsymbol{\sigma}\cdot\mathbf{B}$ dipole coupling of the spin to the magnetic field, and can be derived from the quark model. The first term gives the $N\to\Delta$ transition and the second $\Delta\to N$. Due to charge conservation in electromagnetic transitions, the $H_{\gamma N\Delta}$ can depend only on T_z. There can also be an electric quadrupole transition between the N and Δ states. However, this coupling is very weak compared to the magnetic dipole, and we will not consider its effects.

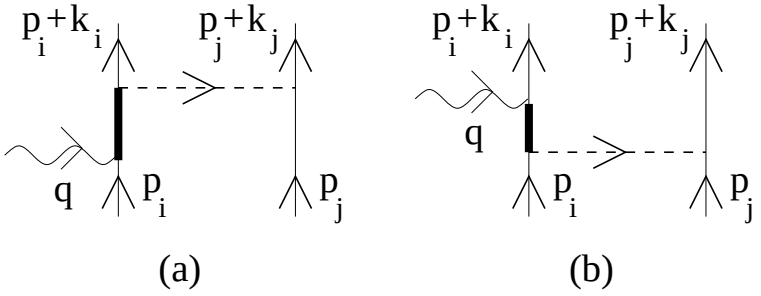

Figure 5.5: Two of diagrams contributing to the $N\Delta$ excitation current. See caption of Fig. 5.1 for notation

The value of the transition magnetic moment $\mu_{\gamma N\Delta}$ obtained from the analysis of γN scattering data in the Δ resonance region is $\simeq 3$ in units of nuclear magnetons. It is about

30% smaller than that predicted by the quark model. The nucleon magnetic current in Eq. (5.10) has an isoscalar term proportional to the isoscalar magnetic form factor $G_M^S(q)$. However, isoscalar terms cannot convert a nucleon to Δ and are absent in $H_{\gamma N\Delta}$. The N to Δ current then follows from Eq. (5.41) as

$$\mathbf{j}_{i,N\to\Delta}(\mathbf{q}) = i\,\frac{\mu_{\gamma N\Delta}}{2\,m_N}\,T_{z,i}\,\mathbf{S}_i\times\mathbf{q}\,\mathrm{e}^{i\mathbf{q}\cdot\mathbf{r}_i}\ , \tag{5.42}$$

while the Δ to N current is obtained from the expression above by replacing $T_{z,i}$ and $\mathbf{S}_i$ by the corresponding adjoint operators.

The main processes contributing to the $N \rightleftharpoons \Delta$ transition current are shown in Fig. 5.5, and can be estimated in perturbation theory by using the one pion-exchange transition potentials derived in Sec. 3.11. By neglecting kinetic energies in the intermediate states, we obtain in coordinate space

$$\begin{aligned}\mathbf{j}_2^{NE,\Delta}(\mathbf{q};ij) &= [v_{NN\to\Delta N}(\mathbf{r}_{ij})]^\dagger\,\frac{1}{m_N-m_\Delta}\,\mathbf{j}_{i,N\to\Delta}(\mathbf{q})\\ &\quad+\mathbf{j}_{i,\Delta\to N}(\mathbf{q})\,\frac{1}{m_N-m_\Delta}\,v_{NN\to\Delta N}(\mathbf{r}_{ij})+(i\rightleftharpoons j)\ .\end{aligned} \tag{5.43}$$

The first (second) term is from the excitation of nucleon i (j). The current above is obviously transverse $\mathbf{q}\cdot\mathbf{j}_2^{NE,\Delta}(\mathbf{q};ij)=0$. It can be expressed in terms of Pauli spin and isospin matrices by making of use of the identities in Eqs. (3.73)–(3.75) satisfied by the spin and isospin transition operators.

The current in Eq. (5.43) is generally overestimated by the above lowest order perturbation theory calculation. It is due to the admixtures of components with nucleons excited to Δ resonances in nuclear wave functions. The diagram (a) in Fig. 5.5, for example, shows a photon induced transition between the component in the initial state in which i is a nucleon to that in the final state in which i is a Δ. In contrast, in diagram (b) i is a Δ in the initial state. The amplitudes of processes due to the $\gamma N\Delta$ coupling can be more accurately calculated using non perturbative approximations for nuclear wave functions with Δ components. The simpler two-nucleon problem is discussed below, and the method has been generalized to light nuclei.

We can consider a Hamiltonian containing nucleon and Δ degrees of freedom. It has the general form

$$\begin{aligned}H_{N+\Delta} &= \sum_i (m_\Delta-m_N)\,P_{i\,\Delta}-\sum_i\left(\frac{1}{2\,m}\,P_{i\,N}+\frac{1}{2\,m_\Delta}\,P_{i\,\Delta}\right)\nabla_i^2\\ &\quad+\sum_{i<j}\ \sum_{B_1,B_2=N,\Delta}\ \sum_{B_1',B_2'=N,\Delta} v_{B_1B_2\to B_1'B_2'}(ij)\ ,\end{aligned} \tag{5.44}$$

where $P_{i\,N}$ and $P_{i\,\Delta}$ are N and Δ projection operators, and $v_{B_1B_2\to B_1'B_2'}(ij)$ are transition potentials when $B_1B_2\neq B_1'B_2'$. Excluding isospin symmetry breaking terms, a minimum of

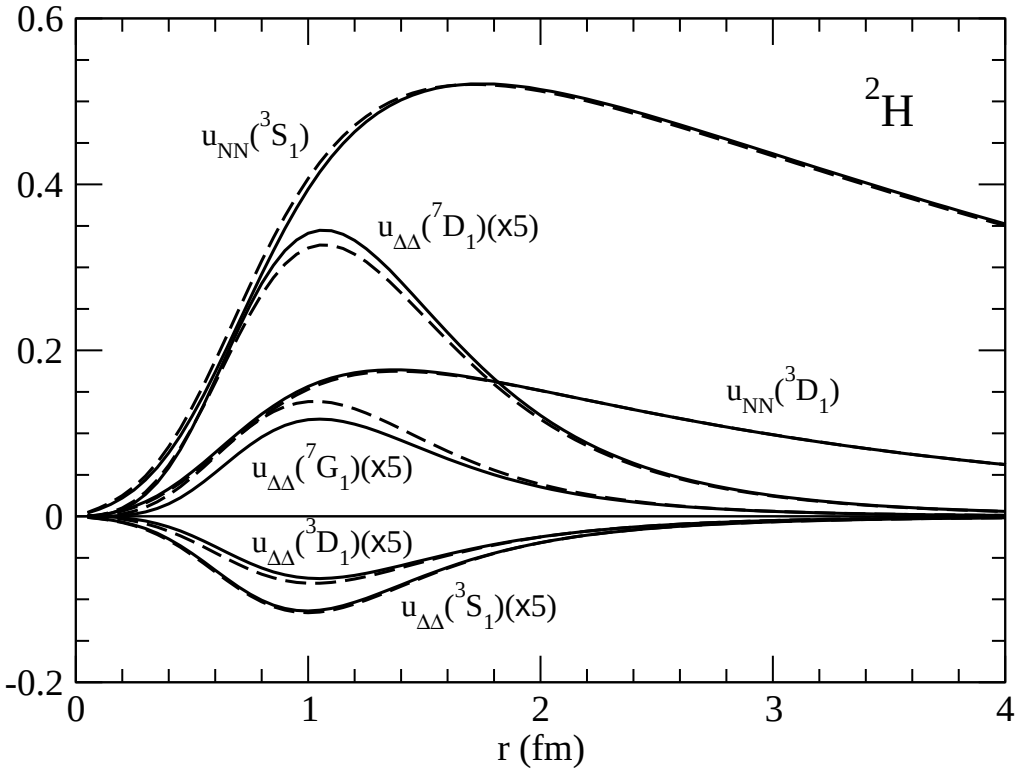

Figure 5.6: The solid lines give the wave functions of all the NN and $\Delta\Delta$ channels in the deuteron obtained by solving the Schrödinger equation with the Hamiltonian (5.44). The dashed lines are obtained with the correlation operator (5.49).

28 operators is needed to describe all the $v_{B_1B_2\to B_1'B_2'}$. These v_{28} models are also successful in explaining the NN elastic scattering data up to 350 MeV in laboratory. Since the Δ has isospin 3/2, the $T = 0$ np states can mix with only the $\Delta\Delta$ states. For example, including the N and Δ degrees of freedom, the deuteron has six coupled channels:

$$(^3S_1)_{NN},\ (^3D_1)_{NN},\ (^3S_1)_{\Delta\Delta},\ (^7D_1)_{\Delta\Delta},\ (^3D_1)_{\Delta\Delta},\ \text{and}\ (^7G_1)_{\Delta\Delta}\ . \tag{5.45}$$

The $T = 1$ pp or np or nn states have admixtures of $N\Delta + \Delta N$ and $\Delta\Delta$ channels, and the important $T = 1,\ J^\pi = 0^+$ state has four coupled channels:

$$(^1S_0)_{NN},\ (^5D_0)_{N\Delta+\Delta N},\ (^1S_0)_{\Delta\Delta},\ \text{and}\ (^5D_0)_{\Delta\Delta}\ . \tag{5.46}$$

The wave functions of channels having Δ's decay asymptotically as $r \to \infty$, and at positive energy only the NN channel goes out to infinity. The v_{28} wave functions for the deuteron and the $T = 1,\ J^\pi = 0^+,\ E = 1$ MeV state are shown in Fig. 5.6 and 5.7.

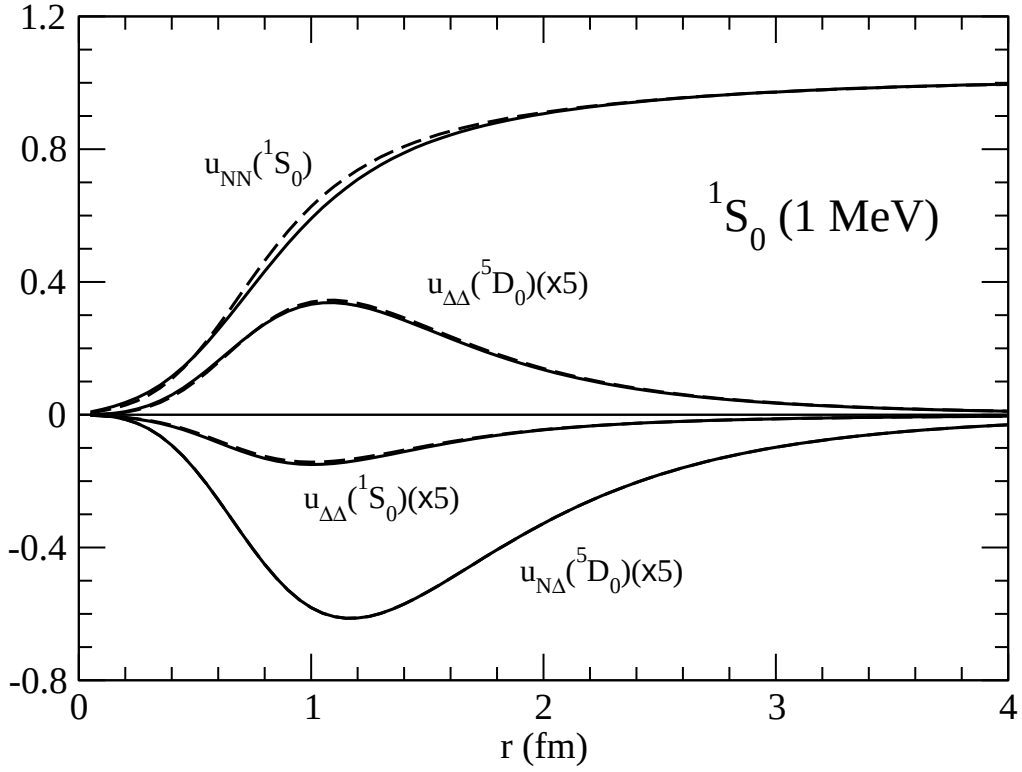

Figure 5.7: The solid lines give the wave functions of all the NN, $N\Delta + \Delta N$ and $\Delta\Delta$ channels in the $T = 1$, $J^\pi = 0^+$ state at $E = 1$ MeV, obtained by solving the Schrödinger equation with the Hamiltonian (5.44). The dashed lines are obtained with the correlation operator (5.49).

Let $\Psi_{NN}(ij)$ be the wave function which contains only the nucleon degrees of freedom, and $\Psi(ij)$ be the full wave function. The $\Psi(ij) \to \Psi_{NN}(ij)$ as $r \to \infty$. In bound states like the deuteron and nuclei, the norm of Ψ_{NN} is less than unit if Ψ is normalized to unity. We can generally define a transition correlation operator $U_{ij}^{\rm TR}$ such that

$$\Psi = \left[1 + U^{\rm TR}(ij)\right] \Psi_{NN}(ij) \ . \tag{5.47}$$

In the first order perturbation theory used to obtain Eq. (5.43) for the current $\mathbf{j}_2^{NE,\Delta}(\mathbf{q}; ij)$, the transition correlation operator is approximated as follows

$$U_{PT}^{\rm TR}(ij) = -\frac{v_{NN\to N\Delta}(ij) + v_{NN\to\Delta N}(ij)}{m_\Delta - m} - \frac{v_{NN\to\Delta\Delta}(ij)}{2\,(m_\Delta - m)} \ , \tag{5.48}$$

in an obvious notation. This approximation is not good at $r \simeq 1$ fm, where the wave functions with Δ's peak, see Figs. 5.6 and 5.7. In this region the wave functions are influenced by the

repulsive core in the diagonal $B_1B_2 \to B_1B_2$ interactions, and the kinetic energies of the channels with Δ's are significant. The above approximation overestimates the amplitudes of some channels with Δ's by factors of order two.

However, a simple and good approximation can be obtained for $U^{\rm TR}$, since in the nuclear energy domain it does not depend too much on the energy and angular momentum of the interacting nucleons. In fact the operator

$$\begin{aligned} U^{TR}(ij) &= u^{\sigma II}(r_{ij})\,(\boldsymbol{\sigma}_i\cdot\mathbf{S}_j\ \boldsymbol{\tau}_i\cdot\mathbf{T}_j + \mathbf{S}_i\cdot\boldsymbol{\sigma}_j\ \mathbf{T}_i\cdot\boldsymbol{\tau}_j) + u^{\sigma III}(r_{ij})\,\mathbf{S}_i\cdot\mathbf{S}_j\ \mathbf{T}_i\cdot\mathbf{T}_j \\ &\quad + u^{tII}(r_{ij})\left(S^{II}_{ji}\ \boldsymbol{\tau}_i\cdot\mathbf{T}_j + S^{II}_{ij}\ \mathbf{T}_i\cdot\boldsymbol{\tau}_j\right) + u^{tIII}(r_{ij})\,S^{III}_{ij}\ \mathbf{T}_i\cdot\mathbf{T}_j\ , \end{aligned} \tag{5.49}$$

gives wave functions of channels with Δ's that are very close to the exact solutions of the two-body Schrödinger equation with the v_{28} potential, as can be seen from Figs. 5.6 and 5.7. Note that the above $U^{\rm TR}$ contains the operators in the transition potentials in Eqs. (3.102) and (3.110). The approximate Ψ_{NN} is calculated from an NN interaction that has the same form as the $v_{NN\to NN}$ in the v_{28}, but its strength parameters are readjusted to make it phase equivalent to v_{28}. The functions $u^{\sigma II}(r)$, $u^{\sigma III}(r)$, $u^{tII}(r)$ and $u^{tIII}(r)$ are extracted from the solutions of the v_{28} Schrödinger equation. The $N \rightleftharpoons \Delta$ transition current can be easily calculated from the full Ψ given by Eq. (5.47).

5.6 Relativistic one-nucleon current

The relativistic expression for the current of a point charge particle like an electron is given by

$$j^\mu(x) = Q\,\overline{\psi}(x)\,\gamma^\mu\,\psi(x)\ , \tag{5.50}$$

$$\langle p',\chi' \mid j^\mu(x) \mid p,\chi\rangle = Q\,{\rm e}^{i\,q\cdot x}\,\overline{u}(p',\chi')\,\gamma^\mu\,u(p,\chi)\ . \tag{5.51}$$

In the equation for j^μ, Q is the charge of the particle and $\overline{\psi}$ and ψ are field operators. In the matrix element of j^μ the p and p' are the initial and final momenta, q is the momentum transfer $q = p' - p$, and χ and χ' are the initial and final spin states. We can easily verify that in the nonrelativistic limit the above current gives the charge density and convection current as in Eqs. (5.5) and (5.8), however, the magnetic moment current in Eq. (5.10) has the Dirac magnetic moments, $e/(2\,m_p)$ for the proton and zero for the neutron. Thus the above equations are not useful for composite objects like the nucleons.

The most general expression for the vector current of a spin half particle is

$$\langle p',\chi' \mid j^\mu(x) \mid p,\chi\rangle = {\rm e}^{i\,q\cdot x}\,\overline{u}(p',\chi')\left[F_1(q^2)\,\gamma^\mu + i\,F_2(q^2)\,\sigma^{\mu\nu}\,q_\nu + F_3(q^2)\,q^\mu\right]u(p,\chi)\ , \tag{5.52}$$

where $\sigma^{\mu\nu}$ is the antisymmetric tensor defined in terms of γ matrices as $\sigma^{\mu\nu} = (i/2)\,[\gamma^\mu\,,\,\gamma^\nu]$. The matrix element of the current depends on the momentum p and the momentum transfer

q or equivalently on p', and for free particles $p^2 = p'^2 = m^2$, where m is the particle mass. In the case of interacting particles p^2 and p'^2 can be different from m^2. The electromagnetic current is conserved, and therefore

$$\frac{\partial}{\partial x^\mu} j^\mu(x) = 0 \ , \tag{5.53}$$

which leads to the following condition

$$\overline{u}(p', \chi') \left[F_1(q^2)\, q_\mu\, \gamma^\mu + i\, F_2(q^2)\, \sigma^{\mu\nu}\, q_\mu\, q_\nu + F_3(q^2)\, q^2 \right] u(p, \chi) \ . \tag{5.54}$$

The $q_\mu \gamma^\mu$ term is zero since the spinors u and $\overline{u}$ satisfy the (free-paricle) Dirac equation, and the $q_\nu q_\mu$ term is also zero because the tensor $\sigma^{\mu\nu}$ is antisymmetric. Therefore the $F_3(q^2) = 0$. Taking the nonrelativistic limit of the Eq. (5.52) we obtain

$$F_1(q^2 \to 0) = Q \ , \qquad F_2(q^2 \to 0) = (\mu - 1)\frac{Q}{2m} \ , \tag{5.55}$$

where $\mu\, Q/(2\, m)$ the magnetic moment of the particle. The form factors at finite values of q^2 are not constrained by the values of Q and the magnetic moment.

The nucleon currents are divided into isoscalar and isovector parts using $(1 \pm \tau_z)/2$ projection operators for the proton and the neutron, as in Sec. 5.1. This gives

$$\begin{aligned} \langle p', \chi' \mid j^\mu(x) | p, \chi \rangle = \mathrm{e}^{i\, q\cdot x}\, \overline{u}(p', \chi') \Bigg[& e\, \gamma^\mu\, \frac{1}{2} \left[F_1^S(q^2) + F_1^V(q^2)\, \tau_z \right] \\ & + i\, \frac{e}{2\, m_N}\, \sigma^{\mu\nu}\, q_\nu\, \frac{1}{2} \left[(\mu_S - 1) F_2^S(q^2) + (\mu_V - 1) F_2^V(q^2)\, \tau_z \right] \Bigg] u(p, \chi) \ . \end{aligned} \tag{5.56}$$

Here χ and χ' give the initial and final spin-isospin states of the nucleon, and the isoscalar and isovector magnetic moments are defined as

$$\mu_S = \mu_p + \mu_n \simeq 0.88 \ , \qquad \mu_V = \mu_p - \mu_n \simeq 4.70 \ , \tag{5.57}$$

in units of $e/(2\, m_N)$. Note that $\mu_S \ll \mu_V$ so that the F_2 form factor associated with the anomalous nucleon magnetic moments is dominantly isovector, and

$$F_1^S(q^2 \to 0) = F_2^S(q^2 \to 0) = F_1^V(q^2 \to 0) = F_2^V(q^2 \to 0) = 1 \tag{5.58}$$

by construction.